

# Assessing Human Bone Collagen Turnover Rate

A Thesis Submitted to the Committee on Graduate Studies in Partial Fulfillment of the Requirements for the Degree of Master of Science in the Faculty of Arts and Science

Trent University  
Peterborough, Ontario, Canada

© Copyright by Olivia Hall 2024  
Anthropology M.Sc. Graduate Program  
September, 2024

## Abstract

Assessing Human Bone Collagen Turnover Rate

Olivia Hall

Understanding tissue turnover rate is crucial for isotopic analysis. Collagen, a main component of bone, is often studied in archaeology and paleontology, yet bone collagen turnover rates across various skeletal elements, remain underexplored. This study addresses this by assessing collagen turnover rates in multiple human skeletal elements using the bomb carbon dating method. Seven donors, aged 54 to 78, from the REST[ES] facility in Québec, were sampled. Turnover rates varied significantly among skeletal elements, ranked from slowest to fastest as follows: ulna, humerus, femur, rib, pelvis, and vertebra. It was shown that turnover rates are not consistent throughout life and are not averaged over a turnover period. For studies aiming to reconstruct temporal variation in life history, vertebrae and ulnae should be used due to their distinct turnover rates. This research provides the most comprehensive list of bone collagen turnover rates for various human skeletal elements.

**Keywords:** Bone collagen, turnover rate, radiocarbon, stable isotope analysis, human physiology, dietary analysis, turnover modeling, bomb carbon dating.

## Acknowledgements

Firstly, I would like to acknowledge the support and guidance I received from Dr. Paul Szpak throughout my thesis. While I am aware that he has said that he “never reads the acknowledgement section of theses”, without him, this work would have been massively overwhelming, and I would never have been able to sort through all the data and information or have functioning results. Thanks to Dr. Shari Forbes for graciously permitting me to collect samples from the donors at the REST[ES] facility. Working in such an esteemed facility was indeed a privilege. As well, thanks to Agathe Ribéreau-Gayon for accompanying me at the REST[ES] facility for two days to take my samples and helping me troubleshoot sample challenges on the fly. I would also like to acknowledge the seven donors I sampled from at the REST[ES] facility, without their donation none of my research would have been possible.

I would also like to thank everyone at TEAL (Trent Environmental Archaeology Laboratory) both past and present for the community and the support that they have provided. This group of people has helped me stay on track while also being a great group of people to spend time both in lab or out for drinks with. Special thanks to Kate Dougherty for always taking the extra time to make sure I had a vegan treat to go along with all her other wonderful cakes and desserts she has made. Also, thanks to Dr. Mathew Teeter for the technical support (especially the 6am support) in the water quality center and on the EA-IRMS, and thanks to Mariah Miller for teaching me everything about setting up and running the EA-IRMS.

I acknowledge here the use of artificial intelligence helped me in a few ways while writing this thesis. Firstly, through edits as Grammarly as well as edits to improve the clarity of my writing using OpenAI 3.5. OpenAI 3.5 was also employed to turn my ideas for models into functional python script, such as taking turnover rates at each year of life and producing the

'percent of tissue attributed to each period of life' from a sample. Not having to do this math in excel with my very basic knowledge of coding saved me probably a month of work.

Thank you to the Ontario Graduate Scholarship for funding the first year of my research, and to the Bagnani Graduate scholarship for the support through my first year as well as funding my trip to Quebec to retrieve my samples and helping to cover conference expenses. Also, thanks to Dr. Szpak's NSERC Discovery Grant for funding all additional costs of this research.

Final thanks go out to my family and friends for helping me get out of the house during the course of my thesis. Going dancing, listening to jazz at the Blackhorse Pub, sharing meals, visiting me in Peterborough, and the endless support made the work bearable and the weekends fun. Thanks mom and dad for funding my undergraduate degree, without that help I would have never found the interesting world of science and isotopes for my master's research! Final thanks to my kitty, who of the time of writing these acknowledgements has just recently passed, her companionship brought comfort during the writing process.

# Table of Contents

Abstract.....	II
Keywords.....	II
Acknowledgements.....	III
Table of Contents.....	V
List of Figures.....	VIII
List of Tables.....	XI
1. Introduction.....	1
2. Background.....	7
Bone Chemistry and Mechanics.....	7
Bone Structure.....	7
Bone Mineral.....	8
Type I Collagen.....	9
Remodeling.....	11
Diet and Isotopic Analysis.....	15
Stable Isotopes and Dietary analysis.....	15
Radiocarbon.....	18
Previous Techniques for Measuring Turnover Rate.....	24
Chemical Output.....	24
Bone Labelling.....	26
Osteon Population Density.....	26
Histological Measurements.....	27
Bomb Carbon Dating.....	27
3. The Current State of Knowledge.....	29
Human Studies.....	29
Differences Between Type of Bone.....	32
Differences Between Sex and Age Groups.....	33
Differences Between Ethnicities.....	34
Differences Between Health and Hormones.....	35

Differences in Activity Levels .....	37
Animal Studies .....	38
Summary of Factors Influencing Bone Turnover Rate .....	44
Issues and Caveats .....	44
4. Materials and Methods .....	48
Materials .....	48
Sample Selection and Acquisition .....	48
Sample Challenges.....	51
Supplemental Datasets .....	52
Methods .....	54
Sample Preparations.....	54
Isotope Ratio Mass Spectrometry .....	55
Analytical Uncertainty .....	56
Sample Preparation for AMS Radiocarbon Dating .....	56
Mathematical Model for Estimating Bone Turnover .....	56
Fixed Rate Model.....	57
Decaying Turnover Rate Model.....	60
Hedges et al. (2007) Model .....	63
Data Treatment.....	64
5. Results .....	67
Stable Isotope Compositions of REST[ES] Donors .....	70
Qualitative Assessments of Measured $\Delta^{14}\text{C}$ Values .....	71
Fixed Rate Model .....	72
REST[ES] Samples.....	73
Supplemental Datasets .....	78
Decaying Turnover Rate Model .....	83
REST[ES] Data.....	83
Supplemental Datasets .....	93
Hedges et al. (2007) Model .....	99

6. Discussion .....	101
Variation between skeletal elements .....	101
Does activity level influence turnover? .....	103
Does health influence collagen turnover?.....	106
Does sex influence collagen turnover? .....	108
Does collagen turnover vary within a skeletal element? .....	109
Models of Bone Turnover.....	111
Fixed rate turnover model.....	111
Decaying rate turnover model.....	112
Hedges et al. (2007) model .....	114
Model accuracy .....	115
Conceptualizing bone collagen turnover .....	116
Is remodeling random? .....	116
Collagen as a “Life Average” .....	121
Implications for palaeodietary studies.....	122
Suggestions for future work .....	122
Comparison of results to previous estimates of turnover.....	125
7. Conclusion .....	131
References .....	134
Appendix 1 .....	146
Appendix 2.....	167

## List of Figures

Figure 2.1. Woven bone cross section characterized by random fibril orientation (A) and lamellar bone cross section characterized by uniform fibril orientation (B) .....	10
Figure 2.2. Visualization of BMUs in a sample of bone (A) and their associated age by colour (B) .....	17
Figure 2.3. Northern atmospheric $^{14}\text{C}$ levels over 100 years, highlighting the Suess effect in the early 1900s (A) and the bomb spike around 1963 (B). Data from Graven et al. (2017), Graven et al. (2022), and Hua et al. (2022) .....	24
Figure 4.1. Subsampling pattern for one femur (TEAL 20506) .....	51
Figure 4.2. Atmospheric $\Delta^{14}\text{C}$ spike for the southern hemisphere. Data are from Hua et al. 2019 where eight monitoring stations were averaged .....	53
Figure 4.3. Expected $\Delta^{14}\text{C}$ for each interval for an individual who died in 2009 (dots) and the third order polynomial function fitted to these data. The solid lines highlight the intersect of an expected $\Delta^{14}\text{C}$ of +136.3‰ and an interval of 31 (3.2% annual turnover).....	60
Figure 4.4. The percentage of the total bone turned over from each year since birth for two different decay constants (50% and 10%). An annual fixed rate turnover of 5% is included to highlight the differences between the two rate types.....	62
Figure 4.5. The average annual turnover rate at each age for the femur from the Hedges et al. (2007) paper for both male and female individuals .....	64
Figure 5.01. $\delta^{13}\text{C}$ values of samples from REST[ES] compared to their corresponding C:N ratios .....	71
Figure 5.02. The $\Delta^{14}\text{C}$ values from the different elements that were measured across the seven donors sampled. ....	72
Figure 5.03. The modeled $\Delta^{14}\text{C}$ values for a fixed turnover rate over life in a bone for turnover intervals of up to 60 years with a year of death of 2020, 2021, or 2022 for the northern hemisphere. For example, an individual that died in 2020 having a bone with an interval of 55 years would have a $\Delta^{14}\text{C}$ value of 195‰ and a bone with an interval of 10 years would have a $\Delta^{14}\text{C}$ value of 16‰. The equation of each 3 <sup>rd</sup> order polynomial curve (prior to the plateau) is also displayed and can be used to generate the fixed turnover rate of any sample from these years....	75
Figure 5.04. Fixed turnover rate results for all the donors across the different elements where $n > 2$ . Elements that produced $\Delta^{14}\text{C}$ values that were too high have been excluded. ....	76

Figure 5.05. The expected $\Delta^{14}\text{C}$ values for bone of any turnover interval for a fixed rate turnover in the southern hemisphere for the years of death. The equation of each 3rd order polynomial curve is also displayed and can be used to generate turnover interval and related fixed turnover rate of any sample from these years.....	79
Figure 5.06. Modelled turnover rates using a fixed rate model for the skeletal elements from the Ubelaker et al. (2022) and the Johnstone-Belford et al. (2022) studies.....	80
Figure 5.07. Fixed turnover rate for elements across all datasets grouped by sex .....	81
Figure 5.09. Fixed turnover rates at each age at death for the different skeletal elements and tissue type analysed in all three datasets. Cortical and trabecular samples are grouped by element .....	83
Figure 5.10. Decay constants (a proxy for bone turnover rate with lower decay constants equating to higher turnover rates) for skeletal elements from all REST[ES] donors. ....	88
Figure 5.11. Decay constants across the skeletal elements sampled at REST[ES] grouped by sex. M = male, F = female.....	90
Figure 5.12. Average percentage of bone formed in each decade of life for the seven elements analyzed from the REST[ES] donors.....	91
Figure 5.13. Age 30 average percentage attributed of each decade of life for the seven elements analyzed from the REST[ES] individuals.....	92
Figure 5.14. Modeled $\Delta^{14}\text{C}$ throughout life for two different decay constants for an individual who died at 94 and was born in 1924. DC refers to decay constant .....	94
Figure 5.15. Decay constants (a proxy for bone turnover rate with lower decay constants equating to higher turnover rates) for each of the elements measured in the two previously published southern hemisphere studies (Ubelaker et al. 2022; Johnstone-Belford et al. 2022). ...	95
Figure 5.16. Decay constants (a proxy for bone turnover rate with lower decay constants equating to higher turnover rates) for the different skeletal elements analyzed in the two southern hemisphere datasets (Ubelaker et al. 2022; Johnstone-Belford et al. 2022) by sex. Male groups are signified by M and female groups are signified by F .....	96
Figure 5.17. Average percentage of bone formed in each decade of life for the seven elements analyzed from the individuals analyzed Ubelaker et al. (2022). C refers to cortical tissue .....	98
Figure 5.18. Average percentage of bone formed in each decade of life for the seven elements analyzed from the individuals analyzed Johnstone-Belford et al. (2022). C refers to the cortical and T refers to trabecular .....	98

Figure 5.19. Estimated decay constants (a proxy for bone turnover rate with lower decay constants equating to higher turnover rates) for the skeletal elements sampled from the REST[ES] donors and in the two Southern Hemisphere studies (Ubelaker et al. 2022; Johnstone-Belford et al. 2022). .....99

Figure 5.20. Estimates produced upper and lower expected  $\Delta 14C$  for every REST[ES] donor (boxes) as well as their actual measured  $\Delta 14C$  values (X). Donor 6 had 8 samples from the femur and so the highest and lowest values are indicated with a line indicating where the other values fell .....100

Figure 6.1 . The percentage of a bone sample at death attributed to each age range from the femur (A and B) and vertebra (C and D) from donor 3. Random remodeling is displayed on the left (A and C) and oldest first remodeling is displaying on the right (B and D) ..... 118

Figure 6.2. The percentage of skeletal element sample that would be attributed to each decade of life from the Ulna and the Vertebra of donor 3 across different ages of life. The innermost ring represents the estimated sample composition of the individual at age 20, and the outermost ring represents the composition at death. Data is produced using a ‘random remodeling’ scenario .120

## List of Tables

Table 3.1. Calculated turnover rates for different ages and skeletal elements from Bryant and Loutit (1963) .....	30
Table 3.2. List and description of possible factors that can affect bone collagen turnover rate. ...	46
Table 4.1. Donor information for the individuals sampled for this research from the REST[ES] facility in Quebec, Canada.....	48
Table 4.2. Sample numbers and the associated donor and element .....	49
Table 4.3. The model used by Hedges et al. (2007) with varying turnover rates based on sex and age .....	63
Table 5.01. Calibrated isotopic and elemental data for all bone collagen samples analyzed in this study. P.S.= pubic symphysis, I.C. = iliac crest, I.P.R= ishiopubic ramus, G.S.N.= greater sciatic notch.....	67
Table 5.02. Results of Dunn’s post-hoc test ( $p$ values) for comparisons of $\Delta^{14}\text{C}$ values among the skeletal elements analyzed. Statistically significant differences ( $p<0.05$ ) are indicated in red.....	72
Table 5.03. . Description of the source of each sample and the estimated fixed turnover rate data. Values are ordered by age at death first and then from lowest to highest annual turnover percent. Samples that had $\Delta^{14}\text{C}$ values that were too high to fit into a fixed rate turnover are indicated with N/A .....	73
Table 5.04. Results of Dunn’s post-hoc test ( $p$ values) for differences in estimated turnover rate based on a fixed rate model between REST[ES] donor elements. Highlighted cells indicate that $p<0.05$ . .....	76
Table 5.05. Dunns post-hoc test ( $p$ values) for differences between the fixed turnover rates for the elements sampled in the supplementary datasets. Statistically significant differences ( $p<0.05$ ) are indicated in red.....	80
Table 5.06. The measured $\Delta^{14}\text{C}$ content from the skeletal elements of each REST[ES] donor, along with the estimated decay constants and the percentages of bone that was formed in each decade of life. DC = Decay constant, as a percent. N/A indicates that the donor was not alive for the specified decade .....	84
Table 5.07. Dunn’s post-hoc test ( $p$ values) for difference in estimated decay constants between element groups using a decaying turnover model. Statistically significant differences ( $p<0.05$ ) are highlighted in red. ....	88
Table 5.08. The average percent of collagen that was produced in each decade of life at death, across the elements analyzed. Decades from which the majority of bone was produced are highlighted in green for each element.....	90

Table 5.09. The average percent of collagen that was produced in five year intervals up until age 30, across the elements analyzed. Values were calculated using the same decay constants that produced the data in Table 5.08. Periods from which the majority of bone collagen was synthesized for each element from are highlighted in green .....	91
Table 5.10. Results of Dunn's post-hoc tests ( $p$ values) for differences in decay constants for each skeletal element group. Statistically significant differences ( $p < 0.05$ ) are indicated in red .....	95
Table 5.11. The average percent of collagen produced in each decade of life at the time of death, across the elements analyzed for the individuals from Ubelaker et al (2022) .....	97
Table 5.12. The average percent of collagen produced in each decade of life at the time of death, across the elements analyzed for the individuals from Johnstone-Belford et al. (2022). C refers to the cortical and T refers to trabecular .....	97
Table 6.1. Qualitative order of skeletal elements from slowest remodeling to fastest bone collagen remodeling.....	102
Table 6.2. The relative confidence in estimated annual turnover rates for bone collagen for different types of bones when using a decaying turnover rate model based on $^{14}\text{C}$ data derived from old individuals.....	114
Table 6.3. The percentage and standard deviation of skeletal element sample that would be attributed to each decade of life from the ulna of donor 3 across different ages of life .....	119
Table 6.4. The percentage and standard deviation of skeletal element sample that would be attributed to each decade of life from the vertebra of donor 3 across different ages of life .....	120
Table 6.5. Average annual turnover rate (%) from age 35-85 in this study using the decay rate model and the study by Bryant and Loutit (1963) for the elements which were measured in both studies. ....	129

## **Chapter 1: Introduction**

In the field of archaeology, skeletal remains serve as invaluable time capsules, offering insights into ancient human populations. Beyond being mere remnants, bones function as storytellers, providing direct glimpses into the lives, environments, diets, and cultural customs of past human populations. While artifacts hint at human-made objects and their potential uses, skeletal remains offer a unique, intimate narrative, shedding light on individual lives within a larger population. Skeletal remains can craft narratives that describe lived experiences of ancient peoples. On a macro scale, features and differences on a bone can tell someone about an individual's sex, appearance, health, and even their typical labour habits (Ortner, 2011). On a micro scale, variations in chemical and isotopic compositions that exist between the bones of people have enabled archaeologists to discern the impact of environments on human populations, distinguish societal differences among classes, identify specialized roles within communities, trace patterns of migration and mobility, and unveil further information about the past (DeNiro, 1987; Makarewicz and Sealy 2015). The analysis of bone on this micro scale is of interest in this thesis.

Bone serves as a reservoir of historical information owing to its biological composition. Collagen is of particular importance for archaeology, as this protein exhibits remarkable preservation capabilities over extended periods (Kucharz, 1992; e.g., Rey-Iglesia et al., 2019, Peters et al., 2023). It is composed of compounds derived from an individual's diet (Ambrose and Norr, 1993) and undergoes continual dissolution and regeneration with fresh elements throughout one's life—a phenomenon termed remodeling (Safadi et al. 2009). As archaeological scientists rely on collagen to deduce crucial life history details, understanding the formation period of this protein is pivotal. This period signifies the duration during which different elements assimilate

into an individual's body via diet while replacing past elements and evidence of old diet. Remodelling involves replacement of old collagen with new collagen and is different from new formation of collagen alone. Bone is assumed to change and remodel, even at a very slow rate for individuals of advanced age, so knowing how turnover rates vary throughout life can provide an understanding of the relative percentages of a sample of bone that were formed during each part of life. For instance, if 100% of bone was made in the last 20 years of life in a 50 year old, the bone is made of tissue and elements from age 30 to age 50. This total period of bone formation is sometimes termed the turnover interval. The turnover rate denotes the percent of collagen that will be dissolved and replaced with new collagen made of new elements, typically discussed on an annual level. This concept is significant for researchers aiming to accurately link bone samples to ancient life histories, underscoring the importance of time as a critical factor demanding consideration in archaeological interpretations.

One of the significant insights revealed by bones involves the dietary habits of ancient populations through stable isotopic analysis. Advancements in technology have allowed for different ratios of carbon and nitrogen isotopes to be measured in increasingly small samples of bone (Fourel et al., 2014; Leichliter et al., 2021). These ratios offer insights into food sources, agricultural practices, social status, and the relative importance of various food types (DeNiro and Epstein, 1978; Schoeninger and DeNiro, 1984). These insights are of major importance in archaeology as the production and consumption of food forms the cornerstone for the development of cities and empires (Reed, 2021). Analyzing diet can tell archaeologists much more about the past than merely what food was consumed. Since isotopic analysis provides insight into variation in diet at the level of the individual rather than the site or population, these data provide highly nuanced understandings of life in the past, encompassing societal structures

and historical transformations. Therefore, in the same way that it is important to understand the temporal context of site occupations through chronometric dating, it is crucial to understand exactly what period of time in the life history is represented in an isotopic analysis of bone to gain an accurate understanding of ancient contexts.

In studies that perform stable isotope analysis on bone collagen, bone turnover rate is often briefly mentioned without much thought being given to the accuracy of the statements. There has been a great deal of emphasis on other important underlying principles of paleodietary reconstruction, such as determining trophic discrimination factors (O'Connell et al., 2001; O'Connell et al., 2012), or determining the routing of different macronutrients to collagen carbon (Jim et al., 2004; Ambrose and Norr, 1993; Ambrose, 2000), but turnover rates, which are also critical for accurate interpretations remain very understudied and are associated with many poorly tested assumptions. There is an important difference between assessing the diet of an individual over the last year of their life and assessing their diet across their whole life. In archaeology, a study by Hedges et al (2007) is largely relied on as *the* source the turnover interval for all bone, either explicitly or implicitly. This study assessed turnover in the midshaft of a femur through  $^{14}\text{C}$  bomb peak dating and these authors concluded that the turnover interval for the femur of an adult human will be more than 10 years of life, and as much as 30 years for older individuals. While this study had a strong experimental design, it is frequently cited in an uncritical manner, extrapolating, or misrepresenting the findings where the results of Hedges et al. (2007) do not apply.

A random search of studies that cite this paper yields a variety of articles that do not analyze the midshaft of the femur, instead measuring the isotopic composition of some other skeletal element. Soncin et al. (2023) state that bone collagen has a turnover interval of about 10

years, citing Hedges et al. (2007), and yet only used bone collagen from rib and tarsal bones. Quinn et al. (2021) analyzed ribs, noting that it has a turnover interval of roughly two to five years, citing Hedges et al. (2007) as the source of this information. Gregoricka and Ullinger (2022) cite Hedges et al. (2007), claiming that ribs have approximately a 10 year turnover interval and femora have up to a 30 year interval, and yet uses various other long bones as well as ribs. While I am not implying that the results of these studies are incorrect due to these assumptions, it is apparent that there is some confusion in the field about what period of time is represented by a sample of bone. Intervals are suggested for different bones that have not been directly studied and for which there is no experimentally quantified turnover rate. There is, therefore, a critical and urgent need for better literature discussing and identifying bone turnover rates, especially as the number of studies employing stable isotope analysis of archaeological materials has grown exponentially in the last few decades.

Apart from the study conducted by Hedges et al. (2007), limited research exists detailing bone turnover from a quantitative perspective across skeletal elements and species. Diverse techniques have been utilized with varying effectiveness to ascertain turnover rates. Challenges persist in distinguishing overall bone turnover from specific intervals, and in quantitatively establishing turnover rates beyond mere classification as relatively 'fast' or 'slow' bones (e.g. Fahy et al., 2017) . A lack of consolidated and accessible turnover rate resources hampers archaeologists' ability to conduct comprehensive analyses using bone collagen.

It is the purpose of this thesis to alleviate this problem in archaeology by assessing the turnover rates across the human skeleton to establish the exact percentage of bone that can be attributed to any year of life. I will utilize a somewhat novel technique that has been employed in fields such as forensic science and environmental science called bomb-carbon dating (e.g.

Calcagnile et al. 2013; Uno et al. 2013). This approach capitalizes on an atmospheric surge in  $^{14}\text{C}$  levels caused by thermonuclear weapons testing that has gradually been dampened due to the combustion of fossil fuels that are highly depleted in  $^{14}\text{C}$  (Carbone et al., 2023). This technique contrasts bone collagen radiocarbon measurements against this curve to gauge the annual introduction of radiocarbon to the bone, thereby assessing turnover rates. I hypothesized that there would be differences not only between different skeletal elements, but also within skeletal elements. While this technique is expected to provide turnover rates across life within a bone, it will also illuminate how distinct lifestyle factors can influence turnover rates and the complexities inherent in determining precise intervals.

Chapter 2 of this thesis will delve deeper into the foundational aspects of both bone biology and isotopic analysis. This exploration aims to provide the reader with a comprehensive understanding of collagen's role within bones, the mechanisms of bone remodeling, and the various factors influencing this process. It will introduce stable isotope analysis and radiocarbon analysis while elucidating how knowledge of turnover rates influences dietary assessments. Additionally, this chapter will examine previous techniques utilized to assess bone collagen turnover rates, highlighting their limitations and underscoring how bomb-carbon dating can address these gaps. Chapter 3 will comprise a literature review encompassing animal and human studies related to bone turnover rates. This extensive review will delineate the existing knowledge base, emphasizing both well-supported findings and areas with insufficient evidence. This chapter aims to underscore the significance of the research on bone collagen turnover rates, summarizing potential influences that can aid in interpretation of isotopic data. Chapter 4 will detail the materials and methods utilized in this thesis. It will contextualize the samples, outlining sample types, donor information, and the employed sampling strategy. Additionally, it will

discuss the laboratory techniques employed to extract collagen from bones, analyze stable isotopes and radiocarbon content of the collagen. The chapter will describe the methods used to convert radiocarbon ratios into turnover rates and present different models used for assessing these rates. Chapter 5 will present the results of stable and  $^{14}\text{C}$  isotope ratio analyses. This chapter will introduce two additional datasets, enhancing the sample size of bone samples and skeletal elements measured. It will qualitatively assess the radiocarbon results and employ fixed-rate and decaying turnover rate models. These results will be compared to the model used in the Hedges et al. (2007) paper, showcasing variability in turnover rates among and within skeletal elements. Chapter 6 will discuss these results in detail to better situate the results within the known literature. The differences between the three models as well as the three datasets will be discussed, as well as how potential influence on turnover rate may have influenced the results that we see. Complications with the past usage of turnover interval and providing exact conclusions will also be discussed, as well as how the results will fit into stable isotope studies. It will also present the results in a way that future studies can pull from when discussing bone turnover rate in the future. Finally, chapter 7 will emphasize the research's significance, stressing the necessity of continued exploration in this field in future studies.

## **Chapter 2: Background**

The study of bone, both as an organ and a tissue, is a very complex topic. Recent technical innovations and a long history of study influence the current state of our knowledge, but many factors related to bone are still not well understood. In this thesis, when referencing bone as a tissue, I will use the word “bone” and when referencing bone as an organ (as in a full femur, mandible, etc.) I will use the term “skeletal element”. This chapter will detail what bone is, in terms of both its form and function, as well as methods commonly used to study the growth and development of bone.

### **2.1 Bone Chemistry and Mechanics**

Bone is a dynamic and living tissue with intricate processes governing its formation and maintenance. It comprises various constituent parts, each possessing distinct properties that significantly influence the functioning of bones. To gain a comprehensive understanding of the turnover rate, which refers to the time taken for a unit of bone to replace itself with new elements, it is essential to delve into the inner workings of bone. In the subsequent section, I will explore this topic in detail.

#### *2.1.1 Bone Structure*

Bone is a vital connective tissue and organ that provides essential support and structure to the body. It is comprised of four key components: inorganic minerals, organic material, lipids, and water. The primary constituents of bone are the organic and inorganic elements, collectively known as the bone matrix (Hill, 1998). The bulk of bone is made of mineralized collagen fibrils, which are thread shaped tissues 10-100 nanometers in size (Weiner and Wagner, 1998).

Approximately 85%–95% of the organic portion of bone is composed of type I collagen

(Kucharz, 1992), which allows for the bone to hold up under tension. The mineral component of bone confers rigidity to the structure of the bone and acts as an ion reservoir (Burr, 2019; Glimcher, 1998). Osteocytes are the cells that makes up the structure of bone, however osteoclasts and osteoblasts also constitute a sizable portion of its cellular composition. Osteoblasts are responsible for producing and regulating the bone matrix, while osteoclasts play a role in removing and dissolving this matrix. There exists a delicate balance between the activities of these two cell types to maintain consistent and ideal bone mass (Hill, 1998; Frost 1987). There are two types of osteons that form within bone, primary osteons which form as a result of rapid growth, and secondary osteons which form as a result of bone being reabsorbed and replaced (Burr, 2019). The bone matrix, consisting of collagen fibers interspersed with minerals, can be categorized into two structural types: cortical and trabecular (Burr, 2019). Cortical bone, which constitutes the majority of bone mass, is dense and primarily responsible for bearing loads. Trabecular bone, characterized by its porous and spongy nature, functions to reduce stress on the bone and absorb shock (Hill, 1998; Burr, 2019; Huiskes et al., 2000). The organization of these structural types is determined by the functional requirements and location of the bone (Burr, 2019).

### *2.1.2 Bone Mineral*

The mineral phase of bone exists in various compounds and phases, but it is not as well understood compared to other components of bone. Bioapatite, which constitutes the mineral component of bone, occupies the gaps within collagen fibrils and is initially deposited as very small calcium phosphate crystals. Due to a high degree of substitution, it can also be deposited as calcium carbonate (Weiner and Wagner 1998; Burr 2019). The deposition of mineral is facilitated by specific collagen sites that promote crystal precipitation. This is why collagen must form

before the mineral component in bone (Farlay and Boivin, 2012; Safadi et al., 2009). This initial deposition process is known as primary deposition and typically takes approximately three weeks per small area of bone called a basic multicellular unit (BMU). Following primary deposition, secondary mineralization occurs as the calcium carbonate is lost, and the bioapatite crystals continue to grow and expand within the bone (Farlay and Boivin, 2012). This mineralization process can take more than a year to complete. The gradual growth of crystals over time is responsible for the link between the size of mineral crystals within bone and the age of the tissue itself (Burr, 2019). Once mineralization is complete, the minerals exist within bone as calcium hydroxyapatite. The entire process of mineralization in bone is not very well defined, however it is thought that the process is mediated by non-collagenous proteins that also exist within bone such as osteocalcin (Glimcher, 1998; Safadi et al., 2009). Over time, the water content within bone decreases, promoting further mineralization. This leads to the development of dense and stiff bones. While mineralization provides essential supportive rigidity to bones, excessive dryness can make bones more susceptible to fractures (Burr, 2019; Farlay and Boivin, 2012). This highlights the critical role of regulating bone turnover. Incomplete mineralization in young bones can result in reduced strength, while over-mineralization in older bones can lead to brittleness. Consequently, the density and overall health of bones are closely related to the tissue's age.

### *2.1.3 Type I Collagen*

Type I collagen is an important component of bone and is also found in many other organs in the body as it is the most widely distributed and abundant structural protein among animals (Kucharz, 1992). In bone, collagen is made up of fibrils that are interspersed with bioapatite mineral. Collagen is made within cells first as tropocollagen and then is deposited into bone as

fibrils, which are sheets about 80-100 nm in diameter (Weiner and Wagner, 1998). These fibrils are arranged differently in two different classes of bone tissue: woven or lamellar (figure 2.1). Woven bone is defined by random orientation of fibrils and is common in areas of rapid growth. Lamellar bone fibres are organized into parallel lines and is formed only on pre-existing bones and has a much slower deposition (Safadi et al., 2009, Kucharz, 1992).

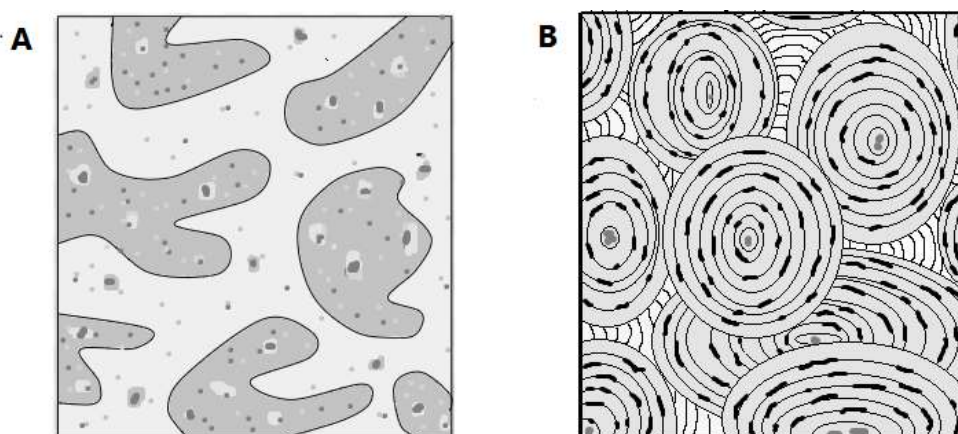


**Figure 2.1.** Woven bone cross section characterized by random fibril orientation (A) and lamellar bone cross section characterized by uniform fibril orientation (B)

Collagen is composed of repeating  $\alpha$ -helices. The amino acids contain various arrangements of carbon, hydrogen, oxygen, nitrogen, and sulfur that are introduced to the body through the digestive system (Kucharz, 1992). Therefore, the chemical composition of collagen is the sum of the chemical composition of all of the constituent amino acids. Each type I collagen fibril has three interwoven  $\alpha$ -chains of about 1000 amino acids each, that together form a right-handed tight triple helix. (Weiner and Wagner, 1998) The tightness of the triple helix occurs because of the repetitive Gly-X-Y pattern that composes the chain. Glycine (Gly) is a very small amino acid, and so having it at every third position reduces the size of each chain and allows it to be tightly coiled (Okuyama, 2008). The X-Y in the pattern can be any other amino acid but is very often proline (X) and hydroxyproline (Y). The high amount of hydroxyproline is unique to collagen and contributes to its stability (Viguet-Carrin et al, 2006). This predictable amount of

each amino acid allows for the percent of elements in a sample of collagen to be anticipated in order to assess collagen purity. For instance, the percent of carbon and nitrogen within a pure collagen sample should be  $41.91 \pm 0.39\%$  and  $15.40 \pm 0.20\%$  respectively (Guiry and Szpak, 2020). If a sample of collagen has a different %C and %N, then it contains more than just collagen and may contain some amount of lipids, non-collagenous proteins, glycoproteins, or residual mineral (Wilson and Szpak, 2022). Once collagen fibrils form in bone, they are stabilized with collagen crosslinks. This is a posttranslational modification through a lysyl oxidase (LOX) reaction which links the fibrils to each other (Hudson et al., 2020). This process is still being researched but it is linked to bone strength and rigidity as well as bone turnover rate (Safadi et al., 2009). Generally, more crosslinks indicates that osteoclast activity is relatively low and results in rigid but brittle bones (Safadi et al., 2009). These crosslinks contribute to the insoluble nature of bone collagen as an increase in LOX has been linked to higher amounts of insoluble collagen (Kucharz, 1992).

#### *2.1.4 Remodelling*

Bone is a dynamic tissue and is constantly replacing itself through the process of remodelling, even after the skeleton is fully grown (Hill, 1998). Remodelling is the process of old bone being reabsorbed and new bone being created, and this happens with both mineral and organic fractions of bone somewhat concurrently (Burr 2019). Each remodelling event occurs within the bone's BMUs (Frost, 1969), which are roughly  $0.05\text{mm}^3$  of bone (Hollinger, 2005). The speed at which these units are remodelled for the entire bone is called the bone turnover rate. The goal of remodelling is theorized to be keeping bone at the optimal volume and strain resistance at any point. By balancing the need for resistant yet strong bones, injury to the bone is reduced (Frost 1987). Remodelling and bone turnover generally refer to the same activity,

however remodelling is more frequently used to describe the process at a cellular or microscopic level, with turnover referring to macroscopic or organ level sum of remodelling (Vaananen, 1993).

Bone turnover rate can be studied at multiple levels (microscopically, macroscopically, organ level), as there are different influences on remodelling at each level. Since bone turnover rate for any skeletal element is the product of thousands of individual BMU's turnover rates, it is important to understand how turnover functions at a cellular level before assessing remodelling at higher levels. These processes can then be applied to better understand the factors that affect the remodelling at the tissue level (i.e., in a sample of a skeletal element) to the level of the remodelling of the whole skeletal element. Remodelling rates can also vary among skeletal elements, and this is not surprising, as Wolff's Law states that differences in the form and function of a bone are correlated with differences in bone architecture and cellular mechanics (Wolff, 1882; Safadi et al., 2009), and each skeletal element has its own unique function in the body.

At the cellular level, bone remodelling is controlled mainly by osteoclasts and osteoblasts. Osteoclasts work to break down and resorb the bone by creating a low pH environment and then producing enzymes which break down the organic matrix (Teitelbaum, 2000). This resorption process in humans takes about 10 days to complete within a single BMU (Safadi et al., 2009). Osteoclasts stimulate two enzymes which dissolve both the organic portion and the mineral portions of bone in the same stage. Osteoblasts create and lay down type I collagen as well as proteoglycans. These cells are also responsible for the ongoing mineralization of bone matrix after the organic portion of bone is created (Blair et al., 2017). This formation process takes approximately three months to complete within a BMU (Safadi et al., 2009; Hill 1998). Based on

the functions of osteoclasts and osteoblasts, both the collagen and mineral portion of bone are replaced during the remodelling process and likely have similar turnover rates. Bone mineral may turn over slightly more slowly than bone collagen due to continuous mineralization over time. It has been estimated that at any time, roughly 20% of cortical bone BMUs are undergoing this remodelling process and occur separate from other BMU remodelling events (Safadi et al., 2009; Hill, 1998), with humans making millions of new BMU's annually (Frost, 1994). The activity of osteoclasts and osteoblasts are interrelated. When osteoclasts are activated to dissolve bone and its components, this triggers the formation of osteoblasts, which then create new bone with fresh elements (Parfitt, 1982). This coupling happens because the osteoclastic process leads to the release of osteoblast-stimulating growth factors like IGF I and II and TGF- $\beta$ . (Pfeilschifter and Mundy, 1987; Safadi et al., 2009; Vaananen, 1993). Osteoblasts indirectly create proteins that are required for the formation of osteoclast precursors, thus creating a cycling of these cells (Blair et al., 2017; Safadi et al., 2009). It is still unknown whether the activation of these two cells start at the same time or if osteoblasts only activate after bone has undergone the osteoclastic phase (Hill, 1998). The number of BMUs in a bone entering the osteoblastic bone formation phase is called the activation frequency (Charles et al., 1987; Ericksen et al., 1986), and the period of time it takes for a single BMU to be completely replaced via these cells, the bone formation period, is denoted by  $\sigma$  (Frost 1969). The events that stimulate the start of a remodelling cycle vary, ranging from hormonal changes to mechanical stress (Vaananen, 1993).

Remodelling can also be examined from the perspective of bone as an organ, where turnover rate is more likely controlled by the mechanics and form of the bone rather than specific cellular processes. The rate of turnover for samples of collagen will not necessarily just be equal to  $\Sigma\sigma$  for every BMU encapsulated in a sample, as each  $\sigma$  is not independent and can occur

simultaneously or overlap. However, the turnover rate is equal to the time it has taken for every individual BMU to have replaced itself at least once. The length of time it has taken for the BMU to be fully replaced can be called the turnover interval. The turnover rate can either remain the same throughout life (fixed rate) or can change according to life stage and age. Stages of life such as infancy, childhood (4-10), adolescence (10-20), growth cessation (20-30), and adulthood into old age can be associated with variable or fluctuating turnover rates. It is important to understand that the turnover interval is not simply the same period that it would take to achieve 100% replacement of the bone. An annual turnover of 5% would not simply take 20 years as it is assumed that each remodelling event would target 5% of a whole sample of BMUs and not 5% of BMUs that have not yet turned over within the interval (Katsimbri, 2017).

The rate also relies on the properties of the sample taken, such as which skeletal element was sampled as well as the location of the sample within the bone. Bone tissue can be either trabecular or cortical, and a sample of bone may consist of either of these or a mixture of both, and this can also influence the rate of remodelling for that particular sample. As well, different locations in a skeletal element (i.e., proximal, anterior, medial) may have different regulations of osteoblasts and osteoclasts, and this is assumed based on different densities of bone matrix in these different areas (Lai et al., 2005; O'Connor and Lanyon, 1982; Skedro et al., 2003). One study found that the pericortical region in skeletal elements of sheep have higher density and therefore slower turnover rates when compared to bone closer to the medullary cavity (O'Connor and Lanyon 1982). In humans, it is believed that the posterior section of the tibia is the densest, followed by medial and lateral sections, with the anterior section being the least dense (Lai et al. 2005). In some animals, proximal bone is more dense than distal portions of bone (Skedro et al. 2003), but the reverse has also been observed in other animals (Holdaway et al. 2011), and these

differences are likely due to biomechanical requirements for the skeletal elements, which vary among species. As will be discussed later, muscle attachments and strain in a bone can also affect properties of the bone and could affect turnover rate. Therefore, on a larger scale, assessments of bone remodelling must be paired with detailed information about where the section of bone originated and must recognize that some averaging of  $\sigma$  for each BMU included in a sample has occurred. This in no way makes larger scale remodelling rates unreliable, however it is important to consider these factors when addressing larger sample level turnover rates of bone.

## **2.2 Diet and Isotopic Analysis**

The elements and mechanics of bone physiology and chemistry are crucial for contextualizing chemical analyses that use bone as an analytical substrate. For example, the foods that animals consume contribute most of the elements that eventually constitute the skeleton. The stable isotope compositions of these elements are widely used in archaeological studies of human diet, health, and life history. Isotopes are atoms that have the same number of protons but differ in their number of neutrons. Stable isotopes are those atoms that do not undergo radioactive decay, whereas radioactive isotopes (radioisotopes) decay into other elements after some amount of time. The following subsections will discuss these two classes of isotopes as they relate to this project.

### *2.2.1 Stable Isotopes and Dietary Analysis*

Stable isotopes are frequently used by researchers to answer questions about the past. A common chemical element used in dietary analysis that has multiple stable isotopes is carbon. Carbon can exist as either  $^{12}\text{C}$  (98.9% of carbon on Earth) or  $^{13}\text{C}$  (1.1% of carbon on Earth) in stable form, as well as the radioactive isotope  $^{14}\text{C}$  (~1 ppt). All forms of carbon enter animals

through the digestive system and are deposited into the tissues that are actively forming or reforming and need carbon (i.e., all organic compounds). Different kinds of food have different ratios of  $^{13}\text{C}$  to  $^{12}\text{C}$ , and different foods can be identified through isotopic analysis if they are isotopically distinct (DeNiro and Epstein, 1978). Further, there is a predictable relationship between the values of the foods and the values of the consumer of the foods. Therefore, if plants such as maize, which have a higher ratio of  $^{13}\text{C}$  to  $^{12}\text{C}$  (reported relative to an international standard in ‰ as  $\delta^{13}\text{C}$ ) than other plants like wheat, individuals who consume more maize will have a higher  $\delta^{13}\text{C}$  compared to those that eat more wheat. Further, marine species tend to also have a higher  $\delta^{13}\text{C}$  than terrestrial species, and therefore it can also be determined if the individual consumed more terrestrial or marine food sources (Schoeninger and DeNiro, 1984). Food sources like maize and marine foods can be distinguished from each other using a second stable isotope system, nitrogen.

Nitrogen isotopes are reported as the ratio of  $^{15}\text{N}$  to  $^{14}\text{N}$  (reported relative to an international standard in ‰ as  $\delta^{15}\text{N}$ ). Higher  $\delta^{15}\text{N}$  values are associated with higher trophic positions (DeNiro and Epstein, 1981; Minagawa and Wada, 1984), and therefore a plant will have a lower  $\delta^{15}\text{N}$  value than a herbivore. By measuring isotopic composition of tissues like bone collagen, which can preserve for tens of thousands of years (e.g., Rey-Iglesia et al., 2019), the diet of an individual can be inferred. This application is also especially useful to archaeologists, as in many cases, bone is all that remains, and in cases where there is no written record of a population's diet, the analysis of bone collagen gives insight into what kind of food people were eating (Makarewicz and Sealy, 2015)

The process of chemical elements entering bone tissue relies on the process of remodelling in bone. When osteoclasts break down a BMU, the chemical elements (C, H, O, N,

S) in the collagen are broken down by the body and excreted. New elements from food that are broken down by the digestive system are then synthesized into collagen and deposited in the BMU. The relationship between the sample's isotopic composition and an individual's diet and life history depends on the timing of the deposition of chemical elements. In other words, the stable isotope composition of bone collagen reflects dietary intake over a specific period. For instance, if the sample includes BMUs that have never remodelled as well as those that remodelled throughout the individual's life up until death, it will represent the integrated diet from early life (when the bone formed) all the way through to the end of life. On the other hand, if the oldest BMUs were deposited quickly during a stage of life like puberty, and very few BMUs remodelled since that point until death, the diet reflected would be more representative of the diet around the time of puberty rather than an average diet from puberty until death. Therefore, it is essential to know the remodelling rate for each skeletal element under study, as this knowledge helps determine the specific period captured in dietary analysis.

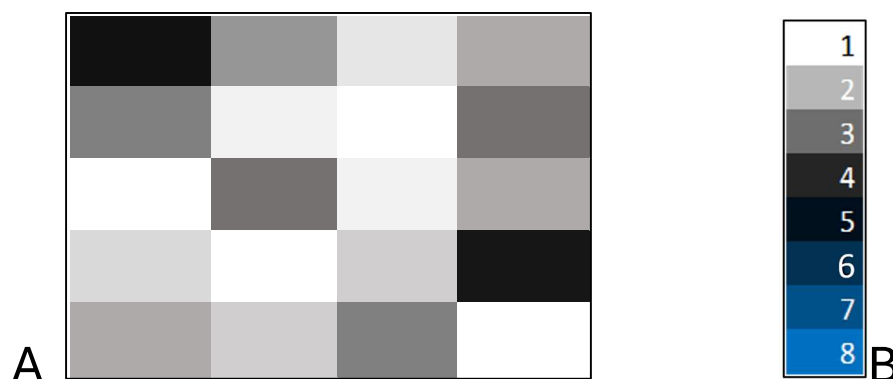


**Figure 2.2.** Visualization of BMUs in a sample of bone (A) and their associated age by colour (B)

Figure 2.2 visualizes bone turnover, where box A represents a sampled section of bone, and each box within A denotes a single BMU. The colour of each BMU indicates its age in years. As

each BMU ages, it goes from white to grey to black and then to blue. Since there are no BMUs older than five years old in box A, this whole sample has a turnover interval of five years, as any BMU that was deposited six or more years prior has been remodelled. It is also possible for samples to be biased based on which BMUs were captured in a sample, as a smaller sample from the bottom left corner of A would only include 3-4 year-old BMUs, and therefore that section would have a smaller turnover interval than the whole sample of bone in box A. However, since each BMU is only  $0.05 \text{ mm}^3$  of bone, there is an assumed averaging effect within a sample of bone.

In summary, bone remodelling is a critical process that influences the stable isotope composition of bone collagen and allows researchers to infer an individual's dietary intake and life history over certain periods. Understanding the remodelling rate for each skeletal element is essential to accurately interpret stable isotope results and gain insights into an individual's diet and life habits.

### *2.2.2 Radiocarbon*

The only naturally occurring radioactive isotope of carbon is  $^{14}\text{C}$ , also called radiocarbon, and it makes up less than 1 ppt of all carbon on Earth. For comparison, the abundance of the rarer stable isotope of carbon ( $^{13}\text{C}$ ) expressed in ppt is  $1.11 \times 10^{10}$ . Typically, radiocarbon is used to determine the geological age of organic material. This is possible due to  $^{14}\text{C}$  decaying into  $^{14}\text{N}$  over time at a known rate. After an organism dies, it is no longer in equilibrium with the environment and no new  $^{14}\text{C}$  will be added through new tissue synthesis.  $^{14}\text{C}$  decay has a half-life of 5,730 years, and can be used to date up to ~50,000 years before present, with anything older no longer having enough  $^{14}\text{C}$  to be accurately quantified (a.k.a. “carbon-dead” material)

(Godwin, 1962; Taylor, 2016).  $^{14}\text{C}$  is produced mainly in nature by energetic radiation of  $^{14}\text{N}$  in the atmosphere from cosmic-ray neutrons. These neutrons collide with the  $^{14}\text{N}$  in the air, as nitrogen (as  $\text{N}_2$ ) makes up 78% of the atmosphere. The collision causes  $^{14}\text{N}$  to gain a proton and become  $^{14}\text{C}$  (Lingenfelter, 1963). The  $^{14}\text{C}$  is quickly oxidized to  $^{14}\text{CO}$  and then  $^{14}\text{CO}_2$  in the atmosphere and mixed thoroughly so that the atmospheric levels of  $^{14}\text{C}$  are generally consistent throughout the northern and southern hemispheres, respectively. Once they reach Earth's surface, these isotopes then enter the carbon cycle and are distributed evenly, fully mixing in a matter of weeks (Bronk, 2008). The sun's energy ensures that there is a constant production of  $^{14}\text{C}$  which offsets any that is lost in the decay process (Taylor, 2016). The amount of  $^{14}\text{C}$  in all organic materials is generally equal to the atmospheric level at the time the organic compounds are synthesized. However, if tissues are formed at different times, they may have different amounts of  $^{14}\text{C}$ . Tissues that are fast forming will be similar to current levels of atmospheric radiocarbon, whereas tissues that contain old carbon will reflect the atmospheric radiocarbon at the time of the tissue formation (Taylor, 2016). This can be visualized, for example, with tree rings, with rings reflecting the atmospheric levels when they formed. This difference between tissues has been noted in the past, such as the slight  $^{14}\text{C}$  differences that were measured between the skin and bone of the Tyrolean Iceman that were attributed to differences in the turnover rate of each tissue (Bonani et al., 1992).

There are a few different ways in which the amount of  $^{14}\text{C}$  in a sample or in the atmosphere is reported. One way that is typically used in geochemical studies is called *percent modern* (pM), which compares the amount of  $^{14}\text{C}$  in a sample directly to an absolute international standard and expressed the  $^{14}\text{C}$  content of the sample in comparison to the 'modern' (1950 AD) amount as a percentage (Stuiver and Polach, 1977). In a similar way, this can be reported as Fm or  $F^{14}\text{C}$ ,

which means *Fraction Modern Carbon*, and is similar to pM, except it accounts for modern correction factors that need to be made in more recent samples (Reimer et al. 2004). Another reporting method is  $\delta^{14}\text{C}$  or  $\Delta^{14}\text{C}$ , which are equal to  $1000(\text{Fm}-1)$ , reported in ‰.  $\Delta^{14}\text{C}$  will be used for reporting measurements of  $^{14}\text{C}$  in this thesis.

Many materials of known age have been analysed by numerous laboratories over the years to measure how much  $^{14}\text{C}$  can be expected in a sample for any year (Reimer et al 2009; Reimer et al. 2013). This is typically done with tree rings, as dendrochronology allows for the age of the trees to be known before analysis. It can also be done with corals but with a higher degree of uncertainty (Taylor, 2016). Originally, it was thought that bone was not a valid material for radiocarbon dating as it often initially yielded dates that were incorrect (Sinex and Faris, 1959). This was due to whole bone (rather than purified collagen) being dated, which included many different components (e.g., collagen and carbonate) and was subject to a higher degree of contamination. Through isolating the primary organic component of bone (high molecular weight fragments of collagen), the data generated by radiocarbon analysis is much more reliable as it is a pure material since the collagen isolation process involves steps which help to remove potential contaminants (Brown et al. 1988; Taylor, 2016; Longin, 1971). Outside of sample purity issues, there are a handful of environmental factors that also effect the reliability of radiocarbon analysis.

Generally, terrestrial organisms equally approximate the  $^{14}\text{C}$  content of the atmosphere within the northern or southern hemisphere regardless of their precise location (Kromer et al., 2001). However, organisms in the ocean are depleted in  $^{14}\text{C}$  compared to terrestrial environments, and this is known as the marine reservoir effect (Alves et al., 2018). This is caused by the exchange of newly created  $^{14}\text{C}$  only occurring at the surface of the oceans mostly in polar

zones. The ocean does not produce any new  $^{14}\text{C}$ , but radioactive decay still occurs, meaning that there will always be less  $^{14}\text{C}$  in the ocean than in the atmosphere. This is especially true since the surface ocean is a larger  $\text{CO}_2$  reservoir than the atmosphere and the intermediate/deep ocean contains  $50\times$  the amount of  $\text{CO}_2$  as the surface ocean (Sigman and Boyle, 2000). This process causes variation in the  $^{14}\text{C}$  content of marine organisms to be related to factors like water temperature rather than atmospheric  $^{14}\text{C}$  levels, which prevents accurate radiocarbon dating on these organisms (Dyke et al., 2019; Reimer 2014). This depletion can affect the  $^{14}\text{C}$  content of humans that consume marine resources, as their tissues may also become depleted in  $^{14}\text{C}$  and therefore not be at equilibrium with the atmosphere (Ascough et al., 2005; Craig et al., 2013). This difference in  $^{14}\text{C}$  can affect any study that is trying to relate atmospheric levels of  $^{14}\text{C}$  with the amount found in a sample, which is an important step of converting a radiocarbon age to a calendar age (i.e., calibration) (Hedges, 2007). Fortunately, the consumption of marine species can easily be assessed with stable isotope analysis.

Increases in fossil fuel production has caused a large amount of  $\text{CO}_2$  depleted in  $^{14}\text{C}$  to be released into the atmosphere, artificially lowering the atmospheric  $^{14}\text{C}$  levels (Baxter and Walton, 1970; Taylor, 2016). This effect started with the industrial revolution, when people began burning fossil fuels, derived mostly from  $^{14}\text{C}$ -dead organic material. The fossil fuels burned and released into the atmosphere were therefore significantly depleted in  $^{14}\text{C}$  compared to the atmospheric levels. This began to drive down the natural atmospheric levels to below zero (Kutschera, 2022), highlighted in figure 2.3 section A. It was estimated by Suess (1955) that this burning resulted in a depression in atmospheric  $^{14}\text{C}$  concentration by about 3% by 1950. This human driven decline in atmospheric  $^{14}\text{C}$  is known as the Suess effect.

The depression of atmospheric radiocarbon caused by industrialization abruptly halted as a result of another atmospheric effect called the bomb pulse. Atmospheric levels of radiocarbon spiked in the mid-1950s as a result of testing of nuclear weapons (predominantly hydrogen bombs). This testing introduced large amounts of artificial  $^{14}\text{C}$  into the atmosphere which almost doubled the amount of  $^{14}\text{C}$  in terrestrial organics between 1955 and 1963 (Figure 2.3, B). In 1963, the United States, United Kingdom, and Soviet Union signed an agreement to stop above-ground nuclear weapons testing, and this caused the rapidly increasing atmospheric  $^{14}\text{C}$  to halt and start to decline towards the levels the atmosphere had been at before the testing (Taylor, 2016; Levin et al., 1997). The speed at which this decline happened was aided not by  $^{14}\text{C}$  decay, but by the increased rate of burning of  $^{14}\text{C}$ -depleted fossil fuels described above. These changes in atmospheric values caused issues for researchers attempting to date samples from around this time with conventional radiocarbon age estimates as the large fluctuations in atmospheric  $^{14}\text{C}$  content over the last 130 years created an exaggerated version of the problem created in a traditional radiocarbon plateau (Baxter and Walton, 1970; Taylor, 2016).

Despite its ineffectiveness in radiocarbon dating, the bomb spike and subsequent gradual decline in atmospheric  $^{14}\text{C}$  has created an opportunity for researchers to use it as a mode to answer questions about biological materials independent of the decay of  $^{14}\text{C}$ . Since the  $^{14}\text{C}$  values for each corresponding year during the peak are known, radiocarbon analysis of organic material that existed and died during the decline in atmospheric radiocarbon has been used to answer questions from determining the age at death of individuals in forensics, conservation questions in ecology, as well as bone turnover rates (Kutschera, 2022; Wild et al., 2000; Kaplan, 2003; Hedges et al., 2008; Calcagnile et al., 2013; Ubelaker et al., 2022). For example, Calcagnile et al. (2013) used radiocarbon measurements of hair, teeth, and bone of a forensic

John Doe case to be able to determine when the individual was born and when he died. The hair measured was associated with the date of death as it is a fast-growing tissue, and so the radiocarbon level in the hair should match with the atmospheric radiocarbon level at the year of death. The teeth are static and do not replace themselves after formation, and so teeth that form at a known age were measured to and linked to a specific year via atmospheric levels, and from there they were able to determine date of birth. This helped confirm the I.D. of the unknown person. Uno et al. (2013) used to peak to test if elephant ivory was modern or harvested before the international ban on harvesting and importing ivory in 1989. By measuring the  $^{14}\text{C}$  values of the ivory, the general age could be determined and deemed either legal (if it contained high  $^{14}\text{C}$  from around the peak) or illegal (if it contained lower, modern  $^{14}\text{C}$ ).

Within only the last few years, however, the atmospheric levels of  $^{14}\text{C}$  have returned to where they were prior to the bomb-peak. Recent (2021) measurements have shown modern atmospheric radiocarbon values to be around  $-4\text{‰}$  (Graven et al., 2022; Hua et al., 2022), and this move below zero is shown in figure 2.3 section C. This return to baseline confines the bomb-spike to the late twentieth and early twenty-first centuries, however both the continuation of the Suess effect and the continuous improvement in precisions of AMS will allow for this method's future use.

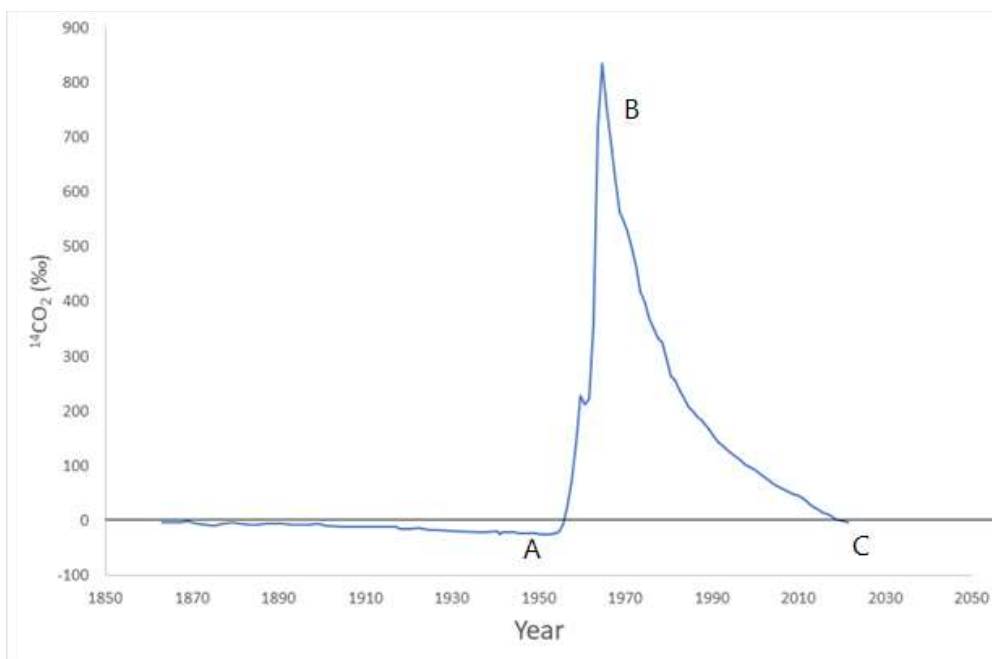


**Figure 2.3.** Northern atmospheric <sup>14</sup>CO<sub>2</sub> levels over 100 years, highlighting the Suess effect in the early 1900s (A) and the bomb spike around 1963 (B). Data from Graven et al. (2017), Graven et al. (2022), and Hua et al. (2022).

## 2.3 Previous Techniques for Measuring Turnover Rate

There have been a handful of techniques that have been employed to assess how quickly a bone turns over, each having strengths and weaknesses. I will quickly review the most frequently employed techniques used to quantify bone collagen turnover rate.

### 2.3.1 Chemical Output

A very early method that was used to determine if skeletal collagen turnover rate had increased or decreased over time was one that measured the output of hydroxyproline in the urine and blood. Since one of the major amino acids in collagen is hydroxyproline, it was suggested that an increase in the output of hydroxyproline would indicate that bone turnover rate had recently sped up, and the reverse would be true if hydroxyproline output decreased (Kivirikko 1970). One of the major issues with this method and the reason it is sparsely used

today is because hydroxyproline does not exist solely in the collagen of bone but exists in collagen that is distributed across a range of other tissues in the body as well, and therefore any results from this method would not independently measure the turnover of *bone* collagen but the entire body's collagen pool.

One method of determining the turnover rate of bone involves assessing the turnover of calcium and strontium in the body. The basis of this method is the fact that roughly 99% of the calcium in the body is stored in the bone, and therefore by measuring the input and excretion of specific isotopes of calcium from the body through a monitored diet including a calcium tracer and measuring blood, urine, and faecal samples, the difference can indicate how much calcium has been absorbed or expelled from the body (Weaver 1998). While this method allows for live sampling and continuous monitoring of turnover over time, there are a few limitations. One major issue is that there can be no specific bone element turnover deduced from the results as the bulk calcium of the body is being measured. As well, discharged calcium may be redeposited into other bone through recycling and would alter the excreted amounts of calcium (Snyder et al., 1975). This method can be altered to look at specific bones through a method outlined in Bryant and Louitt (1963), where an atmospheric peak in strontium allowed for the replacement of calcium with  $^{90}\text{Sr}$  (a radioisotope with a half life of 28.9 years) to be measured. This method allows for the turnover rates of specific bones to be estimated to determine variability in turnover rates among skeletal elements and individuals. While this method may provide more detailed information about bone turnover rate, it only measures the mineral portion of bone, as calcium and strontium are part of bioapatite rather than collagen in bone. While the mineral and collagenous portion of bone are very likely closely linked to each other (Burr 2019), they are not

the same, and therefore results from a method such as this may not have any basis for describing bone collagen turnover rates.

### 2.3.2 Bone Labelling

Bone labelling is a method that has been employed in the past through *in vivo* experimentation to determine bone turnover rates. Typical tracers include tetracycline (Frost, 1969) and calcein (Huja and Beck, 2007) bone labels. These chemicals are visible under by fluorescence microscopy. Once introduced to the body of a living subject, a designated amount of time is allowed to pass before samples of different bones are taken. The chemical tracers will be visible to varying degrees, with a higher percentage of visible tracer linked to a quicker bone turnover rate. Through various mathematical equations that measure the amount of bone that is labelled and the total available bone area, one can calculate the bone formation rate expressed as a percent per year (Huja and Beck, 2007). This technique seems to produce valid data; however, the method has not been performed on humans as sampling the skeletal elements is lethal. Besides the obvious ethical issues, this technique also does not separate collagen from mineral in bone and it is therefore difficult to assess any differences in the turnover rates of bone collagen and mineral.

### 2.3.3 Osteon Population Density

Osteon Population Density (OPD) is another way to measure bone turnover rate, specifically the activity of osteoblasts and osteoclasts, and is very often employed alongside other osteon measurement methods (e.g., Skedros et al., 2003; Burr, 1992). This method works by measuring the number of secondary osteons per section of bone through cross sections and microscopy. Secondary osteons display visible evidence of remodelling within the structure of

the bone and can therefore be used as a proxy for bone produced and as a measure of bone turnover dynamics (Fahy et al., 2017). The number of secondary osteons increases in relation to the number of BMUs that have recently been remodelled and therefore bone that is turning over more quickly will have more secondary osteons than a bone that is turning over more slowly. What makes this method problematic however, is that these cross sections only have visible secondary osteons in elements with a high amount of cortical bone (Fahy et al., 2017). Therefore, OPD only works for measuring the speed of turnover in some skeletal elements. Also, since the method is qualitative rather than quantitative, the remodelling rates are relative and coarse.

#### *2.3.4 Histological Measurements*

Another method that has been used to study bone turnover rate is the histological measurement method. This method estimates turnover rate based on measurements of features like surface area and bone volume. It is assumed in many cases that bone thickness is linked with turnover rate, as thicker bones would have more BMUs and would also have had enough time for increased mineralization which is linked to the thickness of bone (Montoya-Sanhueza and Chinsamy, 2017; Parfitt, 2002). These methods can also measure the loss of bone in older adults, which is linked to an increased turnover rate (Feik et al., 1996). While this method has produced some reasonable results, bone histology can be highly variable among people and can change for various reasons throughout life without altering turnover rate. As well, like other methods, this method does not always provide specific turnover rates and when it does provide turnover expressed per annum, it relies on base information from the tetracycline-labelling method.

#### *2.3.5 Bomb Carbon Dating*

Only few studies have looked at turnover rate of bone using the well-characterized peak in atmospheric  $^{14}\text{C}$  that was described in section 2.2.2. However, a very well-known study that used the bomb carbon dating method is Hedges et al.'s (2007) study of human femoral midshaft collagen from an Australian anatomical collection with birth dates of 1894 to 1951. Here, Hedges and colleagues used the peak to estimate the turnover interval of the femur to be at least 10 years, and average at roughly 30 years. Stenhouse and Baxter (1976) is also a frequently-cited paper to use this method, however they used it to determine the turnover rate of soft tissues in humans.

If bone turnover is linear, then the  $^{14}\text{C}$  values measured from the bone should equal the average of the sum of the atmospheric level for each year within the time of bone turnover. If bone turnover is non-linear, different weight can be given to any year's atmospheric level to account for it having incorporation into the bone. For instance, if bone turnover speeds up as one ages, then atmospheric levels closer to death can be weighted as a higher percentage of bone content. Since it is not well known exactly how turnover increases or decreases over time, this technique allows for multiple scenarios of turnover to be described. This method is ideal as it can provide quantitative turnover rates for isolated bone collagen, minimizing other biological components such as lipids and minerals from influencing the results of the studies and they can be specific to skeletal element and can be used on all types of bone. This technique is the principal technique used in this thesis.

### **Chapter 3: The Current State of Knowledge**

As I will demonstrate, the rate of bone turnover varies across different skeletal elements, and these variations could potentially be influenced by numerous factors. Prior research has offered limited specific turnover rate values for skeletal elements, with much of the existing studies relying on relative comparisons. While these relative insights can be valuable for comparative analysis, it is important to note that precise turnover rates for skeletal elements are still lacking. Furthermore, in order to gain a comprehensive perspective on the potential variations in turnover rates among human skeletal elements, it is informative to consider estimates based on relative turnover rates. Additionally, this analysis will extend to briefly examining animal studies of turnover rates. The outcomes and reasons proposed for turnover rate disparities in animal studies could offer valuable insights when considering the potential variations among human skeletal elements.

#### **3.1 Human Studies**

There are relatively few studies that have quantified human bone turnover rates. These studies have had the greatest influence on the emphasis of other studies and form the framework for the turnover rates cited in chemical analyses (e.g., stable isotopes) of bone collagen. These studies have provided the best quality data to date and the most comprehensive look at bone turnover rate in humans.

Bryant and Loutit (1963) estimated turnover rates using the turnover of calcium and strontium in the skeletal elements to come up with a reference chart for different skeletal elements. They described quantitative results of bone turnover rate in both adolescents and adults, both as full body average and specific skeletal element rates (Table 3.1). These results set

a good baseline against which the results of other studies could be compared, and many subsequent studies have generally aligned well with their results (e.g., Hedges et al., 2007; Parfitt, 2002; Sealy et al., 1995; Fahy et al., 2017; Bell et al., 2001). However, the results from this study cannot be taken as definite, as they are calculated from a small sample of individuals, the majority of which are male. They do not assess other factors that influence the rate of bone turnover, as this could account for the elements that are shown to have a high range in rates (e.g., vertebra range = 3.6-20% turnover per year for adults).

**Table 3.1.** Calculated turnover rates for different ages and skeletal elements from Bryant and Loutit (1963).

	Turnover mean % per year
<b>Adult average</b>	
Cortical bone	1
Trabecular bone	3-10
<b>Adolescents</b>	
One year	100-200
Three to seven	10
Eight - puberty	1
<b>Vertebra</b>	
One year	72
Five to six	20
Ten	30
Adult	8
<b>Bone (age 36-86)</b>	
Rib	4.7
Vertebra	8.3
Skull	1.8
Patella	3.6
Ilium	
Femur	
Proximal	

	Distal	6.5
	Shaft	2.9
Tibia		5.7
		2.5
		2.0
		1.1

Hedges et al.'s (2007) study has been especially influential. This study is cited in archaeological studies when the turnover rate of bones in humans is discussed, often in the context of techniques like stable isotope analysis. In this paper, the researchers measured  $^{14}\text{C}$  from femoral collagen of adult humans who died after the atmospheric spike in  $^{14}\text{C}$  during the mid-20th century (all of whom were born prior to the bomb peak), and this spike allowed for the turnover of collagen to be calculated. The most often cited conclusion of this paper is that collagen in an adult femur reflects more than a 10-year period, meaning less than 10% bone turnover per year. Additionally, in adolescence, male turnover rate is higher than the female rate, but adolescents in general have a higher turnover rate than adults. In fact, the adolescent femur from age 10–15 was shown to turn over at a rate of roughly 10–30% per year (Hedges et al., 2007). This makes sense in light of the fact that adolescent humans go through a large growth event during these years, and the new bone being placed down would offset the amount of old bone, increasing the turnover rate. This increased turnover in adolescent bone is also consistent with Bryant and Loutit's (1963) work.

Another relatively comprehensive study done by Fahy et al. (2017) used osteon population density (OPD) as a measure of relative bone turnover rate within ten different bones sampled from ten English Medieval skeletons. Using a higher OPD as an indicator of a bone undergoing more remodelling (when age is controlled), Fahy et al. (2017) were able to create a

list of the relative turnover rates of different skeletal elements in humans. However, the OPD method does not work well in skeletal elements with a high amount of trabecular bone, and therefore bones such as vertebrae and the pelvis were not studied. The results of this study created a list of bones from highest to lowest OPD. The humerus was seen to have the highest OPD, indicating that it potentially has the highest bone turnover rate among the elements measured, along with metacarpals and ribs also sharing a relatively high turnover rate. Other bones such as tibiae, radii and clavicles had lower turnover, with the occipital bone having the lowest turnover rate of all. They also noted that females generally had higher OPD values than males. From this, Fahy et al. (2017) was able to recommend that when all elements are present for analysis, the occipital bone is optimal for studies which aim to measure long periods of life. Interestingly, this study also indicated that the rib and femur have similar turnover rates, yet many researchers still believe the rib to be relatively fast and the femur to be relatively slow (e.g. Cheung et al., 2017; Drtikolova Kaupova et al., 2021) As detailed in section 2.2.3, OPD only produces relative turnover rates that cannot be compared across species. While the humerus had the fastest turnover rate in these humans studied, this qualitative result may not be the case in all species, age groups, or humans with different activity levels. As well, it is still unclear what period is represented in any given sample of bone. What's more, both Fahy et al. (2017) and Hedges et al. (2007) take a small sample from the bones they study and assume that the turnover rate will be equal within a skeletal element, an assumption which is unproven and inconsistent with the results presented by Matsubayashi and Tayasu (2019).

### *3.1.1. Differences Between Type of Bone*

Since OPD is unable to measure turnover rates of trabecular bone, some researchers have compared cortical to trabecular bone turnover rates via other methods. While it is often assumed

that trabecular bone has a higher turnover rate than cortical bone (Bryant and Louitt, 1963; Hill, 1998; Cox and Sealy, 1997), this may not always be the case. Parfitt (2002) measured relative bone turnover rate within humans for both cortical and trabecular bone using the histological measurement method. The results of this study indicated that within just one skeletal element (the ilium), different turnover rates exist and that the turnover rate in central cortical bone, despite being slower than central trabecular bone, is still faster than the outer section of trabecular bone. Thus, while trabecular bone in general has a faster remodelling rate than cortical bone, not all sections of bone are equal, and this must also be taken into consideration. Nonetheless, other studies have used the general difference in turnover rate between these two types of bone in humans to create a life-history, assuming cortical bone represents general life events and trabecular bone represents near-death events (Ubelaker et al., 2006). Trabecular bone is still widely considered to be characterized by faster remodelling than cortical bone (Huiskes et al., 2000; Eriksen, 2010; Currey, 2006; Shin et al., 2004).

### *3.1.2 Differences Between Sexes and Age Groups*

Other factors that have been observed to affect the turnover rate of bone within humans are sex and age. Age was a factor that was identified in the Bryant and Louitt (1963) and Hedges et al. (2007) studies, with the main finding being that adolescents have a faster bone turnover rate than adults. These results make sense as these early years are when the human body experiences the most growth, and so new bone is laid down to support this growth (Burr, 2019). What these papers did not account for, however, is how bone remodelling might differ between sexes in adolescents and juveniles, while also grouping all adults into the same category without recognizing differences that may occur in turnover between 20 and 80-year-old individuals. This is typically how turnover is discussed, with adults grouped into one category.

Feik et al. (1996) looked at the trends in bone turnover seen in adult men and women using the histological measurement method. Their findings indicated that not only are there differences between sex, but there are differences in different adult age groups, at least within the human femur. For instance, adult men and women have a relatively stable turnover rate until middle adulthood, and after this, postmenopausal women see a significant increase in bone turnover rate and men see a small increase. In late adulthood, men and women have the greatest variance in remodelling rate, and these remain different up until around age 70, when the sexes have little difference and experience relative stability in turnover rate (Feik et al., 1996). These results have not been contested, however, with other studies indicating that there is no *overall* turnover rate difference between premenopausal and postmenopausal women, and that there is only an increase in bone absorption (with no increase in bone formation) (Balena et al., 2009).

There have been many other studies which have noted age and sex differences in bone turnover (Han et al., 1997; Fahy et al., 2017; Mulhern, 2000; Cox and Sealy, 1997). The consensus in these studies is that in both adolescence and adulthood, women have a higher bone turnover rate in some skeletal elements when compared to men, and that bone turnover rate slightly increases as one ages until around age 70. These changes and differences have been suggested to be due to hormonal differences, differences in activity levels, or differences in the overall bone sizes (Han et al., 1997; Fahy et al., 2017; Mulhern, 2000). Based on measurements of hormones in adult men, bone turnover rate decreases from young adulthood to older adulthood (Fatayerji and Eastell 1999).

### *3.1.3. Differences Between Ethnicities*

Another factor that may influence the turnover rate is ethnicity. One study found that between black and white women, the iliac bone turnover was 25% slower in black relative to white women, which could be due to differences in overall bone mass (Han et al., 1997). Another similar study saw that bone turnover rate in black people was 35% slower than white people (Weinstein and Bell, 1988). Other studies have noted population differences as well (Mulhern, 2000; Stout and Lueck 1995) where the bone remodelling rate of archaeological skeletons were assessed. In these studies, each population had a slightly different remodelling rate, and all differed from modern populations. It can therefore be concluded that even if age and sex are kept consistent, differences in bone turnover rates may still exist among people of different ethnicities.

#### *3.1.4. Differences Between Health and Hormones*

Another factor that has been seen to potentially alter the bone turnover rate in humans, is health and hormonal changes. Conditions that affect hormones, or health issues related to diet and mobility all have the potential to alter bone turnover rate. Studies have shown that a deficiency of vitamin D can increase the turnover rate of bone, as it can cause the deactivation of bone formation regulators, which results in bone being dissolved and replaced more frequently (Kong et al., 2013). These results have been seen elsewhere and have also suggested that vitamin D deficiency paired with low dietary calcium intake could be the reason that people who have plant-based diets have also been shown to have faster turnover rates and are more prone to bone-related injuries (Itkonen et al., 2020). One study used these results to explain why there was seasonal variation in turnover rate within a population, showing 20–30% higher turnover rates in the winter. Due to vitamin D deficiency being the most common during winter months, Woitage et al., (1998) concluded that vitamin D deficiency was the cause of seasonal differences in

turnover rate. Bone turnover rate can also increase by 50% in people who have Paget's disease (Kucharz, 1992). Since hormones play a role in the regulation of bone turnover rate (Hill, 1998), studies have also shown that conditions that affect hormone levels such as hyperparathyroidism can cause the increase or change in the rate of bone turnover in humans (Parfitt, 1996). It has also been noted that injury can alter the rate at which bone turns over. Generally, bone turnover rate increases around the site of injury in humans as more bone is needed to heal the injury (Ingle et al., 1999).

Another disease to note that can affect bone turnover rate is osteoporosis. Different types of this disease effect the collagen in different ways. The main markers for this disease are changes in the activity levels of osteoblasts and/or osteoclasts. Since collagen turnover rate is measured as % collagen loss/% collagen gain per year, with osteoblasts creating new bone, and osteoclasts in charge of dissolving bone, it is obvious that unbalanced changes in these cells would affect turnover rate. These changes also alter the density and porosity of bone which is why this disease is known to make bone more brittle. Typically, the brittleness of bone in osteoporosis is associated with increased bone turnover and more porous cortices (Shigdel et al., 2015). However, the quality of bone collagen is a stronger indicator of bone fragility, as newer bone collagen has had less time to create enough crosslinks to add rigidity to the bone. Further, aging is linked to a decrease in overall collagen content, which also adds to the fragility of skeletal elements from older individuals (Rouhi, 2012). Most commonly, osteoporosis is associated with an increase in osteoclastic activity, and either no change or an increase in osteoblastic activity. In this case, bone turnover will be increased as bone is being built and dissolved more frequently. Other diseases like osteopetrosis (reduced osteoclast activity) or osteopenia (decreased osteoblast activity) are more likely to reduce the turnover rate of the bone

(Rouhi, 2012). Osteoporosis can also be related to calcium deficiency and has been shown to be associated with a very high turnover rate (Melton et al., 1997). Therefore, with diseases of the bone such as those mentioned here, factors could be at play that could either increase or decrease bone turnover rate. Further, the effects of these diseases can be counteracted with drugs such as alendronate, which decreases osteoclastic activity (Arlot et al., 2005) and therefore slows the turnover rate in high turnover rate osteoporosis patients.

### *3.1.5. Differences in Activity Levels*

The final factor I will discuss is level and type of activity. Only a few studies have assessed how activity type and level effects bone turnover in humans, typically by assessing different groups of athletes. Fehling et al. (1995) measured the density of bone in impact athletes (volleyball players and gymnasts) and cardio athletes (swimmers) through dual-energy X-ray absorption (DEXA). They found that the impact athletes had a higher bone density and therefore a lower turnover rate, whereas the swimmers showed a lower bone density and a higher turnover rate. Bennell et al. (1997) conducted a similar study using the same method but went further by directly measuring overall turnover rate through the assessment of turnover markers in blood and urine. Interestingly, they did not observe any significant difference in turnover markers between athletes and individuals with low activity levels. However, it is important to note that their method accounted for the total remodelling occurring in all skeletal elements, and therefore, they couldn't definitively conclude if turnover rate in specific skeletal elements were affected by specific activities. These results were also seen in a study that measured the chemical outputs of runners, which suggested that there may be a regulating skeletal response to changes in turnover in some skeletal elements (Zanker and Swaine, 2000). However, based on these studies, it remains inconclusive whether activity level in humans can directly affect bone turnover.

Moreover, these studies do not consider age-related changes in activity or how different sexes may respond to varying activity levels. Therefore, while these studies have provided valuable insights into the potential relationship between activity and bone turnover, more research is needed to fully understand its impact on bone turnover in humans.

### **3.2 Animal Studies**

It is also important to consider studies that have been done on different species to assess bone turnover rate as variation across species or among skeletal elements could be useful in determining the factors that can affect human bone remodelling. There are multiple studies that have produced data for non-human species. This information is compiled here to gain a better overall understanding of what is known about the turnover rate of skeletal elements in different animal species.

Several studies have examined bone turnover rates and the factors influencing them in small animals, particularly rodents. Interestingly, small-bodied creatures like mice, squirrels, rats, and small birds appear to exhibit infrequent bone remodelling, although the reasons for this remain unknown (Enlow and Brown, 1958; Shipov et al., 2013; Enlow and Brown, 1957; Currey, 2006). Their bones may be too thin to endure the remodelling process, and the short lifespan of these animals may further limit significant remodelling (Currey, 2006; Kirkwood, 1992). A detailed study by Montoya-Sanhueza and Chinsamy (2017) focused on bone formation and absorption in Cape dune mole-rats (*Bathyergus suillus*), supporting previous findings of low remodelling rates and overall bone turnover. The study suggested that the small bones of these animals cannot withstand the increased osteoclast activity associated with high turnover rates. Interestingly, even within this slowly remodelling rodent species, researchers observed a slightly

higher remodelling rate in female rodents compared to males, similar to what has been observed in humans (Feik et al., 1996; Montoya-Sanhueza and Chinsamy, 2017).

Montoya-Sanhueza et al. (2021) examined the longest-living rodent (*Bathyergus suillus*) to investigate whether a turnover rate could be identified based on their extended lifespan. By measuring osteons and employing histological measurements, they discovered that forelimb bones undergo significantly higher rates of remodelling compared to hind limb bones. Specifically, the humerus displayed the fastest remodelling, followed by the femur, ulna, and tibia. The researchers hypothesized that these bones undergo more remodelling due to the rodents' digging behaviour, necessitating increased turnover and bone modelling to support the bones experiencing greater forces (Montoya-Sanhueza et al., 2021). This observation aligns with the pattern observed in both animals and humans, where bones subjected to greater stress undergo more remodelling—a finding supported by numerous previous studies (Sykut et al., 2020; Skedros et al., 2013; Daegling and Hotzman, 2003). Therefore, when assessing bone turnover rates in future studies, it is crucial to consider the influence of bone stress. Furthermore, the hypothesis that reduced turnover rates in small animals result from their short lifespan was not supported and instead attributed to the fragility of their thin bones (Montoya-Sanhueza et al., 2021).

The bone turnover rate of dogs (*Canis familiaris*) has also been extensively studied. Marotti (1963) assessed the rate of turnover in different long bones of dogs via protein labelling. They gave the dogs the fluorescent chemical a few days before euthanizing them, and the chemical allowed for the growth of new bone that included this chemical to be seen microscopically. The results showed the turnover rates were fastest in the ulna, then radius, tibia, and femur, with the humerus being the slowest. These results were quite different from what has

been seen in other species, such as humans, in which the humerus had one of the fastest turnover rates (Fahy et al., 2017). This highlights the importance of the analysis of individual species since the difference in remodelling seems to be vast and potentially related to function for species. Huja et al. (2006) looked at remodelling differences between the mandible and maxilla in dogs by injecting them with tracers and then slaughtering the animals after some time had passed. They found that not only was there a difference between the mandible and maxilla, but there was a difference in turnover rate based on location within the bone as well. Bone turnover rate was significantly higher in the mandible (annual turnover rate of 36.9%) than in the maxilla (annual turnover rate of 19.1%), with both being much higher than the femur (annual turnover rate of 6.4%). Within the maxilla, the anterior portion of the bone had a higher turnover rate than the posterior portion (Huja et al., 2006). In younger dogs the femur had significantly higher turnover (annual turnover rate of 72%) than the mandible (annual turnover rate of 51%) and maxilla (annual turnover rate of 25%) (Huja and Beck, 2007). This speaks to the rapid growth occurring in the femur of young dogs but suggests a more gradual rate exists in the jaw bones. Bone characteristics also vary based on the life stage of dogs. Lactating dogs had greater bone turnover rates than other dogs, likely due to hormonal changes associated with lactation (Vajda et al., 1999).

Dogs have also been used to test more general models of bone turnover. Contrary to studies that have shown that skeletal elements important for absorbing shock undergo the most turnover (Montoya-Sanhueza et al. 2021), it has also been shown that, in dogs, skeletal elements that are immobilised and undergo no strain also tend to have higher turnover rates than bones which perform their regular function (Marotti and Marotti, 1966). Physical activity differences can therefore have different effects on the bone turnover rate, highlighting the importance in

acknowledging factors like mobility and activity when assessing differences in the turnover rate of bone. It is possible that, in humans, factors like handedness could contribute to increased activity levels in certain limbs and cause left to right differences in turnover rate. As movement is also related to age, turnover differences due to age could also be attributed to differences in movement abilities. However, it should also be noted that this is not the case in all species, as multiple studies on bears show that despite long periods during hibernations where they have no movement, bears reduce their turnover rates during these periods to protect their bone strength (McGee-Laurence et al., 2015; McGee et al., 2008; Wojda et al., 2013).

Bone turnover in larger terrestrial mammals has been studied to some degree as well. Similar to what other studies have seen in their analyses, in mule deer (*Odocoileus hemionus hemionus*), OPD was used to confirm that the rib bones have a much higher turnover rate than limb bones, and limb bones had relatively similar turnover rates (Skedros et al., 2003). This study further observed slight variations in turnover rates within bones, possibly attributable to differences in stress distribution across the bone (Skedros et al., 2003). Another study, using red deer (*Cervus elaphus*), saw that not only are ribs one of the fastest turning over bones, but they turn over cyclically. Turnover rates in rib bones vary throughout the year, with lower turnover during certain periods and peaks corresponding to antler growth (Baxter et al., 1999). Thus, while rib bones may represent a stage of life closer to death, this phase might be skewed to reflect only a specific season of the year. Studies using stable isotopes on deer have also shown that the mandible of this animal has comparable isotopic values to distal appendicular elements such as phalanges and metatarsals, and thus they concluded that these elements have comparable turnover rates (Sykut et al., 2020).

In the Asiatic wild ass (*Equus hemionus*), through various histological measurements, it was found that the femur had the slowest turnover rate, representing the longest period of time, and was somewhat similar to metatarsals, with the tibia being found to turnover slightly faster (Nacarino-Meneses et al., 2016). Sika deer (*Cervus nippon*) were used to determine if turnover rate is the same in all parts of the femur and if time is equally represented within the bone, measured through the bomb-carbon dating method (Matsubayashi and Tayasu, 2019). Different layers of bone exhibited varying turnover rates, with the section closest to the medullary cavity demonstrating the fastest turnover. Furthermore, the study showed that samples from the femur did not equally represent the entire lifespan during which the bone underwent remodeling; instead, they primarily represented the period of most rapid growth during adolescence (Matsubayashi and Tayasu, 2019). Another study using sheep (*Rupicapra rupicapra*) used histological measurements of the iliac crest to determine if bone mineral density and turnover rate was consistent across seasons. Their results showed that there was a decrease in bone mass in the winter and an increase in the summer, suggesting that these seasons have differing bone turnover rates (Arens et al., 2007)

Marine species have also been a topic of interest for bone turnover rate. A study using stable isotope analysis on pinnipeds (*Odobenus rosmarus divergens*, *Pusa hispida*, *Phoca* spp.) and sea otters (*Enhydra lutris*) concluded that there is stable isotopic variability between skeletal elements within the individuals. They found that elements that typically have higher amounts of trabecular bone, such as the scapula, vertebrae, and distal limb bones, all grouped together isotopically (Clark et al., 2017). They concluded the grouping was likely due to the fact that these bones would have relatively similar turnover rates. They also indicated that these were likely the faster turning over skeletal elements, compared to more dense cortical bone (Clark et

al., 2017). This same variation between skeletal elements has also been noted in cetaceans (Smith et al., 2020). Other studies of pinnipeds have seen that for the mandible and maxilla, the bone turnover rate was said to be roughly five years, based on analyses of how nitrogen isotopes are integrated into the tissue (Riofrío-Lazo, 2013). This study, however, did not have strong evidence for their conclusions regarding quantitative turnover rates. Similar to what has been seen in other species, younger individuals have faster bone turnover rates. In *Otariidae*, this was confirmed by sampling multiple crania and measuring weaning signals isotopically and using this to determine when bone had fully turned over. The crania of <1 year old *Otariidae* completely turned over in 8–10 months (Newsome et al., 2006).

There are numerous other species that have been less intensively studied but still provide some baseline information. In one study, a single racoon (*Procyon lotor*) sample had multiple elements assessed and used the difference in stable isotope composition of each element to estimate which skeletal elements turned over the fastest (Hyland et al., 2022). Turnover was most rapid in the pelvis and the ribs, attributed to these bones containing more trabecular bone, similar to what has been seen in other species. Also, it was suggested that the locomotion pattern of racoons placed more stress on these skeletal elements, including the lumbar vertebrae, which may also account for their higher turnover rate. Bones with lower turnover such as the limb bones may have these low rates due to remodelling limiting strength, a cost not every bone can afford (Hyland et al., 2022). Another species that has received a small amount of attention is the macaque. In a study by Burr (1992) they compared macaque (*Macaca mulatta*) bone turnover rate to human bone turnover rate to test if macaque skeletal elements would make a good proxy for humans. While the rib turns over faster in the macaque than in humans, the macaque femur turns over more slowly than in humans (Burr, 1992). However, a similar study conducted by

Schock et al. (1972), using a histological measurement-based method, found that macaques exhibit bone remodelling rates similar to humans. These discrepancies highlight the ongoing debates and complexities surrounding animal turnover rates, making comparisons to humans or other species more challenging. Furthermore, the discordant findings may signal the limitations of some of these methods for quantifying bone turnover.

### **3.3. Summary of Factors Influencing Bone Turnover Rate**

Through analysing both humans and non-human animals, certain trends related to bone turnover have been observed. These trends are summarized in table 3.2.

It is possible that other factors, not discussed here, may dramatically change bone turnover rate. For example, while studies examining how health can affect bone turnover focused on bone-related ailments such as osteoporosis and vitamin D deficiency, it is more than likely that any other type of rare and common lifestyles and diseases can alter bone collagen turnover rate to varying degrees. Even smoking and drinking alcohol have been suggested to affect bone turnover rate (Woitage et al., 1998), however this has not been thoroughly studied. Therefore, it is crucial to continue characterizing turnover rates in multiple skeletal elements across various species to improve the accuracy and precision of estimates and improve our understanding of the range of factors that influence bone turnover.

#### *3.3.1 Issues and Caveats*

While previous studies on animals and humans have provided important information about bone remodelling rates in some species, especially in a relative and qualitative sense, there is certain information that most of these studies lack, making them less useful where more quantitative estimates of bone turnover rate are desirable. For example, widely used methods

such as OPD and histological analyses produce results that are difficult to compare directly with other techniques. With more explicit quantitative turnover rates, such as those derived from bomb-pulse dating, comparisons between species can be made and we can understand exactly what is represented by chemical analyses of bone collagen, such as stable isotope analysis. Few studies have been able to provide explicit numeric turnover rates (e.g., Huja et al., 2006; Hedges et al. 2007), but the results of these studies have been informative and powerful because turnover rates expressed per annum can be directly compared across skeletal elements, sexes, populations, and species. To perform inter-species comparisons in the future, emphases should be placed on quantitatively defining turnover rates. Based on the review of the literature, no previous study, or series of studies, has comprehensively and quantitatively defined the turnover rate of skeletal elements in any species, including humans. Being the focus of many archaeological studies, humans are, therefore, especially important in the context of understanding bone turnover rates from a quantitative perspective.

**Table 3.2.** List and description of possible factors that can affect bone collagen turnover rate.

<b>Factor</b>	<b>Summary and trends</b>	<b>Cited by</b>
Bone type and Bone region	Cortical and trabecular bone exhibit distinct turnover rates, likely due to their specific functions. Cortical bone, responsible for strength and rigidity, benefits from slower turnover rates to preserve its structural integrity. On the other hand, trabecular bone, which absorbs shock and withstands strain, tends to have higher turnover rates. This difference in turnover can be attributed to factors such as increased vascularity and porosity in trabecular bone. Additionally, different sections of a bone, such as the anterior or medial regions, have the potential to display variations in turnover rates.	Bryant and Louitt, 1963; Burr, 2019; Clark et al., 2017; Cox and Sealy, 1997; Currey, 2006; Eriksen, 2010; Hill, 1998; Huiskes et al., 2000; Hyland et al., 2022; Lai et al., 2005; Parfitt, 2002; Sealy et al., 1995; Shin et al., 2004; Ubelaker et al., 2006.
Sex and age	Differences in turnover rates between sexes can be attributed to hormonal variations, growth rates, and overall body sizes. Age-related differences also arise due to varying growth rates and hormonal changes associated with age. Young individuals who are experiencing rapid growth tend to have the fastest bone turnover rates, while women generally exhibit equal or faster turnover rates compared to men depending on their life stage.	Bryant and Louitt, 1963; Cox and Sealy, 1997; Fahy et al., 2017; Feik et al., 1996; Han et al., 1997; Hedges et al., 2007; Montoya-Sanhueza and Chinsamy, 2017; Mulhern, 2000; Vajda et al., 1999.
Health	The impact of health conditions on turnover rates has been extensively studied in humans, and some animal models have confirmed similar trends. Diseases, dietary deficiencies, injuries, and various conditions have been linked to changes in turnover rates. In most cases, these changes tend to increase turnover rates, although it is important to note that the detrimental effects of accelerated turnover may be more significant than the effects of decreased turnover. Further studies are needed in all species to better understand the relationship between health and turnover rates, with the expectation that findings will align between animals and humans.	Hill, 1998; Ingle et al., 1999; Rouhi, 2012; Itkonen et al., 2020; Kong et al., 2013; Kucharz, 1992; Melton <i>et al.</i> , 1997; Parfitt, 1996; Woitage et al., 1998.
Turnover intervals	While bone collagen is constantly changing, major remodeling occurs at different intervals based on factors such as age or time of year. The effects of seasons on	Arens et al., 2007; Baxter et al., 1999; McGee-Laurence et al., 2015; McGee et al., 2008; Woitage et

Factor	Summary and trends	Cited by
	<p>turnover rates are still not fully understood, as humans have shown higher turnovers in winter, while animals like deer and sheep exhibit greater turnover in spring and summer. Bears also display interval-based changes, reducing their overall turnover during hibernation. Consequently, bone turnover does not represent a yearly average and is more reflective of periods of high turnover.</p>	<p>al., 1998; Wojda et al., 2013.</p>
<p>Ethnicity and species</p>	<p>Differences in DNA can significantly influence bone characteristics, including size, shape, and remodeling patterns. These differences are particularly evident between species, with notable variations observed among similar but distinct species. Lifespan, size, and specific activities performed by each group have been linked to these inter-species differences. Human studies have also demonstrated differences in turnover rates among different populations, often attributed to variations in general body size or activity levels.</p>	<p>Burr, 1992; Currey, 2006; Han et al., 1997; Kirkwood, 1992; Montoya-Sanhueza et al. 2021; Mulhern, 2000; Stout and Lueck, 1995; Weinstein and Bell, 1988;</p>
<p>Strain and activity</p>	<p>Bone collagen turnover rates are influenced by the forces exerted on each bone. Bones subjected to high levels of strain and limited mobility tend to exhibit increased turnover rates, likely due to the need to repair microfractures resulting from shock absorption. Conversely, bones with low turnover rates may be less capable of compromising strength, as bones with higher turnover rates often display increased porosity, which can lead to increased fragility.</p>	<p>Bell et al., 2001; Daegling and Hotzman, 2003; Hill, 1998; Hyland et al., 2022; Marotti and Marotti, 1966; Montoya-Sanhueza et al., 2021; O'Connor et al., 1982; Skedros et al., 2013; Sykut et al., 2020.</p>

## **Chapter 4: Materials and Methods**

### **4.1. Materials**

#### *4.1.1 Sample selection and acquisition*

Samples for this research were acquired from the Research in Experimental and Social Thanatology / *Recherche en Sciences Thanatologiques [Experimentales et Sociales]* site, also referred to as REST[ES], which is a facility associated with the Université du Québec à Trois-Rivières (UQTR). REST[ES] is a high-security outdoor facility which houses the remains of individuals who have donated their bodies to UQTR for forensic science research purposes. This facility is the first of its kind in Canada, and the research mainly includes forensic and ecological studies on topics around human decomposition. The donors that are housed in the facility are recently deceased (within the last three years) and are in various states of decomposition. Human ethics approval for sample collection from the donors was approved by UQTR under the Director of the REST[ES] facility, Shari Forbes with certification numbers CER-19-261-07.10 and SCELERA 22-06. The research completed here is considered to be secondary use of these samples and is consistent with the existing research agreement, which was ratified by Trent University. The donors provided detailed information about their life prior to death and the facility is able to use this information for research and to understand physiological and demographic differences between the individuals. This information is detailed in table 4.1.

**Table 4.1.** Donor information for the individuals sampled for this research from the REST[ES] facility in Quebec, Canada

<b>Donor #</b>	<b>Health details</b>	<b>Birth Year</b>	<b>Death Year</b>	<b>Sex</b>
3		1951	2020	F
5	Metastatic melanoma	1948	2020	M
6	Metastatic melanoma	1944	2021	M
10	Lung neoplasia	1943	2021	M
11	Metastatic lung cancer	1967	2021	M

Donor #	Health details	Birth Year	Death Year	Sex
12	Lung neoplasia, on Alendronate for Osteoporosis	1948	2021	F
17	Paralysis	1949	2022	M

Donors were chosen based on state of decomposition. It was important to keep other tissues unaltered as these donors are being used in various other research projects and thus, only individuals with accessible skeletal material were sampled. The elements chosen from each donor was also based on the accessibility of the element, and therefore equal numbers of every skeletal element could not be obtained. A variety of different skeletal elements were collected from each donor as indicated in table 4.2. For each element, a small ~100 mg section was removed from the bone for further processing. In a few cases, the small section of bone was subdivided to increase the sample size. For TEAL 20506, two ~100 mg sections were taken from the same mandible since it was the only mandible available from all donors and may highlight any differences in turnover rate within the same element. Similarly, 20526 was subdivided as this bone provided the unique opportunity to sample both cortical (A) and trabecular (B) regions from the same rib.

**Table 4.2.** Sample numbers and the associated donor and element

Donor Number	TEAL Number	Skeletal Element	Side/Specifications
3	20491	Femur	Right
3	20492	Rib	Left
3	20493	Vertebra	Thoracic
3	20494	Ulna	Right
3	20495	Public symphysis	
3	20496	Iliac Crest	
3	20497	Humerus	Left
5	20498	Femur	Right
5	20499	Rib	Right
5	20500	Ulna	Right
5	20501	Pubic symphysis	
5	20502	Vertebra	Thoracic
5	20503	Iliac crest	
5	20504	Humerus	Left

<b>Donor Number</b>	<b>TEAL Number</b>	<b>Skeletal Element</b>	<b>Side/Specifications</b>
6	20505 A1	Femur	Right
6	20505 A2	Femur	Right
6	20505 B1	Femur	Right
6	20505 B2	Femur	Right
6	20505 C1	Femur	Right
6	20505 C2	Femur	Right
6	20505 D1	Femur	Right
6	20505 D2	Femur	Right
6	20506 A	Mandible	
6	20506 B	Mandible	
6	20507	Ulna	Left
6	20508	Rib	Left
6	20509	Pubic symphysis	
6	20510	Humerus	Left
6	20511	Iliac crest	
10	20512	Femur	Right
10	20513	Rib	Left
10	20514	Ulna	Right
10	20515	Pubic symphysis	
10	20516	Vertebra	Lumbar
10	20517	Humerus	Left
10	20518	Ischiopubic ramus	Right
11	20519	Femur	Right
11	20520	Rib	Right
11	20521	Pubic symphysis	
11	20522	Ulna	Left
11	20523	Humerus	Left
11	20524	Greater sciatic notch	
12	20525	Femur	Right
12	20526 A	Rib	Left
12	20526 B	Rib	Left
12	20527	Vertebra	Lumbar
12	20528	Humerus	Left
17	20529	Ulna	Right
17	20530	Femur	Left
17	20531	Rib	Left
17	20532	Vertebra	Lumbar
17	20533	Humerus	Left
17	20534	Ischiopubic ramus	

TEAL 20505 was a unique sample of a femur. Instead of a small section being removed from the femur, a whole cross section was taken. This cross section allowed for multiple samples to be taken from a similar region of bone to assess variability in turnover in different areas of the femur. The cross section was subdivided into 8 sections, from the medial, lateral, anterior, and posterior area of bone, as well as sampling from the pericortical area and the perimedullary region of bone. This sampling strategy is illustrated in figure 4.1

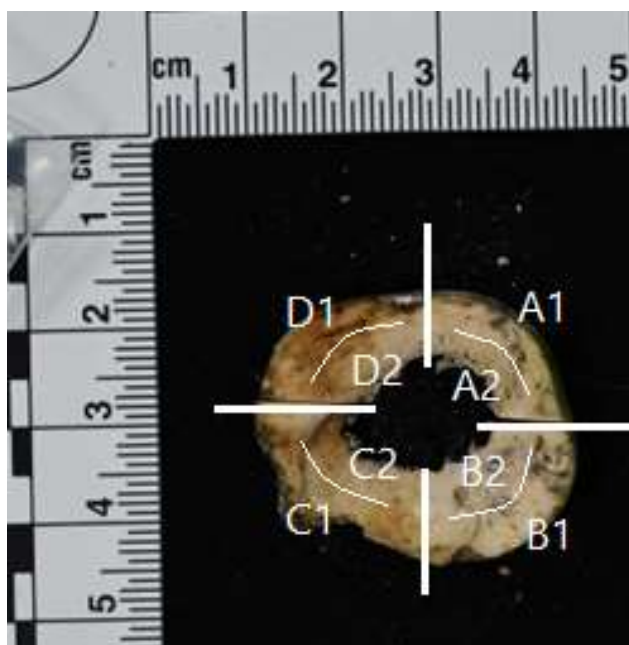


**Figure 4.1.** Subsampling pattern for one femur (TEAL 20506).

#### *4.1.2 Sample Challenges*

While the goal of this thesis is to provide a general estimate of the turnover rate of each skeletal element, it is important to address the biases within the selected samples. The age range of the donors is limited, with the donors' age at death ranging from 54 to 77 years. This is only a 23 year range, which only covers adult – late adult age groups. This age group is also more prone to specific health issues and lower activity level patterns which could potentially differentiate

their bone collagen turnover rates from other demographics of adults. Specifically, it is possible that osteoporosis could have affected any of the donors to varying degrees, which would affect turnover rates in the effected bones. Moreover, many of the donors had some form of cancer, which could have impacted bone health, however the relationship between cancer and turnover rate of bones is not well studied. Despite the fact that this sample group may hinder the results from being applied across all demographic age categories, it also opens up pathways to discover how turnover is influenced by health, movement, and age by comparing the turnover rates of this study with results from other studies. For instance, the inclusion of osteoporotic donors as well as a donor who took medications to limit the effects of osteoporosis (donor 12) provides an opportunity to directly test the effectiveness of that drug. A donor who experienced paralysis in the last years of life (donor 17) provides a direct opportunity to test the turnover rate of bone that experienced no movement whatsoever. There are many ways in which this sample grouping provides more research opportunities rather than restricting them.

There is also the potential issue that this age range puts some of the life of the donors on the left side of the atmospheric radiocarbon spike, and thus could influence the results due to there being more than one year with certain amounts of atmospheric  $^{14}\text{C}$ . This issue will be assumed to not influence the results at all as most of the individuals were around the age of puberty when the atmospheric levels were at their highest. Since puberty is thought to be a time of higher bone turnover due to bone growth (Bryant and Loutit, 1963), as well as the fact that these people lived for around 60 years after the peak, it is assumed that all bone from before the peak has been turned over at least once for all the donors.

#### *4.1.3. Supplemental datasets*

Data from two additional studies were collected in order to increase sample size and number of elements sampled. The two studies reported the bone collagen  $\Delta^{14}\text{C}$  values for various skeletal elements from individuals with known ages of birth and death that lived in the post nuclear age (Johnstone-Belford et al. 2022; Ubelaker et al. 2022). In these studies,  $\Delta^{14}\text{C}$  was measured to calculate 'lag time', which is the difference between the death date and the year associated with the  $\Delta^{14}\text{C}$ . This lag time concept is relevant in forensics when determining a precise year of death for unidentified remains is the goal. The samples used in these studies are from the southern hemisphere, where the radiocarbon spike in the 1950s was less pronounced compared to the northern hemisphere spike (Figure 4.2). The date of deaths for these individuals included 2006, 2010, and 2013-2018. The Ubelaker et al. (2022) study utilized 68 samples from six females and eleven males who were all born in 1963 and died at age 43 to 54. Four elements were sampled from each person: the parietal, the occipital, the femur, and the vertebra. The study by Johnstone-Belford et al. (2022) included 72 samples in total across 18 individuals. This study assessed differences in  $\Delta^{14}\text{C}$  for cortical and trabecular differences bone in the femur and rib of each individual. Of the 18 samples individuals, 3 were female and 15 were male, and they ranged in age from 64 to 94, with the dates of death ranging from 2016 to 2018.

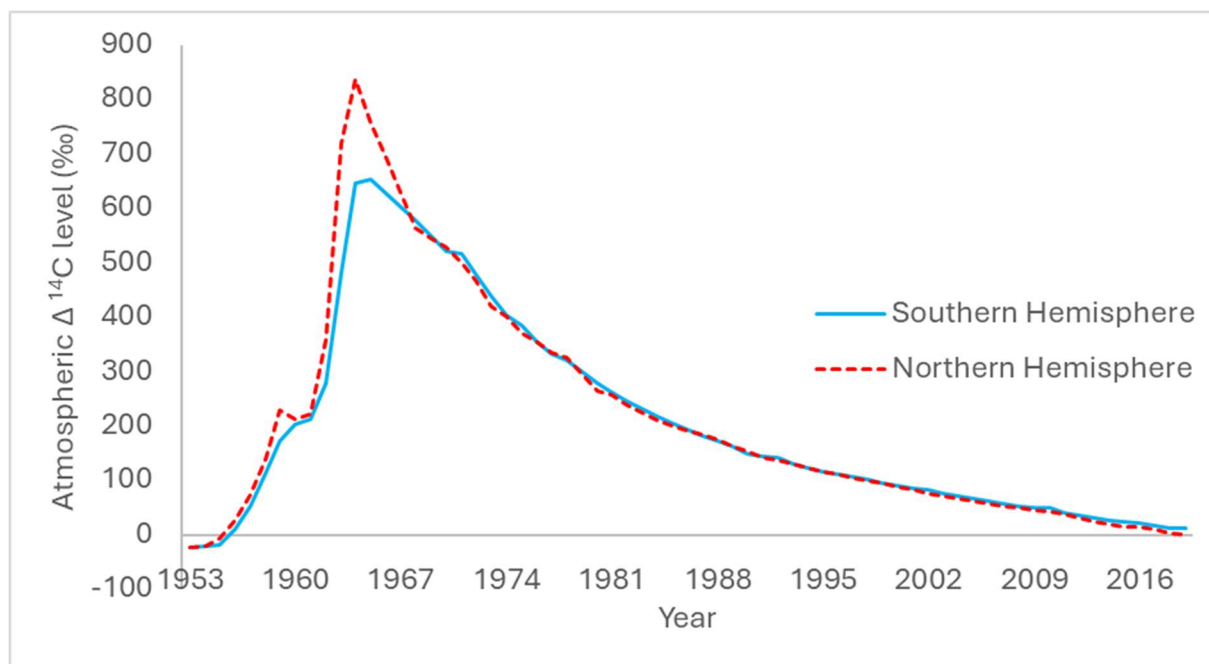


**Figure 4.2.** Atmospheric  $\Delta^{14}\text{C}$  spike for the southern hemisphere. Data are from Hua et al. 2019 where eight monitoring stations were averaged.

## 4.2. Methods

### 4.2.1 Sample Preparation

Two radiocarbon dead bone samples (Hollis Mine Mammoth) and two samples of known  $\Delta^{14}\text{C}$  (specify which one) were processed alongside all of the samples in order to determine background  $^{14}\text{C}$  levels and assess the consistency of the sample pretreatments. The collagen isolation process started with the removal of lipids from the samples. The removal of lipids is an important process when isolating collagen as lipids contain a large amount of carbon and may have a different turnover rate than collagen (Guiry *et al.*, 2016). These factors could have an impact on the estimated turnover rates as these are based on the  $^{14}\text{C}$  content of all carbon in the sampled material. The lipid extraction process involved one hour of sonication at room temperature, with the samples suspended in a 2:1 solution of chloroform and methanol (Folch and Stanley, 1957). The solution was then replaced with fresh chloroform-methanol solution, and

this sonication process was repeated twice more for a total of three treatments. This sequence effectively removed the lipids, allowing them to be separated from the bone samples and subsequently discarded. This pretreatment is important, as ultrafiltration alone cannot remove lipids (Guiry et al 2016). The efficacy of this pretreatment can be confirmed by assessing the resulting C:N ratios of the collagen (Guiry and Szpak, 2020). Samples were left to dry at room temperature in a fumehood before moving onto the next step. The next phase involved demineralization, where the samples were placed in 8 mL of 0.5 M hydrochloric acid. This demineralization process lasted for 48 h at room temperature while the samples were kept in continuous motion using an orbital shaker. Complete demineralization was indicated by the bone samples being soft and rubbery. Once complete demineralization was achieved, the samples were rinsed to neutrality using Type I water. Following the neutralization, the water was decanted and 3 mL of 0.01 M hydrochloric acid was added to the tube, and the samples were transferred to an oven. Here, they were refluxed at a temperature of 65°C for 36 h. Once the reflux process was concluded, the solution containing the solubilized collagen underwent an ultrafiltration process with Amicon 30 kDa molecular weight cutoff ultrafilters. The solubilized collagen was added to the ultrafilter and the solution was centrifuged at 3000 rpm for 20 min. This caused smaller, non-collagenous molecules to filter through the membrane of the ultrafilter, and the remaining solution was placed in a 4 mL vial. These vials were then frozen and subsequently subjected to lyophilization under vacuum conditions using a freeze dryer.

#### *4.2.2 Isotope Ratio Mass Spectrometry*

Prior to sending the samples to UC Irvine for AMS radiocarbon dating, stable isotope and elemental analyses were performed on 0.5-0.6 mg aliquots of each collagen sample (except for the  $^{14}\text{C}$  standards) after weighing the samples into tin capsules.  $\delta^{13}\text{C}$ ,  $\delta^{15}\text{N}$ , %C, and %N values

were obtained using a EuroEA 3000 Elemental Analyzer (EuroVector SpA) coupled with a Nu Horizon continuous flow isotope ratio mass spectrometer at the Trent University Water Quality Center. To assess analytical precision, a 7% sample duplication rate was employed.  $\delta^{13}\text{C}$  and  $\delta^{15}\text{N}$  values were calibrated relative to VPDB and AIR using a three-point calibration curve based on USGS40 ( $\delta^{13}\text{C} = -26.39 \pm 0.04 \text{ ‰}$ ,  $\delta^{15}\text{N} = -4.52 \pm 0.04 \text{ ‰}$ ), USGS63 ( $\delta^{13}\text{C} = -1.17 \pm 0.04 \text{ ‰}$ ,  $\delta^{15}\text{N} = +37.83 \pm 0.06 \text{ ‰}$ ), and USGS66 ( $\delta^{13}\text{C} = -0.67 \pm 0.04 \text{ ‰}$ ,  $\delta^{15}\text{N} = +40.83 \pm 0.06 \text{ ‰}$ ) (Qi et al., 2003; Schimmelmann et al., 2016). To ascertain accuracy and precision, in-house standards of caribou bone collagen (SRM-1,  $\delta^{13}\text{C} = -19.39 \pm 0.09 \text{ ‰}$ ,  $\delta^{15}\text{N} = 1.85 \pm 0.19 \text{ ‰}$ ), polar bear bone collagen (SRM-14,  $\delta^{13}\text{C} = -13.63 \pm 0.09 \text{ ‰}$ ,  $\delta^{15}\text{N} = 21.50 \pm 0.22 \text{ ‰}$ ), marine fish collagen (SRM-26,  $\delta^{13}\text{C} = -16.17 \pm 0.10 \text{ ‰}$ ,  $\delta^{15}\text{N} = 14.69 \pm 0.18 \text{ ‰}$ ) and alanine (SRM-28,  $\delta^{13}\text{C} = -16.27 \pm 0.09 \text{ ‰}$ ,  $\delta^{15}\text{N} = -1.94 \pm 0.18 \text{ ‰}$ ) were incorporated into each run. These standards have C:N ratios that closely resemble the anticipated range for human bone collagen, and their  $\delta^{13}\text{C}$  and  $\delta^{15}\text{N}$  values encompass the upper and lower limits expected for the samples.

#### 4.2.3. Analytical Uncertainty

Analytical uncertainty was estimated using the method outlined in Szpak et al. (2017). The random error or  $u(Rw)$  for the measurements was calculated to be  $\pm 0.07 \text{ ‰}$  for  $\delta^{13}\text{C}$  and  $\pm 0.21 \text{ ‰}$  for  $\delta^{15}\text{N}$ . This determination was derived from replicates of calibration standards, check standards, and sample duplicates. The systematic error, or  $u(bias)$  was calculated at  $\pm 0.09 \text{ ‰}$  for  $\delta^{13}\text{C}$  and  $\pm 0.28 \text{ ‰}$  for  $\delta^{15}\text{N}$  based on the difference between the observed and known  $\delta$  values of the standards. The overall analytical uncertainty was calculated to be  $\pm 0.13 \text{ ‰}$  for  $\delta^{13}\text{C}$  and  $\pm 0.32 \text{ ‰}$  for  $\delta^{15}\text{N}$ .

#### 4.2.4 Sample Preparation for AMS Radiocarbon Dating

In a quartz tube, 2.0-2.4 mg of collagen from each sample was combusted with 40-50 mg of CuO and silver wire. Radiocarbon-dead collagen and standard collagen with known age were also combusted in duplicate in order to assure quality control standards were met. These samples were then graphitized at 525°C for 2.5 h. The samples were pressed and loaded into a 0.5 MV NEC-AMS at the KCCAMS laboratory at the University of California Irvine.

#### *4.2.5. Mathematical Model for Estimating Bone Turnover*

The  $\Delta^{14}\text{C}$  data generated by AMS can be utilized to calculate the turnover rate of the measured element. This relies on knowledge of two key factors: the  $\Delta^{14}\text{C}$  content of the sample ( $C_{\text{measured}}$ ) and the atmospheric  $\Delta^{14}\text{C}$  content at any year of life ( $C_y$ ) from the year of birth ( $b$ ) to the year of death ( $d$ ). Additionally, we must assign a weight to each  $C_y$ , which can also be thought of as the turnover rate ( $x$ ) for each year ( $x_y$ ). In cases where it is assumed that all years are evenly represented (a fixed rate turnover), this weight will be equal in every year prior to death over the interval for turnover. The turnover interval is  $100\%/x$  (a turnover rate of 10% would have a turnover interval of 10 years). This is how turnover rate is frequently discussed, as a suggested annual turnover rate of roughly 3% by Hedges et al (2007) is often taken to mean a roughly 30 year turnover interval for the adult human femur.

However, when it is assumed that each year is not evenly represented within a bone collagen sample (fluctuating rate turnover), a specific weight ( $x_y$ ) can be assigned for each year. For instance, if the element has a decreasing rate of turnover and a decay constant ( $Z$ ) of 0.5, the earliest year of life can be weighted as 0.5, the next would be 0.25, the next would be 0.125, and so forth until the year of death. In the case of a fluctuating turnover model, each year, the turnover rate is applied to the previous year's expected  $\Delta^{14}\text{C}$  contents and this continues until the

individual's death, pointing to what their final  $\Delta^{14}\text{C}$  values should be ( $C_{\text{expected}}$ ). If the  $C_{\text{expected}}$  matches the  $C_{\text{measured}}$ , then the model used is a feasible solution for that sample's turnover rates.

#### 4.2.6. Fixed rate model

The equation defining the  $C_{\text{expected}}$  for any given  $x$  is as follows:

$$\sum_{y=i}^d C_y x = C_{\text{expected}} \quad \text{Eq. (1)}$$

Where  $d$  refers to the year of death,  $C_y$  refers to the  $\Delta^{14}\text{C}$  value at any given year ( $y$ ),  $x$  refers to the turnover rate, and  $i$  refers to the starting year for a given turnover interval, or  $i = d - (1/x + 1)$ ,

For a fixed rate turnover, each potential  $x$  will produce a different  $C_{\text{expected}}$ , which can be compared to the  $C_{\text{measured}}$ . When the expected and measured  $\Delta^{14}\text{C}$  values match, this suggests that the estimated turnover rate is plausible.

To demonstrate how a fixed model works for estimating turnover rates of skeletal elements from radiocarbon values, I present a small forensic case study where radiocarbon values for certain skeletal elements were given but were not used to measure turnover. The data from Calcagnile et al. (2013) provides  $\Delta^{14}\text{C}$  values of various tissues to confirm the age of an unidentified body, reporting the  $\Delta^{14}\text{C}$  values of the occipital bone collagen. Using eq (1), I was able to determine the possible turnover rate of this bone.

The individual used in this example was born in 1973 and died in 2009, so was 36 years old at the time of death. A collagen sample from the occipital of this individual had a  $\Delta^{14}\text{C}$  of +136.3 ‰ ( $C_{\text{measured}}$ ). Manipulating eq. (1) to include the information from this individual to predict the estimated  $\Delta^{14}\text{C}$  ( $C_{\text{estimated}}$ ) given a value of  $x$ , where  $x$  is then manipulated to get the prediction close to the observation ( $C_{\text{measured}}$ ) is demonstrated by eq. (2).

$$(C_{2009}x) + (C_{2008}x) + \dots (C_i x) = C_{\text{expected}} \quad \text{Eq. (2)}$$

Assessing what the expected turnover rate would be with an interval of the entire life of the individual ( $i=37$  years, annual turnover rate of 2.7%) would yield a  $\Delta^{14}\text{C}$  content that is too high, as demonstrated in the eq. (3).

$$\begin{aligned} (C_{2009}2.7\%) + (C_{2008}2.7\%) + \dots (C_{1973}2.7\%) &= C_{\text{expected}} & \text{Eq. (3)} \\ (45.8 \times 0.027) + (49.4 \times 0.027) + \dots (418.6 \times 0.027) &= 174.5 \end{aligned}$$

Considering a much more rapid turnover rate or an annual turnover rate of 10% ( $i = 10$  years) would yield a  $\Delta^{14}\text{C}$  content that is too low, as demonstrated in the eq. (4).

$$\begin{aligned} (C_{2009}10\%) + (C_{2008}10\%) + \dots (C_{1999}10\%) &= C_{\text{expected}} & \text{Eq. (4)} \\ (45.8 \times 0.10) + (49.4 \times 0.10) + \dots (94.1 \times 0.10) &= 64.8 \end{aligned}$$

An iterative process reveals that when  $x=3.2\%$  and  $i = 31$  year, this provides the closest match for both sides of the equation, demonstrating that with this equal turnover framework, the occipital bone represents the last 31 years of life, as shown in eq. (5).

$$\begin{aligned} (C_{2009}3.2\%) + (C_{2008}3.2\%) + \dots (C_{1979}3.2\%) &= C_{\text{expected}} & \text{Eq. (5)} \\ (45.8 \times 0.032) + (49.4 \times 0.032) + \dots (295.8 \times 0.032) &= 137.3 \end{aligned}$$

We can confirm this interval by creating a trendline of the expected  $\Delta^{14}\text{C}$  for every interval of turnover. For this case, a final year of life in 2009 creates the trendline in Figure 4.3. This trendline which fits the plotted results in a 3<sup>rd</sup> order polynomial, produces the equation seen in Figure 4.3. This equation can be used to quickly determine the interval and fixed turnover rate for any skeletal element from this individual that has a measured  $\Delta^{14}\text{C}$  value. For instance, by letting  $y = +136.3 \text{ ‰}$ , the equation yields an  $x$  of 3.2%, again informing us that (if turnover is fixed) this individual's occipital bone had an annual turnover rate of 3.2% over 31 years.

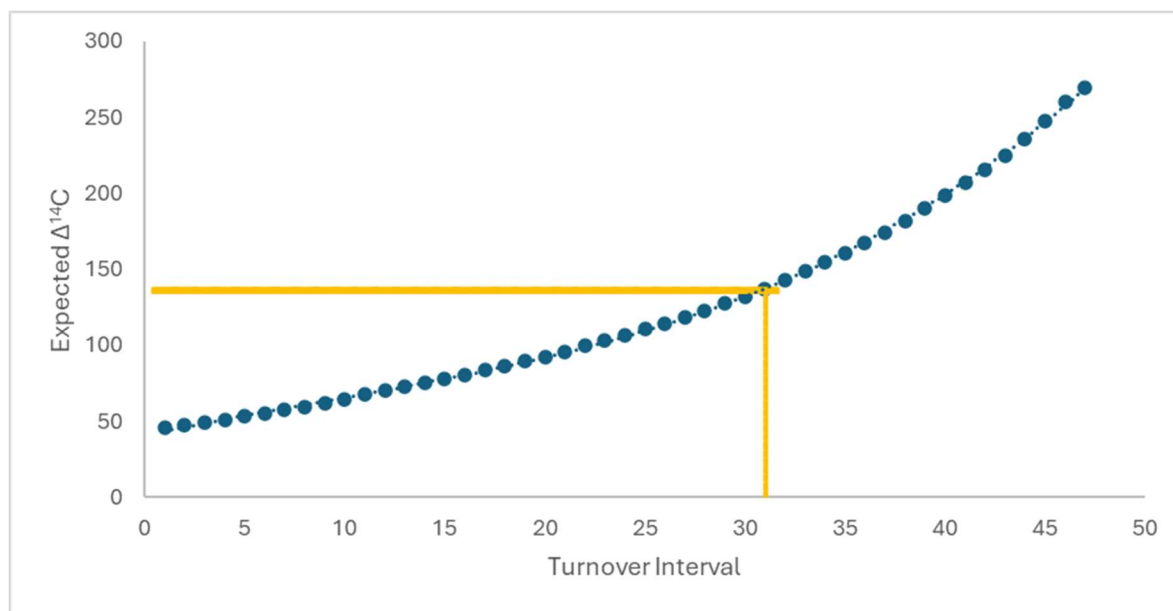


**Figure 4.3.** Expected  $\Delta^{14}\text{C}$  for each turnover interval interval for an individual who died in 2009 (dots) and the third order polynomial function fitted to these data. The solid lines highlight the intersect of an expected  $\Delta^{14}\text{C}$  of +136.3‰ and an interval of 31 (3.2% annual turnover).

#### 4.2.7. Decaying turnover rate model

In a scenario where the turnover rate can fluctuate year to year, there are countless possible models that would lead to the expected  $\Delta^{14}\text{C}$  matching the measured  $\Delta^{14}\text{C}$  of a sample. Under a fluctuating turnover model, any year's atmospheric  $^{14}\text{C}$  can be given any weight, however this leads to endless possible solutions, some of which are clearly illogical and inconsistent with everything that is known about bone biology. For example, if a bone collagen sample was taken from someone who was born in 1950 and died in 2024 and had a  $\Delta^{14}\text{C}$  value of 334 ‰, this could mean that 100% of the sampled bone was formed or replaced in 1977, when the northern hemisphere had an atmospheric value of close to 334 ‰. In this scenario, no new bone tissue would have formed in any year after 1977 and all of the previous bone was replaced in this year as well. This would be highly unlikely as the remodeling of bone, however small, keeps the bone from becoming too ridged and dry (Safadi et al., 2009). While there are an infinite number of scenarios that *could* work in the equation under a fluctuating turnover rate

(i.e., could produce a feasible solution), logic must be used to eliminate some of these possibilities. Therefore, I applied a decaying turnover rate model as it provides a static decay constant ( $Z$ ) which determines each annual turnover rate, and it makes the most sense based on what is known about bone remodeling and aging (Feik et al., 1996; Frost, 1997; Fahy et al., 2017).

To illustrate the concept of an exponential decay function, consider the following example. Suppose we have a function with a decay constant of 50%. This means that at birth, the function exhibits 100% turnover. By  $x_1$ , it decreases to 50%, then to 25% by  $x_2$ , and so on until death. This pattern is depicted in Figure 4.4. This is mathematically expressed using eq. (6).

$$x_y = (x_y - 1)(1 - Z) \quad \text{Eq. (6)}$$

Where  $x_y$  refers to the turnover rate ( $x$ ) at any given year in life ( $y$ ).  $Z$  represents the decay constant as a decimal, and it is assumed that  $x_0 = 100\%$ . In this scenario, the percentage of bone turned over in any given year is defined by  $e^{-0.693}$ .

With a decay constant of 10%, the annual turnover rates would be as follows in eq. (7) ( $e^{-0.105}$ ).

$$\begin{array}{rcl} X_0 & & = 100\% \\ X_1 & = 100\% \times (1 - 0.10) & = 90\% \\ X_2 & = 90\% \times (1 - 0.10) & = 81\% \\ X_3 & = 81\% \times (1 - 0.10) & = 72.9\% \end{array} \quad \text{Eq. (7)}$$

This process continues until the individual's year of death. Determining the 'correct' decay constant for a sample involves an iterative process of testing various decay constants within the original equation until the result matches the real measured  $\Delta^{14}\text{C}$  of that sample.

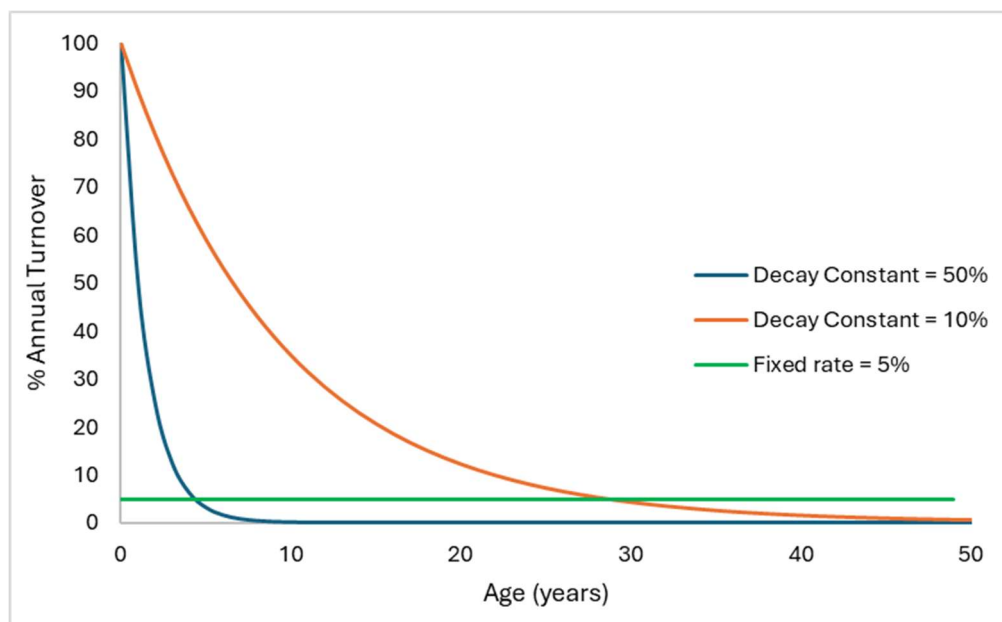


**Figure 4.4.** The percentage of the total bone turned over from each year since birth for two different decay constants (50% and 10%). An annual fixed rate turnover of 5% is included to highlight the differences between the two rate types.

This decay function stresses that bone experiences more change in early life before growth is complete. The years close to death in older individuals therefore have low turnover rates, and the bone is mostly represented by tissue that was formed earlier in life. Figure 4.4 shows how at lower decay constants, a higher percentage of the total bone is replaced in only a few years. At a 50% decay constant, the percent turned over each year quickly becomes less than 1% and bone formed during the later years of life would not significantly influence the bone's  $\Delta^{14}\text{C}$  content.

Because each individual's specific birth and death years are known, and the atmospheric  $\Delta^{14}\text{C}$  content is well understood, decay constants ( $Z$ ) were substituted within eq. (8) until the  $C_{\text{expected}}$  matches the  $C_{\text{measured}}$ , thus indicating a possible decay constant and turnover rates for that sample.

$$C_{\text{expected}(y)} = (1 - Z^a) \times C_{\text{expected}(y-1)} + C_y Z^a \quad \text{Eq. (8)}$$

Here,  $C_{\text{expected}(y)}$  refers to the estimated  $\Delta^{14}\text{C}$  content that the individual would have had at any year of life ( $y$ ).  $Z$  refers to the decay constant,  $a$  refers to the age of the individual at the desired year, and  $C_y$  refers to the atmospheric  $\Delta^{14}\text{C}$  content within that year. This equation can be worked backwards until birth ( $b$ ), where  $C_{\text{expected}(b)}$  is thought to be equal to  $C_y$ .

It must be noted that the turnover interval is not especially meaningful in this scenario, as the years included within the interval are unevenly represented. These decay functions can also provide an estimate of the rate of bone turnover at any age, giving a rough estimation of how much bone is changing at each point in an individual's life, although these earlier rates must be taken with a grain of salt and are associated with much more uncertainty.

#### 4.2.7. *Hedges et al. (2007) model*

An alternative model presented by Hedges et al. (2007) has produced the estimated turnover interval most frequently cited in today's literature. Hedges and colleagues established a sex-specific turnover model, employing a fluctuating turnover pattern (Figure 4.5). The general shape of the curve broadly resembles the exponential decay function discussed previously but is more linear in nature. This approach involved delineating inflection points where the turnover rate transitioned, gradually decreasing each year until reaching the subsequent inflection point. The age of these inflection points was determined based on life stages for each sex, and turnover rates were derived from an average best fit for the sampled femora. The specific values used to generate the curves in Figure 4.5 are presented in Table 4.3

**Table 4.3.** The model used by Hedges et al. (2007) with varying turnover rates based on sex and age.

Inflection Point	Age (Males)	Annual Turnover rate (%)	Age (Females)	Annual Turnover rate (%)
Birth	0	50 ± 20	0	50 ± 20
Adolescence	17	13.7 ± 1.3	15	6 ± 4
Cessation of growth	25	3 ± 1.5	19	4 ± 1
Death definitely occurred	100	1.5 ± 0.7	100	3 ± 1

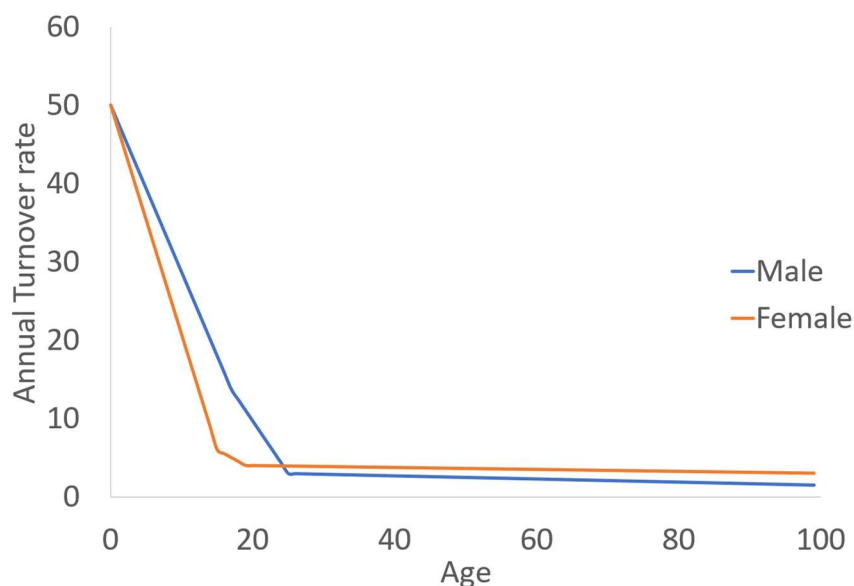


**Figure 4.5.** The average annual turnover rate at each age for the femur from the Hedges et al. (2007) paper for both male and female individuals.

The Hedges et al. (2007) study only analyzed femur samples, which allowed for the femurs from REST[ES] and other published datasets to be tested using the parameters of this model. Each femur sample's expected  $\Delta^{14}\text{C}$  were modeled using Hedges et al.'s (2007) turnover rates for each age and compared to the real measured  $\Delta^{14}\text{C}$  of each femur sample. This was done with the average as well as both upper and lower limits of turnover rates at each inflection point. The expected and measured  $\Delta^{14}\text{C}$  were statistically compared to determine if the Hedges et al. (2007) can accurately predict the remodelling patterns of an adult femur.

#### 4.2.8. Data Treatment

The results of the stable isotopic analysis were used to determine if a large portion of each individual's diet came from marine resources, in order to assess whether or not the marine

reservoir effect has influenced the  $\Delta^{14}\text{C}$  values of the samples. The ocean experienced a more dampened increase in  $\Delta^{14}\text{C}$  content caused by nuclear weapons testing (Dutta 2016), and therefore, the contribution of substantial amounts of marine protein in the diet may produce inaccurate turnover estimates. A study from Canada found that Canadian diets are very homogenous due to food industrialization (Bataille et al., 2020), which highlights that an appreciable amount of marine protein in Canadian diets is rare, outside of some Inuit communities. However, a range indicative of a highly marine influenced diet may still be useful. Schoeninger and DeNiro (1984) suggested that  $\delta^{13}\text{C}$  values of  $-16.5\text{‰}$  or higher coupled with  $\delta^{15}\text{N}$  values of  $+13.6\text{‰}$  are considered to be indicative of a high percent marine diet. An isotopic study of fingernails of the Uummannaq Inuit population of Greenland, who mainly eat marine protein, found that their values were above  $+12\text{‰}$  for  $\delta^{15}\text{N}$  and above  $-20\text{‰}$  for  $\delta^{13}\text{C}$  (Buchardt et al. 2007).

The  $\Delta^{14}\text{C}$  values were each substituted into different equations to determine the turnover rate of the sample through an iterative process that attempted to match the  $\Delta^{14}\text{C}$  content of the measured sample with the modeled  $\Delta^{14}\text{C}$  content based on Equations 1 and 2 (varying the number of years included in the interval and the relative weighting of each year). The results of the models were compared to one other within an individual to determine if bone turnover rate varied among and within different skeletal elements. Differences in turnover rate within the same skeletal element across different individuals informed inferences about how life history factors could affect bone collagen turnover rate.

All distributions were first tested for normality using a Shapiro Wilk test. For comparisons of results (i.e. decay constants, fixed turnover rates) between two groups, such as males and females, an F-test was performed to assess the equality of variance, followed by a t-

tests (when variances were equal) or a Welch's t-test (when variances were unequal). If distributions were found to be not normal, a Mann-Whitney U test was performed. For comparisons involving three or more groups, a one-way analysis of variance (ANOVA) was performed when all distributions were normal, followed by Levene's test to assess equality of variances. When variances were equal, a *post hoc* Tukey's HSD test was performed and when variances were unequal, a Dunn's *post hoc* test was performed. A Kruskal Wallis test was used in place of the ANOVA to assess differences in three or more groups when one or more of those groups were characterized by a non-parametric distribution.

In order to estimate the percentage of each sample that can be attributed to each period of an individual's life, Python script was employed using the Google Colaboratory software to model how the bone tissue would change with each resulting turnover rate for the decaying model, and this python script that was generated with the assistance of A.I. is shown in figure S.1. (OpenAI. 2024). This model uses a selection of 100 BMUs and randomly replaces a specified percentage of the BMUs based on the annual turnover for each year. This was done for all years until the age of each individuals' death. At death, each of the 100 BMUs in the model indicated the last year they were 'turned over', and these years were collected to summarize the percentages of BMUs that came from each period of life in the sample. Since the BMUs were randomly changed, variation would exist between runs of the same model, and therefore for each sample, the model was run 1,000 times and the average and standard deviation from each decade of life was recorded.

## Chapter 5: Results

**Table 5.01.** Calibrated isotopic and elemental data for all bone collagen samples analyzed in this study. P.S.= pubic symphysis, I.C. = iliac crest, I.P.R= ishiopubic ramus, G.S.N.= greater sciatic notch

Donor #	Sex	Age	Element	Side	Sample ID	$\delta^{13}\text{C}$	$\delta^{15}\text{N}$	%C	%N	C:N Atomic	$\Delta^{14}\text{C}$ (‰)
3	F	69	Femur	R	20491	-18.05	10.94	42.5	15.0	3.30	+ 199.07
			Rib	L	20492	-17.96	11.02	41.1	14.5	3.29	+ 176.77
			Vertebra		20493	-17.88	10.89	41.6	14.8	3.29	+ 48.94
			Ulna	R	20494	-18.07	11.30	41.2	14.8	3.25	+ 337.44
			P.S		20495	-17.89	10.39	40.3	14.4	3.27	+62.70
			I.C.		20496	-18.03	10.51	41.2	14.6	3.29	+89.55
			Humerus	L	20497	-18.13	11.20	41.8	14.7	3.32	+ 302.02
5	M	72	Femur	R	20498	-17.93	10.76	41.8	14.9	3.26	+ 302.72
			Rib	R	20499	-17.88	10.69	40.5	14.7	3.20	+ 241.87
			Ulna	R	20500	-17.90	10.99	40.1	14.6	3.21	+ 391.82
			P.S		20501	-18.12	10.27	41.3	14.7	3.27	+ 101.15
			Vertebra		20502	-17.97	10.35	40.5	14.5	3.26	+ 53.56
			I.C.		20503	-18.03	11.44	40.8	14.6	3.26	+ 166.96
			Humerus	L	20504	-17.86	10.46	40.3	14.6	3.22	+ 275.74
6	M	77	Ulna	L	20507	-17.36	11.12	41.0	14.7	3.25	+ 173.61
			Rib	L	20508	-17.51	10.71	41.3	14.9	3.23	+ 88.32
			P.S.		20509	-17.63	10.50	39.9	14.3	3.25	+ 29.59
			Humerus	L	20510	-17.16	11.20	41.3	15.1	3.19	+ 215.11
			I.C		20511	-17.42	10.57	41.0	14.9	3.20	+ 84.66
10	M	78	Femur	R	20512	-17.07	11.13	40.8	14.5	3.28	+ 132.72
			Rib	L	20513	-17.55	10.78	40.3	14.6	3.22	+ 57.34
			Ulna	R	20514	-16.93	11.64	41.4	15.1	3.20	+ 205.48
			P.S.		20515	-17.71	10.63	40.1	14.2	3.29	+ 33.99

Donor #	Sex	Age	Element	Side	Sample ID	$\delta^{13}\text{C}$	$\delta^{15}\text{N}$	%C	%N	C:N Atomic	$\Delta^{14}\text{C}$ (‰)
			Vertebra		20516	-17.61	11.15	41.4	15.0	3.22	+ 45.03
			Humerus	L	20517	-16.94	11.66	41.1	14.8	3.24	+ 222.30
			I.P.R	R	20518	-17.79	10.58	41.6	14.8	3.27	+ 29.86
11	M	54	Femur	R	20519	-17.30	10.62	40.8	14.5	3.27	+ 180.69
			Rib	R	20520	-16.91	10.42	41.2	14.9	3.24	+ 94.37
			P.S.		20521	-16.95	10.18	40.4	14.5	3.25	+ 66.86
			Ulna	L	20522	-17.09	10.40	41.4	15.1	3.20	+ 155.24
			Humerus	L	20523	-17.04	10.55	40.9	14.8	3.22	+ 140.83
			G.S.N.		20524	-16.80	10.29	40.8	14.6	3.26	+ 58.70
12	F	73	Femur	R	20525	-17.37	10.99	41.0	14.8	3.22	+ 164.30
			Vertebra		20527	-16.41	10.31	40.2	14.7	3.19	+ 32.59
			Humerus	L	20528	-17.86	10.68	42.3	14.3	3.46	+ 131.12
17	M	73	Ulna	R	20529	-17.09	11.35	40.4	14.5	3.25	+ 405.51
			Femur	L	20530	-17.30	10.74	41.2	14.8	3.23	+ 201.41
			Rib	L	20531	-17.35	11.02	40.6	14.5	3.26	+ 219.42
			Vertebra		20532	-17.48	11.04	49.3	18.0	3.20	+ 41.08
			Humerus	L	20533	-17.20	11.14	39.4	14.4	3.20	+ 229.73
			I.P.R.		20534	-17.35	11.84	51.3	18.4	3.26	+ 182.20
6	M	77	Femur	R	20505 A1	-17.25	10.78	40.4	14.8	3.19	+ 167.50
			Femur	R	20505 A2	-17.35	11.11	40.9	14.7	3.24	+ 161.44
			Femur	R	20505 B1	-17.12	10.47	40.3	14.9	3.16	+ 139.19
			Femur	R	20505 B2	-17.44	11.07	41.4	15.1	3.20	+ 122.01
			Femur	R	20505 C1	-17.37	11.02	40.9	14.9	3.20	+ 151.05
			Femur	R	20505 C2	-17.37	11.03	40.1	14.6	3.20	+ 174.01
			Femur	R	20505 D1	-17.30	10.48	40.5	14.8	3.19	+ 87.10
			Femur	R	20505 D2	-17.24	10.94	40.5	14.9	3.18	+ 162.90
			Mandible		20506 A	-17.34	11.07	40.8	14.7	3.24	+ 141.80

Donor #	Sex	Age	Element	Side	Sample ID	$\delta^{13}\text{C}$	$\delta^{15}\text{N}$	%C	%N	C:N Atomic	$\Delta^{14}\text{C}$ (‰)
			Mandible		20506 B	-17.39	11.11	41.3	14.8	3.25	+ 107.5
12	F	73	Rib	L	20526 A	-16.70	10.34	40.6	14.9	3.21	+ 54.30
			Rib	L	20526 B	-16.66	10.58	53.9	19.4	3.25	+ 45.00

## 5.1. Stable isotope compositions of REST[ES] donors

The stable isotope data for all the bone collagen samples analyzed in this study are presented in Table 5.01. The quality control criteria for all but 7 out of 53 samples analyzed are within the very stringent acceptable range of 3.00-3.28 for the atomic C:N of modern bone collagen (Guiry and Szpak, 2020); six samples had atomic C:N ratios between 3.29 and 3.32, and one had an atomic C:N ratio of 3.46. There was a statistically significant correlation between the C:N ratios and  $\delta^{13}\text{C}$  values for these bone collagen samples (Pearson's  $r$ ;  $r=-0.45$ ,  $p<0.001$ ) (figure 5.01). Removing any samples that produced C:N ratios above 3.28, still produced a significant correlation between C:N and  $\delta^{13}\text{C}$  (Pearson's  $r$ ;  $r=-0.32$ ,  $p=0.03$ ). It is therefore possible that some lipids remained in some of the samples with higher C:N ratios as they are not removed by ultrafiltration (Guiry et al., 2016), but the relative abundance of these lipids was very small as evidence by the low variation in  $\delta^{13}\text{C}$  for these individuals (Table 5.01). The elemental concentrations (%C and %N) are very similar to what is expected for modern mammalian bone collagen (Guiry and Szpak, 2020). While all of the  $\delta^{13}\text{C}$  values were above  $-20$  ‰ (likely due to a relatively high amount of maize-foddered animal protein in the diet) (Jahren and Kraft 2008), there were no  $\delta^{15}\text{N}$  values greater than  $+12$  ‰, suggesting negligible impact of marine foods. Since the samples are not within the marine-influenced diet range, it can be concluded that any  $\Delta^{14}\text{C}$  values produced were not affected by the marine reservoir effect to any significant extent.

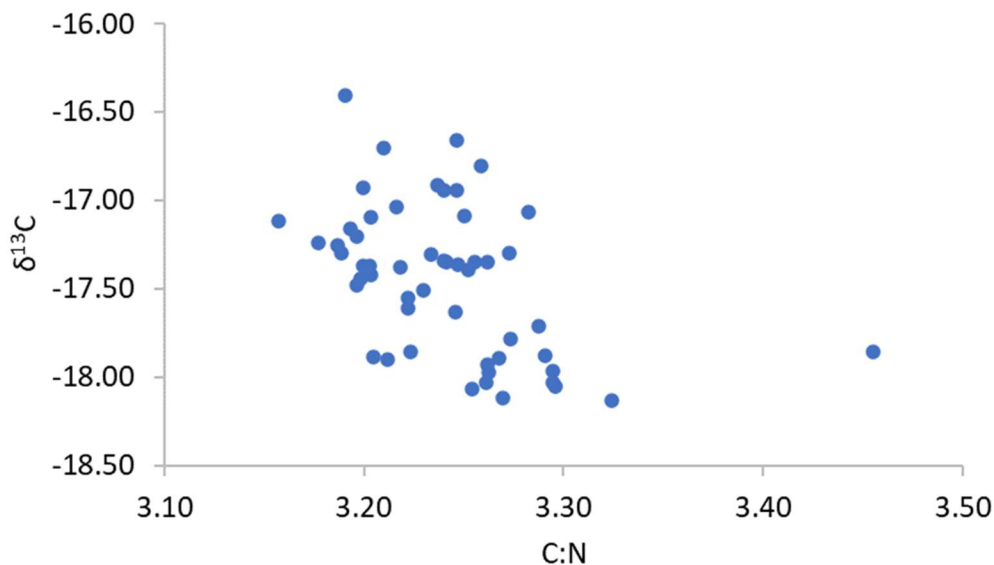


**Figure 5.01.**  $\delta^{13}\text{C}$  values of samples from REST[ES] compared to their corresponding C:N ratios

## 5.2. Qualitative assessments of measured $\Delta^{14}\text{C}$ values

In general, the samples with the highest  $\Delta^{14}\text{C}$  values will contain more BMUs that were formed when the atmospheric  $^{14}\text{C}$  content was at or near its peak, implying that they have the longest turnover intervals weighted towards earlier in life (Figure 5.02). The  $\Delta^{14}\text{C}$  values from the REST[ES] donors vary primarily due to variation in the rate of turnover since their death years are similar. A maximum difference in  $\Delta^{14}\text{C}$  of about 20 ‰ could be the result of variable year of death for these individuals, but this would require a very rapid turnover rate in the last years of life (100% annually). More realistically, because annual turnover rate should be relatively low at the end of life, variation in death year will have a minimal impact on the  $\Delta^{14}\text{C}$  values. Therefore, it is reasonable to make comparisons of the  $\Delta^{14}\text{C}$  values observed among the different skeletal elements for the REST[ES] donors as most of the variation in these values is caused by different turnover rates.

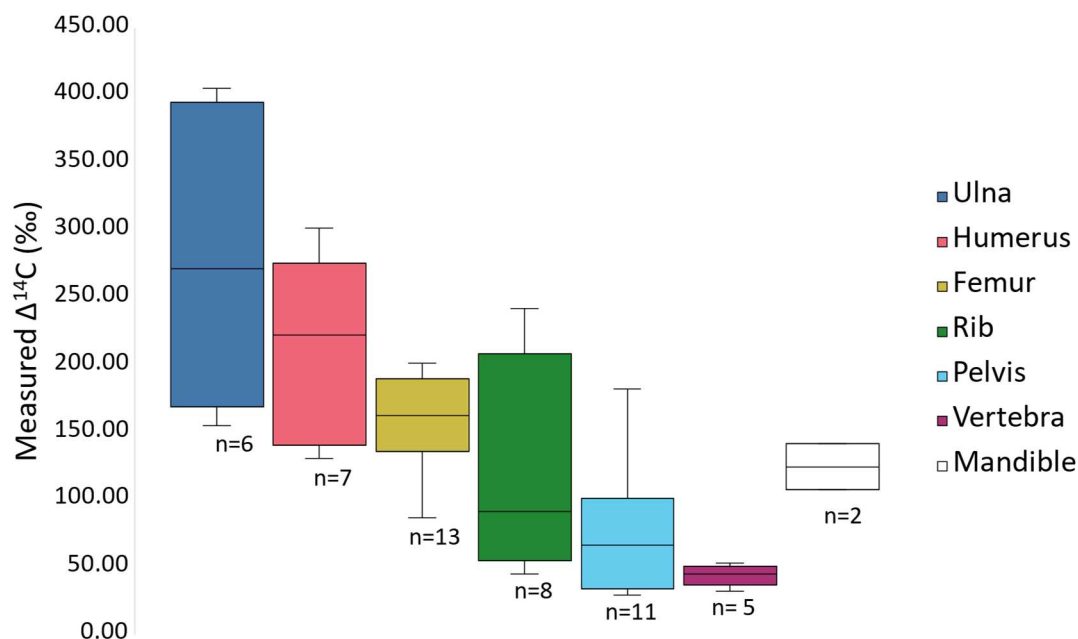


**Figure 5.02.** The  $\Delta^{14}\text{C}$  values from the different elements that were measured across the seven donors sampled.

Different skeletal elements varied significantly with respect to when their BMUs were formed as reflected in their  $^{14}\text{C}$  content (ANOVA test;  $p < 0.01$ ,  $df = 6$ ). Specifically, the pelvis and vertebra were consistently different, with lower measured  $\Delta^{14}\text{C}$  values than long bones (Table 5.02).

**Table 5.02.** Results of Dunn's post-hoc test ( $p$  values) for comparisons of  $\Delta^{14}\text{C}$  values among the skeletal elements analyzed. Statistically significant differences ( $p < 0.05$ ) are indicated in red.

Element	Humerus	Rib	Femur	Pelvis	Vertebra	Mandible
<b>Ulna</b>	0.66	0.02	0.12	<0.01	<0.01	0.12
<b>Humerus</b>		0.04	0.26	<0.01	<0.01	0.21
<b>Rib</b>			0.25	0.25	0.05	0.97
<b>Femur</b>				0.01	<0.01	0.53
<b>Pelvis</b>					0.27	0.46
<b>Vertebra</b>						0.17

### 5.3. Fixed rate model

#### 5.3.1. REST[ES] Samples

Estimates of turnover rates and intervals using the fixed rate model (as described in section 4.2.5) are presented for the REST[ES] donors in Table 5.03 and Figure 5.03. There were 10 cases out of the 53 samples analyzed where the measured  $\Delta^{14}\text{C}$  was so high that a fixed turnover rate or interval could not be calculated. In these cases, even if the turnover interval spanned the donor's entire life, the expected  $\Delta^{14}\text{C}$  would still be too low to match the measured  $\Delta^{14}\text{C}$ . This indicates that more bone turnover must have occurred during years with a higher amount of atmospheric  $^{14}\text{C}$  and therefore a fixed turnover rate through life is untenable. These instances are indicated with "N/A" for the interval and fixed turnover rate in Table 5.03.

**Table 5.03.** Description of the source of each sample and the estimated fixed turnover rate data. Values are ordered by age at death first and then from lowest to highest annual turnover percent. Samples that had  $\Delta^{14}\text{C}$  values that were too high to fit into a fixed rate turnover are indicated with N/A

TEAL Number	Donor Number	Age at death	Skeletal Element	Side/ Specification	Turnover Internal (x)	Annual turnover (%)
20519	11	54	Femur	Right	55.8	1.8
20522			Ulna	Left	52.4	1.9
20523			Humerus	Left	50.2	2
20520			Rib	Right	41.4	2.4
20521			Pubic symphysis		34	2.9
20524			Greater sciatic notch		31.2	3.2
20494			3	69	Ulna	Right
20497	Humerus	Left			N/A	N/A
20491	Femur	Right			55.5	1.8
20492	Rib	Left			52.8	1.9
20496	Iliac Crest				37.9	2.6
20495	Public symphysis				30.2	3.3
20493	Vertebra	Thoracic			25	4
20500	5	72	Ulna	Right	N/A	N/A
20498			Femur	Right	N/A	N/A
20504			Humerus	Left	N/A	N/A
20499			Rib	Right	N/A	N/A

<b>20503</b>			Iliac crest		51.5	1.9
<b>20501</b>			Pubic symphysis		40.5	2.5
<b>20502</b>			Vertebra	Thoracic	26.9	3.7
<b>20529</b>	17	73	Ulna	Right	N/A	N/A
<b>20533</b>			Humerus	Left	N/A	N/A
<b>20531</b>			Rib	Left	N/A	N/A
<b>20530</b>			Femur	Left	59.7	1.7
<b>20534</b>			Ischiopubic ramus		57.3	1.7
<b>20532</b>			Vertebra	Lumbar	25.9	3.9
<b>20525</b>			12	73	Femur	Right
<b>20528</b>	Humerus	Left			48.6	2.1
<b>20526 A</b>	Rib	Left			29.6	3.4
<b>20526 B</b>	Rib	Left			25.7	3.9
<b>20527</b>	Vertebra	Lumbar			19.9	5
<b>20510</b>	6	77	Humerus	Left	59.8	1.7
<b>20505 C2</b>			Femur	Right	55	1.8
<b>20507</b>			Ulna	Left	54.9	1.8
<b>20505 A1</b>			Femur	Right	54.1	1.9
<b>20505 D2</b>			Femur	Right	53.5	1.9
<b>20505 A2</b>			Femur	Right	53.3	1.9
<b>20505 C1</b>			Femur	Right	51.8	1.9
<b>20506 A</b>			Mandible		50.4	2
<b>20505 B1</b>			Femur	Right	50	2
<b>20505 B2</b>			Femur	Right	47	2.1
<b>20506 B</b>			Mandible		44.3	2.3
<b>20508</b>			Rib	Left	40	2.5
<b>20505 D1</b>			Femur	Right	39.7	2.5
<b>20511</b>			Iliac crest		39.1	2.6
<b>20509</b>			Pubic symphysis		18.3	5.5
<b>20517</b>			10	78	Humerus	Left
<b>20514</b>	Ulna	Right			58.8	1.7
<b>20512</b>	Femur	Right			48.9	2.1
<b>20513</b>	Rib	Left			30.7	3.3
<b>20516</b>	Vertebra	Lumbar			25.7	3.9

20515			Pubic symphysis		20.6	4.9
20518			Ischiopubic ramus	Right	18.5	5.4

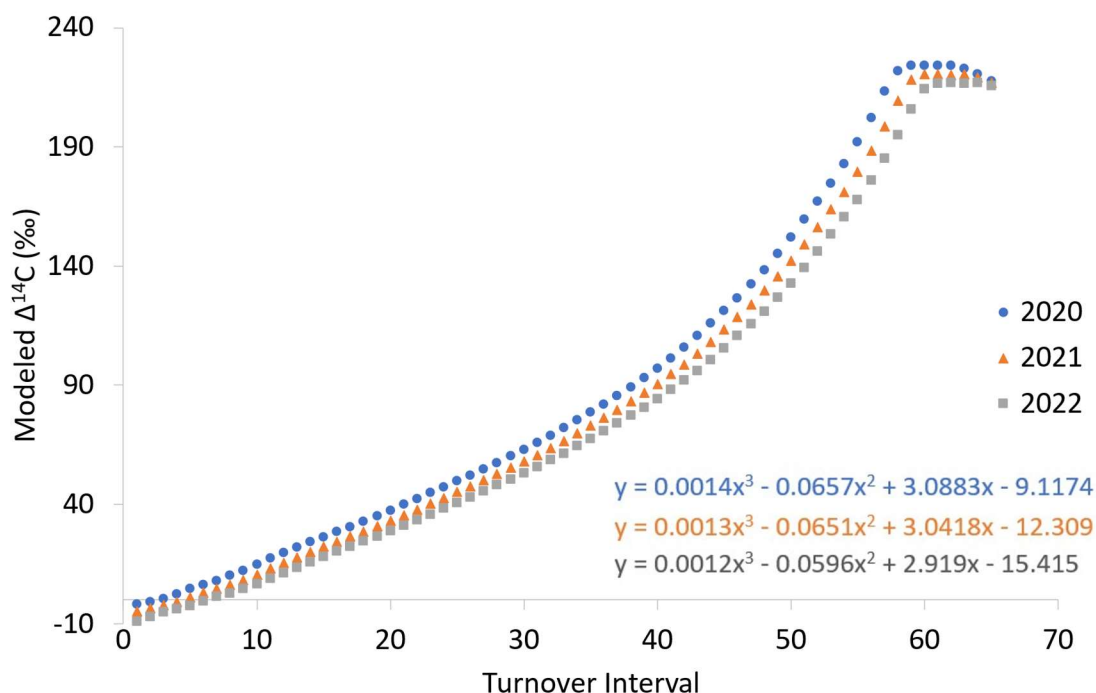


**Figure 5.03.** The modeled  $\Delta^{14}\text{C}$  values for a fixed turnover rate over life in a bone for turnover intervals of up to 60 years with a year of death of 2020, 2021, or 2022 for the northern hemisphere. For example, an individual that died in 2020 having a bone with an interval of 55 years would have a  $\Delta^{14}\text{C}$  value of 195‰ and a bone with an interval of 10 years would have a  $\Delta^{14}\text{C}$  value of 16‰. The equation of each 3<sup>rd</sup> order polynomial curve (prior to the plateau) is also displayed and can be used to generate the fixed turnover rate of any sample from these years.

The results of the fixed rate calculations showed similar results to what the assessment based on  $\Delta^{14}\text{C}$  values alone measured. Three ulnae, four humeri, two ribs, and one femur produced  $\Delta^{14}\text{C}$  which were too high to fit in the model. Consistently, the vertebra and the samples from various locations in the pelvis had the highest fixed rate within each donor, with long bones consistently having the lowest fixed rate and ribs falling between the two categories (Figure 5.04).

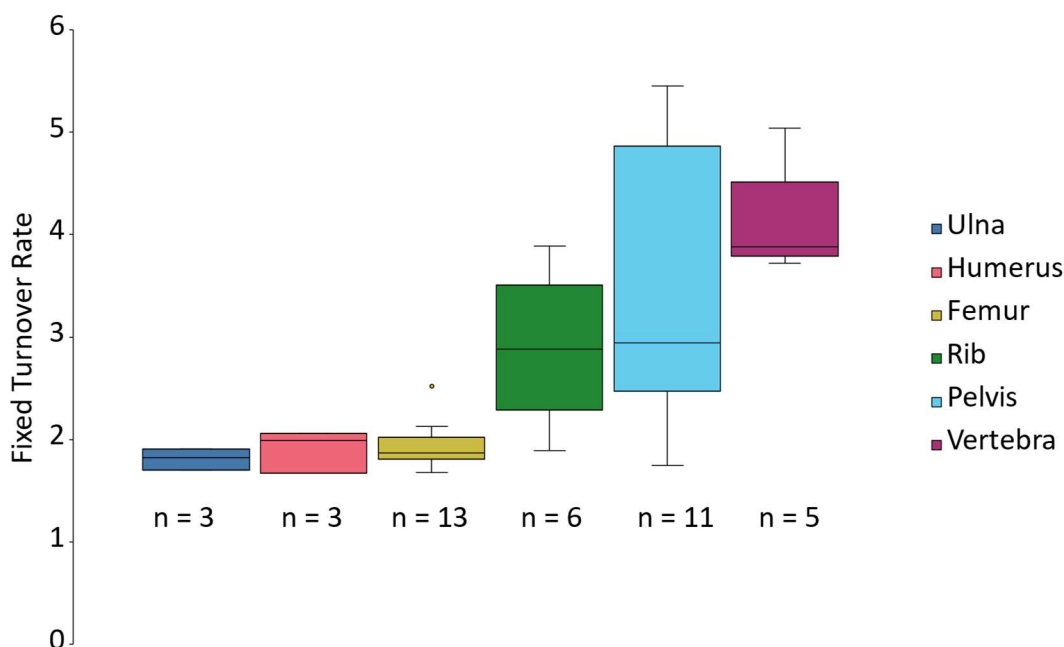


**Figure 5.04.** Fixed turnover rate results for all the donors across the different elements where  $n > 2$ . Elements that produced  $\Delta^{14}\text{C}$  values that were too high have been excluded.

A Kruskal-Wallis H test ( $\chi^2 = 23.48$ ,  $p < 0.001$ ) indicated that there were significant differences between the turnover rates of these elements. The turnover rates of the vertebrae were different from all long bones; the estimated turnover rate of the pelvis and rib were significantly different from both the femur and the ulna (Table 5.04).

**Table 5.04.** Results of Dunn's post-hoc test ( $p$  values) for differences in estimated turnover rate based on a fixed rate model between REST[ES] donor elements. Highlighted cells in red indicate that  $p < 0.05$ .

	Ulna	Humerus	Femur	Rib	Pelvis	Vertebra
Ulna		0.658	0.605	0.035	0.014	0.002
Humerus			0.963	0.111	0.057	0.009
Femur				0.019	0.002	<0.001
Rib					0.821	0.193
Pelvis						0.213

Although the sample size was not large enough that vast generalizations can be made about patterns in turnover across elements, differences were explored to give indications about

what patterns may emerge within an element category. Two kinds of vertebra were sampled: the lumbar and thoracic. The annual turnover rate of the lumbar vertebra averaged 3.2% (n=2) and the thoracic 2.2% (n=3) which suggested that these two types of vertebrae are similar but perhaps not identical (Figure 5.04).

Different locations sampled on the pelvis included the pubic symphysis (n=5), ischiopubic ramus (n=2), iliac crest (n=3), and the greater sciatic notch (n=1). The pelvis had a mean annual turnover rate range of 2.9% across all sampling sites within specific individuals (Figure 5.04), with the lowest turnover rate belonging to the ischiopubic ramus (annual turnover rate of 1.7%) and the highest to the pubic symphysis (annual turnover rate of 5.5%). The ischiopubic ramus was characterized by a wide range of estimated annual turnover rates, ranging from 1.7 to 5.4%, which suggests that the amount of variability in the turnover rates seen within the pelvis is not due only to various locations being included, and that the large range for this element is due to individual differences in turnover rate that exist even within the same location sampled. The pubic symphysis, with more samples, had a range of estimated annual turnover rates between 2.5% and 5.5%, smaller than the ischiopubic ramus, but still large enough to potentially represent different periods of an individual's life. Some donors that had different features from their pelvises sampled had a large degree of variation in estimated rates (e.g., the iliac crest and pubic symphysis of Donor 6 had estimated turnover rates that was 2.6% compared to 5.5% respectively), while others had little variation (e.g., the pubic symphysis and ischiopubic ramus of Donor 10 had estimated turnover rates that ranged from 4.9% to 5.4%). These results suggest that both sampling location within an individual and inter-individual variation can influence the turnover rate in the pelvis, meaning that a turnover rate for this skeletal element would be difficult to predict.

Two samples were taken from neighboring locations along the body of the mandible of one individual. The two samples produced estimated fixed annual turnover rates of 2% and 2.3%, which falls roughly within the middle of the estimated turnover rates estimated for this individual. Two samples from the same rib were divided based on one having more cortical bone and the other having more trabecular bone. The rib sample with the higher proportion of visible cortical bone had a turnover rate of 3.4% and the rib sample with a higher proportion of trabecular bone had a higher estimated annual turnover rate of 3.9%. While these intra-element samples showed a relatively small difference in estimated turnover rates relative to the difference in turnover rates across all bones of their respective donors, absolute differences of 0.3% (mandible) and 0.4% (rib) suggested that skeletal elements were not homogenous with respect to their turnover rates. This finding is further supported by the multiple samples collected from the same femur (Figure 4.1). This cross sectioned femur had annual turnover rates that ranged from 1.8% to 2.5%, highlighting that even within close proximity in the same skeletal element there can be a large difference in the amount of time encapsulated by the tissue. Also, there was no discernible pattern in the turnover rates from the cross section, with all sides exhibiting seemingly random variation in the modeled turnover rates. There also was no difference in mean or variance between the outer portion (number 1) and inner portion (number 2) of the femur bone (t-test;  $t = 0.89$ ,  $df = 6$ ,  $p = 0.40$ . f-test;  $f = 4.74$ ,  $p = 0.23$ ).

### 5.3.2. Supplemental Datasets

The expected  $\Delta^{14}\text{C}$  values and the equation of the line for each turnover interval using a fixed rate model according to year of death for the published southern hemisphere datasets (Ubelaker et al. 2022; Johnstone-Belford et al. 2022) are presented in figure 5.05. The  $\Delta^{14}\text{C}$  values and modelled turnover interval calculated using the equations of the lines from figure 5.06

are presented in table S3. Figure 5.06 illustrates the various turnover rates for the range of skeletal elements assessed across the two studies.

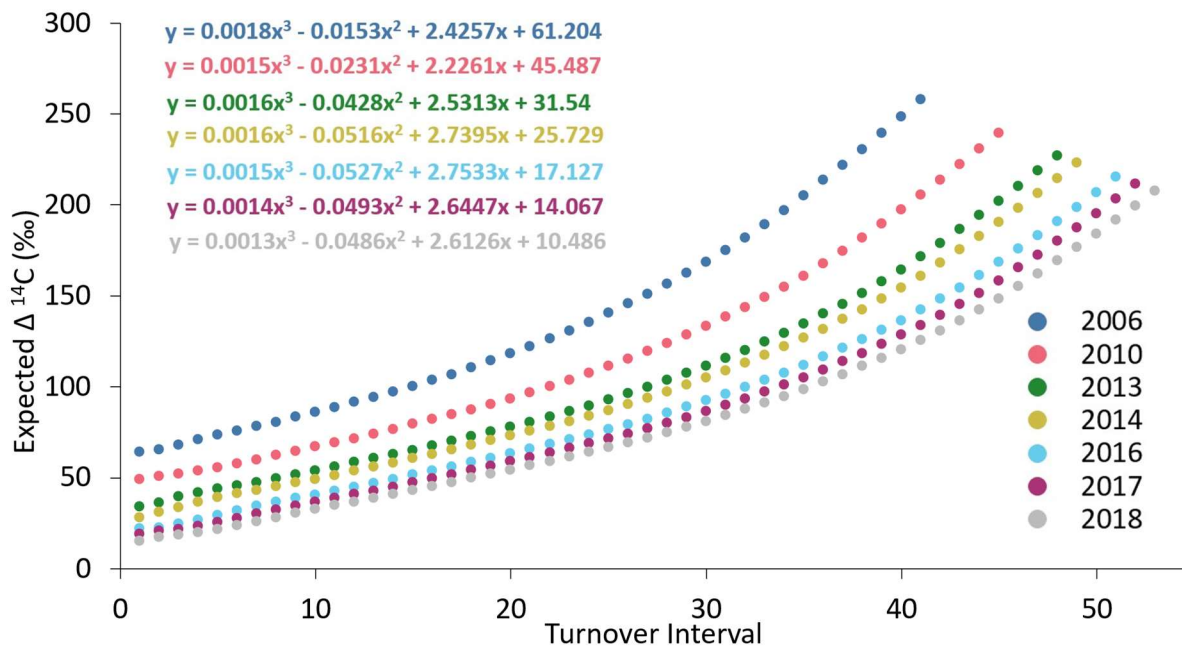


**Figure 5.05.** The expected  $\Delta^{14}\text{C}$  values for bone of any turnover interval for a fixed rate turnover in the southern hemisphere for the years of death. The equation of each 3<sup>rd</sup> order polynomial curve is also displayed and can be used to generate turnover interval and related fixed turnover rate of any sample from these years.

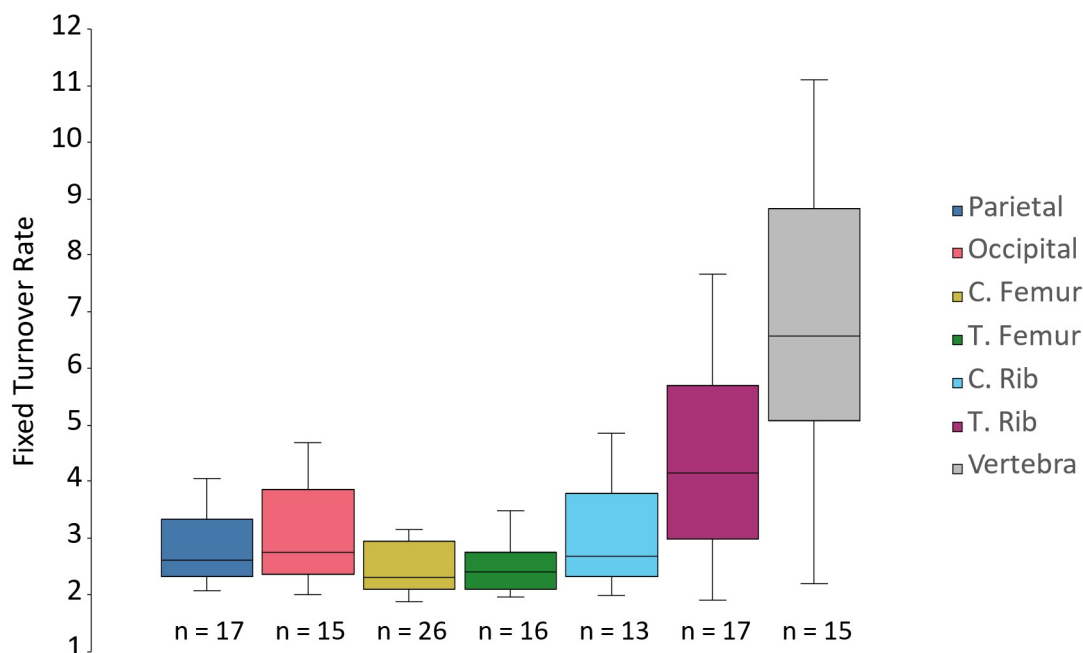


**Figure 5.06.** Modelled turnover rates using a fixed rate model for the skeletal elements from the Ubelaker et al. (2022) and the Johnstone-Belford et al. (2022) studies.

A Kruskal-Wallis H test ( $\chi^2=43.66$ ,  $p<0.001$ ) indicated that there was a significant difference in fixed turnover rates among elements. The results of a Dunn's post-hoc test (table 5.05) indicated that the vertebra had a significantly higher turnover rate from all groups except the trabecular rib. The turnover rate of trabecular rib samples also differed significantly from both femur bone types as well as the parietal bone. All skeletal elements except the vertebrae had measured  $\Delta^{14}\text{C}$  values that were too high to be modelled with the fixed rate function. Therefore, datapoints are missing and these groups are not necessarily representative of their element type.

**Table 5.05.** Dunns post-hoc test ( $p$  values) for differences between the fixed turnover rates for the elements sampled in the supplementary datasets. Statistically significant differences ( $p<0.05$ ) are indicated in red.

	Parietal	Occipital	C. Femur	T. Femur	C. Rib	T. Rib	Vertebra
Parietal		0.610	0.216	0.389	0.776	0.025	<0.001
Occipital			0.086	0.183	0.817	0.105	0.001
C. Femur				0.766	0.127	<0.001	<0.001
T. Femur					0.256	0.002	0.001
C. Rib						0.054	<0.001

<b>T. Rib</b>							0.100
---------------	--	--	--	--	--	--	-------

When compared to the northern hemisphere REST[ES] dataset, only the cortical femur, cortical rib, and vertebra overlap as elements that were sampled in both cases. The REST[ES] femora had an average turnover rate of 1.9%/year (range 1.7% to 2.5%/year). The Ubelaker et al. (2022) and Johnstone-Belford et al. (2022) datasets had significantly higher estimated turnover rates for femur, at 2.7%/year with a range of 1.9% to 7.2%/year (Mann Whitney U test;  $U=36$ ,  $p<0.001$ ). For the cortical rib, the REST[ES] dataset has an average annual turnover rate of 2.9% (range 1.9% to 3.9%) and the Southern hemisphere datasets had an average of 3.0%/year (range 2.0% to 4.9%). A t-test indicated that there was not a significant difference between these groups (t-test;  $t=3.34$ ,  $df=19$ ,  $p=0.74$ ). For vertebra, the REST[ES] dataset had an average annual turnover rate of 4.10% with an absolute range of 0.27%/year. In the supplementary datasets, the vertebra had a significantly higher estimated annual turnover rate, with an average of 7.02% and an absolute range of 13.31% (Mann Whitney U test;  $U = 9$ ,  $p = 0.009$ )

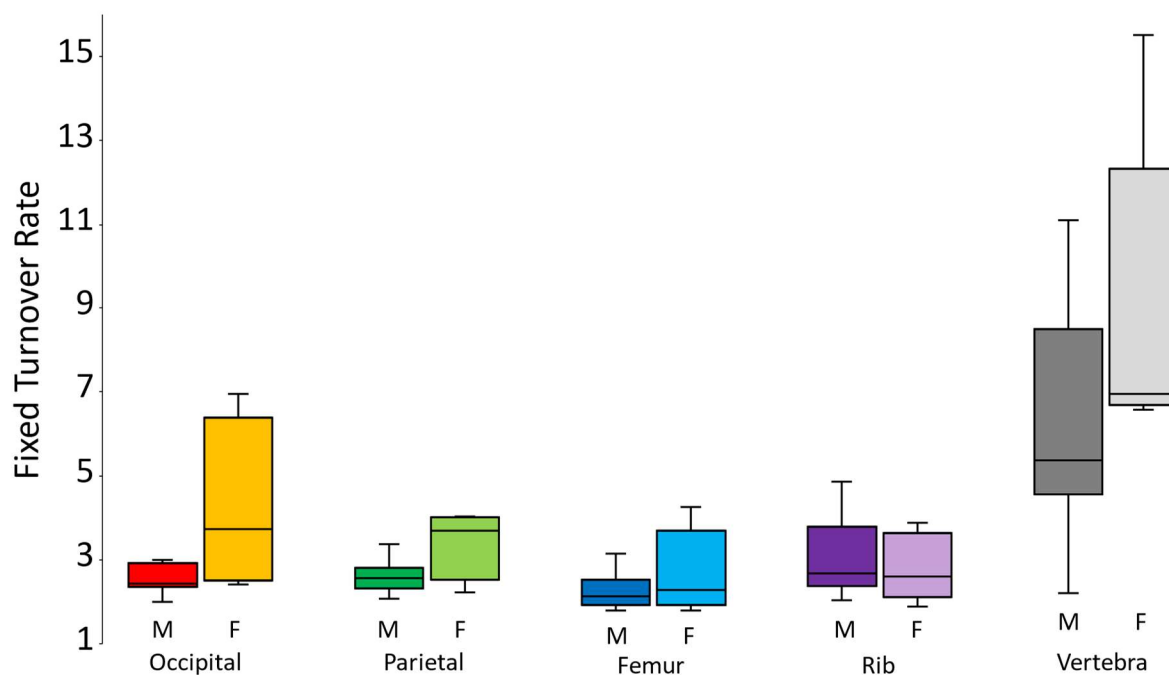


**Figure 5.07.** Fixed turnover rate for elements across all datasets grouped by sex.

Across all datasets, differences in annual turnover rate based on a fixed-rate model within elements were assessed based on sex (figure 5.07). This analysis included the occipital, parietal, cortical femur, cortical rib, and vertebra as they had enough data from each sex in order to assess differences. There were no statistically significant differences between sexes for the occipital (Mann-Whitney U test;  $U=9$ ,  $p=0.190$ ), femur (Mann-Whitney U test;  $U=115$ ,  $p=0.437$ ), rib (Mann-Whitney U test;  $U=32$ ,  $p=0.663$ ), and vertebra (Mann-Whitney U test;  $U=13.5$ ,  $p=0.126$ ). Only the parietal had a significant difference between the two sex groups tested (t-test;  $t=2.908$ ,  $df=14$ ,  $p=0.022$ ).

The range in ages at death in these studies provided an opportunity to assess if the turnover rate varied based on age, which would have important implications for the validity of implicit or explicit assumptions of fixed turnover rates used in stable isotope studies. Figure 5.09 displays the fluctuations seen in estimated turnover interval in each category from all datasets based on age. There is a high degree of variability in turnover rate across individuals at different ages and bone type. Under a fixed rate turnover model, as an individual ages, there should be no change in turnover rate within a single element. However, the high amount of variation within an element prevents any detection of these correlations. Moreover, with the finding that some samples had measured  $\Delta^{14}\text{C}$  values that were too high to have uniformly remodeled over the course of the individual's life, the fixed rate model is unlikely to accurately reflect turnover rate at any age.

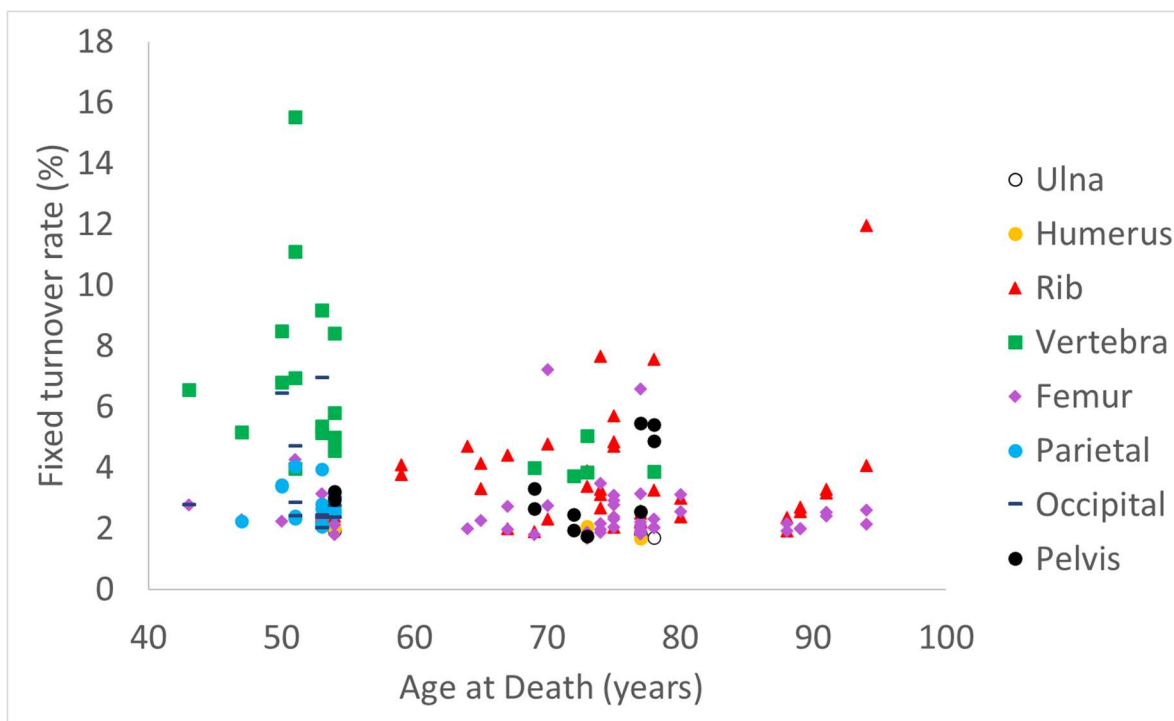


**Figure 5.09.** Fixed turnover rates at each age at death for the different skeletal elements and tissue type analysed in all three datasets. Cortical and trabecular samples are grouped by element.

#### 5.4. Decaying turnover rate model

The  $\Delta^{14}\text{C}$  values for some of the REST[ES] donors were too high to fit into a model where equal parts of the bone came from every year of life, and this indicates that a larger proportion of the bone must have formed during years with higher  $\Delta^{14}\text{C}$  values (i.e., closer to the bomb peak) and not remodeled, consistent with a decreasing turnover rate over time. Therefore, the decaying turnover rate model was used to explain how bone turns over in an individual's life.

##### 5.4.1 REST[ES] Data

The decay constants and the percentage of tissue from each decade of life for each of the skeletal elements of the REST[ES] donors are presented in Table 5.06. The decay constant is an



Donor	Skeletal element	$\Delta^{14}\text{C}$	DC (%)	0-10	10-20	20-30	30-40	40-50	50-60	60-70	70-80
	I.C.	167.0	6.4	0.01 ± 0.08	1.28 ± 1.15	10.74 ± 3.07	24.35 ± 4.24	27.02 ± 4.31	20.75 ± 4.04	13.11 ± 3.27	2.74 ± 1.64
	P.S.	101.1	5.3	0	0.14 ± 0.37	2.66 ± 1.65	12.43 ± 3.29	24.45 ± 4.17	28.56 ± 4.44	25.36 ± 4.35	6.40 ± 2.34
	Vertebra	53.6	4.1	0	0.00 ± 0.04	0.20 ± 0.45	2.47 ± 1.60	11.99 ± 3.22	28.18 ± 4.51	42.94 ± 5.10	14.23 ± 3.62
6	Humerus	215.1	6.6	0.01 ± 0.09	1.64 ± 1.27	11.88 ± 3.19	25.12 ± 4.27	25.58 ± 4.38	18.89 ± 3.86	11.41 ± 3.20	5.48 ± 2.30
	Femur	174.0	6.0	0.00 ± 0.03	0.61 ± 0.79	7.07 ± 2.56	20.08 ± 4.07	25.96 ± 4.30	22.59 ± 4.13	15.64 ± 3.54	8.05 ± 2.74
	Ulna	173.6	6.0	0.00 ± 0.03	0.60 ± 0.76	7.07 ± 2.66	20.01 ± 3.99	26.51 ± 4.58	22.80 ± 4.27	15.75 ± 3.44	7.26 ± 2.66
	Femur	167.5	5.9	0.00 ± 0.03	0.55 ± 0.75	6.44 ± 2.45	18.81 ± 3.88	26.18 ± 4.28	23.16 ± 4.18	16.26 ± 3.61	8.60 ± 2.68
	Femur	162.9	5.9	0.00 ± 0.03	0.51 ± 0.71	5.99 ± 2.31	18.40 ± 3.72	25.82 ± 4.29	23.37 ± 4.26	16.97 ± 3.80	8.94 ± 2.90
	Femur	161.4	5.9	0	0.45 ± 0.66	5.86 ± 2.44	18.06 ± 3.91	25.67 ± 4.29	23.67 ± 4.34	17.20 ± 3.80	9.10 ± 2.87
	Femur	151.0	5.7	0.00 ± 0.03	0.35 ± 0.60	4.92 ± 2.17	16.85 ± 3.88	25.23 ± 4.15	24.08 ± 4.22	18.38 ± 3.89	10.19 ± 2.91
	Mandible	141.8	5.6	0	0.24 ± 0.49	4.03 ± 1.96	15.09 ± 3.56	24.34 ± 4.40	25.00 ± 4.21	19.94 ± 4.01	11.36 ± 3.16
	Femur	139.2	5.6	0.00 ± 0.05	0.25 ± 0.51	3.86 ± 1.87	14.65 ± 3.60	24.52 ± 4.26	25.29 ± 4.49	20.19 ± 4.10	11.24 ± 3.09
	Femur	122.0	5.3	0.00 ± 0.03	0.12 ± 0.33	2.57 ± 1.58	11.81 ± 3.34	22.61 ± 4.24	26.19 ± 4.47	22.59 ± 4.12	14.10 ± 3.38
	Mandible	107.5	5.1	0.00 ± 0.03	0.06 ± 0.25	1.69 ± 1.27	9.20 ± 2.92	20.74 ± 4.15	26.73 ± 4.34	25.22 ± 4.41	16.35 ± 3.67
	Rib	88.3	4.7	0	0.03 ± 0.17	0.74 ± 0.88	5.92 ± 2.28	16.99 ± 3.70	26.35 ± 4.51	28.91 ± 4.59	21.06 ± 4.07
	Femur	87.1	4.7	0	0.02 ± 0.14	0.68 ± 0.83	5.74 ± 2.33	16.59 ± 3.65	26.30 ± 4.29	29.13 ± 4.41	21.54 ± 4.19

Donor	Skeletal element	$\Delta^{14}\text{C}$	DC (%)	0-10	10-20	20-30	30-40	40-50	50-60	60-70	70-80
	I.C.	84.7	4.6	0	0.01 ± 0.10	0.64 ± 0.80	5.25 ± 2.26	16.09 ± 3.81	26.17 ± 4.37	29.87 ± 4.39	21.97 ± 4.13
	P.S.	29.6	3.2	0	0	0.00 ± 0.06	0.12 ± 0.35	1.72 ± 1.32	10.48 ± 3.06	33.77 ± 4.70	53.89 ± 5.06
<b>10</b>	Humerus	222.3	6.5	0.02 ± 0.13	1.49 ± 1.19	11.49 ± 3.23	24.61 ± 4.33	25.76 ± 4.46	18.82 ± 3.82	11.72 ± 3.22	6.10 ± 2.39
	Ulna	205.5	6.3	0.01 ± 0.09	1.03 ± 1.00	9.59 ± 2.84	22.71 ± 4.32	25.78 ± 4.25	20.47 ± 4.08	13.29 ± 3.31	7.12 ± 2.58
	Femur	132.7	5.4	0	0.15 ± 0.37	2.85 ± 1.69	12.16 ± 3.23	22.83 ± 4.31	25.80 ± 4.36	21.85 ± 4.00	14.37 ± 3.53
	Rib	57.3	4.0	0	0.00 ± 0.03	0.07 ± 0.27	1.42 ± 1.18	7.67 ± 2.65	20.60 ± 4.11	33.59 ± 4.75	36.64 ± 4.88
	Vertebra	45.0	3.7	0	0.00 ± 0.03	0.02 ± 0.13	0.59 ± 0.77	4.46 ± 2.10	16.10 ± 3.74	33.84 ± 4.49	44.99 ± 4.81
	PS	34.0	3.3	0	0	0.00 ± 0.06	0.17 ± 0.42	2.06 ± 1.41	11.06 ± 3.21	32.17 ± 4.63	54.54 ± 4.98
	IPR	29.9	3.2	0	0	0.00 ± 0.03	0.10 ± 0.30	1.46 ± 1.20	9.04 ± 2.84	30.57 ± 4.63	58.84 ± 4.83
<b>11</b>	Femur	180.7	11.2	5.36 ± 2.19	38.21 ± 4.79	35.13 ± 4.58	15.22 ± 3.50	5.03 ± 2.12	1.05 ± 1.07	N/A	N/A
	Ulna	155.2	10.3	2.63 ± 1.61	29.58 ± 4.49	37.58 ± 4.97	20.34 ± 4.06	8.05 ± 2.71	1.81 ± 1.31	N/A	N/A
	Humerus	140.8	9.7	1.61 ± 1.27	24.18 ± 4.18	37.65 ± 4.71	23.60 ± 4.26	10.43 ± 2.98	2.52 ± 1.54	N/A	N/A
	Rib	94.4	7.9	0.19 ± 0.42	8.24 ± 2.71	29.23 ± 4.61	33.01 ± 4.59	22.49 ± 4.29	6.84 ± 2.60	N/A	N/A
	P.S.	66.9	6.7	0.03 ± 0.16	2.54 ± 1.59	17.39 ± 3.48	33.67 ± 4.63	33.36 ± 4.64	13.02 ± 3.35	N/A	N/A
	G.S.N.	58.7	6.3	0.01 ± 0.11	1.42 ± 1.20	13.65 ± 3.46	32.27 ± 4.63	36.72 ± 4.78	15.92 ± 3.65	N/A	N/A
<b>12</b>	Femur	164.3	6.4	0.01 ± 0.11	1.20 ± 1.10	10.72 ± 3.19	23.97 ± 4.40	26.80 ± 4.39	20.51 ± 3.99	13.20 ± 3.48	3.59 ± 1.84

Donor	Skeletal element	$\Delta^{14}\text{C}$	DC (%)	0-10	10-20	20-30	30-40	40-50	50-60	60-70	70-80
	Humerus	131.1	5.9	0.00 ± 0.04	0.47 ± 0.71	6.12 ± 2.35	18.97 ± 3.89	26.49 ± 4.47	24.74 ± 4.44	17.86 ± 3.72	5.36 ± 2.29
	Rib	54.3	4.2	0	0.00 ± 0.05	0.24 ± 0.51	2.94 ± 1.71	12.83 ± 3.46	27.61 ± 4.42	39.34 ± 5.03	17.04 ± 3.72
	Rib	45.0	3.9	0	0.00 ± 0.04	0.09 ± 0.29	1.64 ± 1.25	9.10 ± 2.94	25.35 ± 4.43	43.06 ± 4.78	20.75 ± 4.08
	Vertebra	32.6	3.5	0	0	0.01 ± 0.10	0.45 ± 0.67	4.75 ± 2.23	19.54 ± 4.01	47.32 ± 5.05	27.93 ± 4.51
17	Ulna	405.5	10.9	4.18 ± 2.00	35.27 ± 4.59	35.45 ± 4.66	16.45 ± 3.71	5.91 ± 2.35	2.00 ± 1.48	0.63 ± 0.78	0.11 ± 0.33
	Humerus	229.7	7.5	0.10 ± 0.31	5.23 ± 2.28	22.28 ± 4.25	29.44 ± 4.58	22.02 ± 4.33	12.94 ± 3.39	6.52 ± 2.35	1.49 ± 1.23
	Rib	219.4	7.3	0.07 ± 0.26	4.47 ± 2.12	20.61 ± 4.00	29.39 ± 4.48	22.87 ± 4.07	13.75 ± 3.53	7.09 ± 2.64	1.75 ± 1.34
	Femur	201.4	7.1	0.04 ± 0.19	3.28 ± 1.72	18.16 ± 3.98	28.67 ± 4.46	24.07 ± 4.40	15.20 ± 3.62	8.48 ± 2.75	2.09 ± 1.41
	IPR	182.2	6.8	0.01 ± 0.11	2.30 ± 1.44	15.03 ± 3.68	27.22 ± 4.39	25.47 ± 4.31	17.33 ± 3.94	10.07 ± 3.03	2.57 ± 1.66
	Vertebra	41.1	4.0	0	0.00 ± 0.03	0.10 ± 0.32	1.79 ± 1.34	9.56 ± 2.92	25.70 ± 4.26	42.57 ± 4.78	20.27 ± 3.83

The ulna typically had the highest decay constants (and therefore slowest turnover), but with considerable variation (Figure 5.10), while vertebrae consistently had the lowest decay constants (and therefore the fastest turnover rates). With the exception of the vertebra, each element had a large range of estimated decay constants meaning that turnover rate is much more variable within an element than has traditionally been assumed. A Kruskal-Wallis H test demonstrated that there were significant differences in the decay constants among elements ( $\chi^2 = 23.03, p = <0.001$ ), as summarized in Table 5.07.

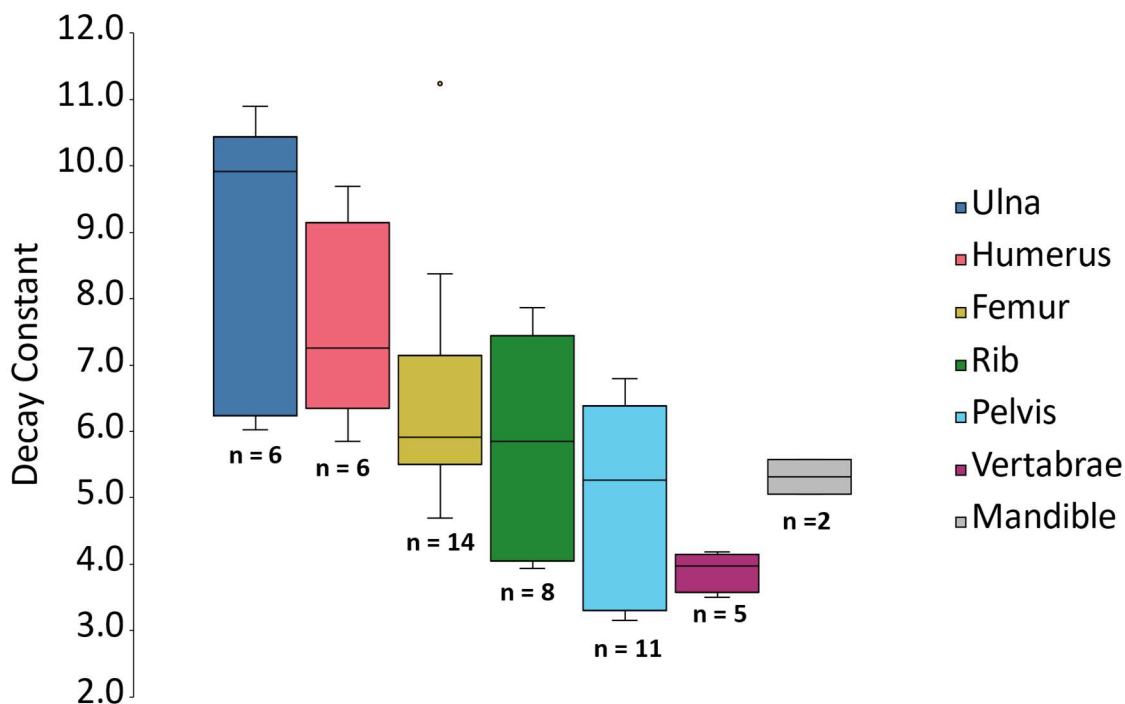


**Figure 5.10.** Decay constants (a proxy for bone turnover rate with lower decay constants equating to higher turnover rates) for skeletal elements from all REST[ES] donors.

**Table 5.07.** Dunn's post-hoc test ( $p$  values) for difference in estimated decay constants between element groups using a decaying turnover model. Statistically significant differences ( $p < 0.05$ ) are highlighted in red.

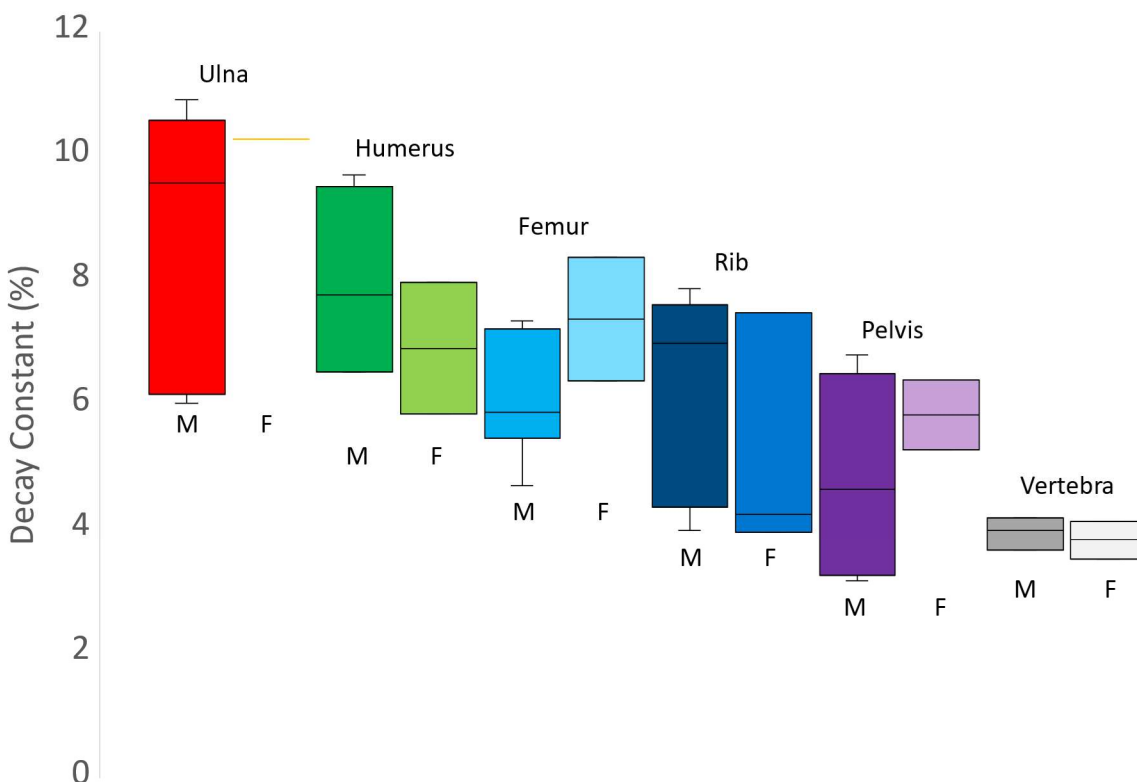
	Ulna	Humerus	Femur	Rib	Pelvis	Vertebra	Mandible
Ulna		0.634	0.073	0.035	0.002	<0.001	0.056
Humerus			0.220	0.110	0.009	<0.001	0.115
Femur				0.546	0.072	0.005	0.363
Rib					0.326	0.033	0.595
Pelvis						0.161	0.963
Vertebra							0.344

At death, donor 17 had the highest degree of variation in the  $^{14}\text{C}$  of the elements sampled, with the ulna having a decay constant of 10.9% and the vertebra having a decay constant of 4.0%. The least amount of variation at death was seen in donor 12, with a decay constant of 6.4 in the femur and 3.5 in their greater sciatic notch.

Elements that were sampled in multiple locations display both low and high rates of bone turnover. The most variation at death was observed in the femur of donor 6, with an absolute range

in calculated decay constant of 1.3%. For the subsection of this femur that had the fastest turnover rates, the last 17 years of life accounts for the production of just over 50% of the total bone collagen, however with the slowest remodeling subsection of this femur, these last 17 years account for less than 25% of the total bone collagen makeup (Table 5.06). For donor 6, 52% of the pubic symphysis bone collagen turned over in the last seven years of life, while only 21% of the bone collagen in the iliac crest turned over in the same period of time. Donor 6 also had a mandible sample split into two samples, which yielded decay constants of 5.1% and 5.6%. The subsampled rib from donor 12 had yielded decay constants of 3.9% and 4.2%. Also, two different kinds of vertebra were sampled, the thoracic and the lumbar. The thoracic (donor 3 and 5) has an average decay constant of 4.2%, and the lumbar (donor 10, 12, and 17) was 3.7%. It is important to recall that similar decay constants can still lead to large differences in what periods are represented in bone.

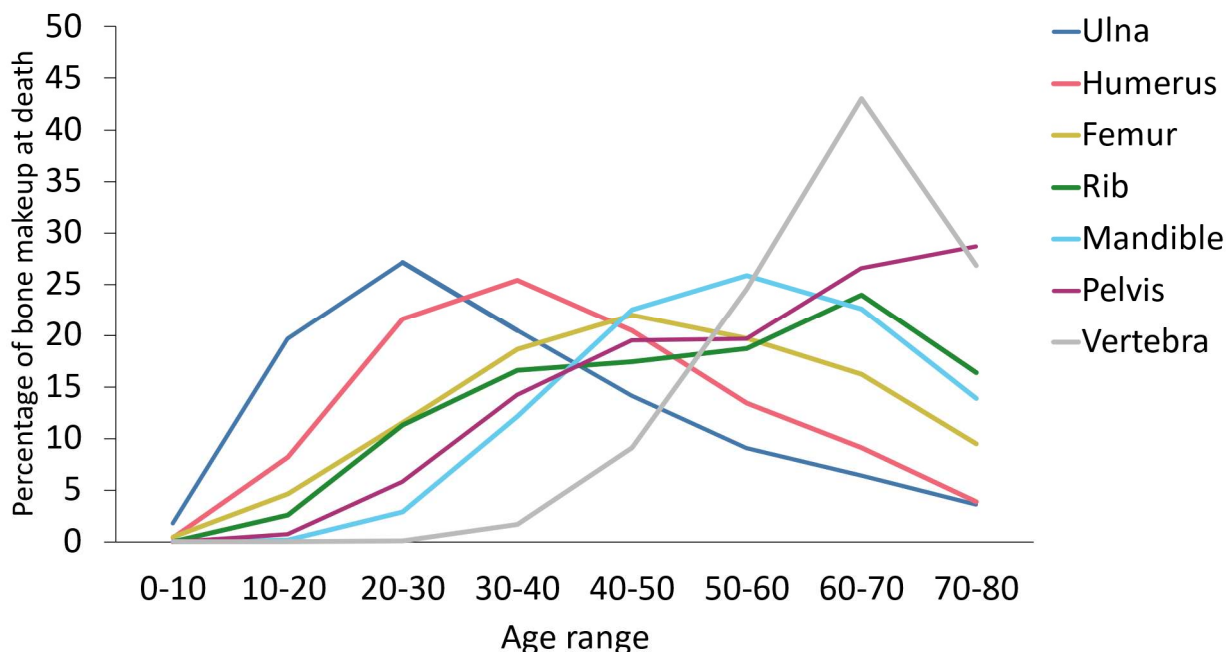
While there were only two female donors sampled, the differences between male and female decay constants for each element were compared in order to assess if any differences based on sex were visible. The low sample size of females made it so statistical analysis comparing the results were not possible. Figure 5.11 illustrates the decay constants of males and females by skeletal element, and highlights that generally there is overlap between the sexes suggesting no differences between the sexes in bone collagen remodeling rates, but the small sample size precludes any conclusions from being drawn.



**Figure 5.11.** Decay constants (a proxy for bone turnover rate with lower decay constants equating to higher turnover rates) across the skeletal elements sampled at REST[ES] grouped by sex. M = male, F = female.

**Table 5.08.** The average percent of collagen that was produced in each decade of life at death, across the elements analyzed. Decades from which the majority of bone was produced are highlighted in green for each element.

Element	Decade							
	0-10	10-20	20-30	30-40	40-50	50-60	60-70	70-80
Ulna	1.8 ± 1.7	19.7 ± 15.2	27.1 ± 14.6	20.5 ± 2.6	14.1 ± 9.4	9.0 ± 9.8	6.5 ± 7.4	3.6 ± 4.1
Humerus	0.4 ± 0.6	8.2 ± 9.0	21.6 ± 12.2	25.4 ± 3.6	20.5 ± 6.4	13.4 ± 7.9	9.1 ± 5.7	3.9 ± 2.5
Femur	0.5 ± 1.5	4.7 ± 10.5	11.5 ± 11.3	18.7 ± 7.3	22.0 ± 6.0	19.7 ± 7.9	16.3 ± 7.2	9.5 ± 6.0
Mandible	0 ± 0	0.2 ± 0.1	2.9 ± 1.7	12.2 ± 4.2	22.5 ± 2.6	25.9 ± 1.2	22.6 ± 3.7	13.9 ± 3.5
Rib	0.1 ± 0.1	2.6 ± 3.1	11.3 ± 12.2	16.6 ± 14.7	17.5 ± 6.9	18.7 ± 7.5	24.0 ± 15.9	16.4 ± 13.4
Pelvis	0.0 ± 0.0	0.7 ± 1.0	5.8 ± 6.9	14.2 ± 13.1	19.6 ± 12.7	19.7 ± 8.8	26.6 ± 9.4	28.7 ± 26.2
Vertebra	0 ± 0	0 ± 0	0.1 ± 0.1	1.7 ± 1.2	9.1 ± 4.5	24.5 ± 6.8	43.1 ± 5.8	26.9 ± 13.3



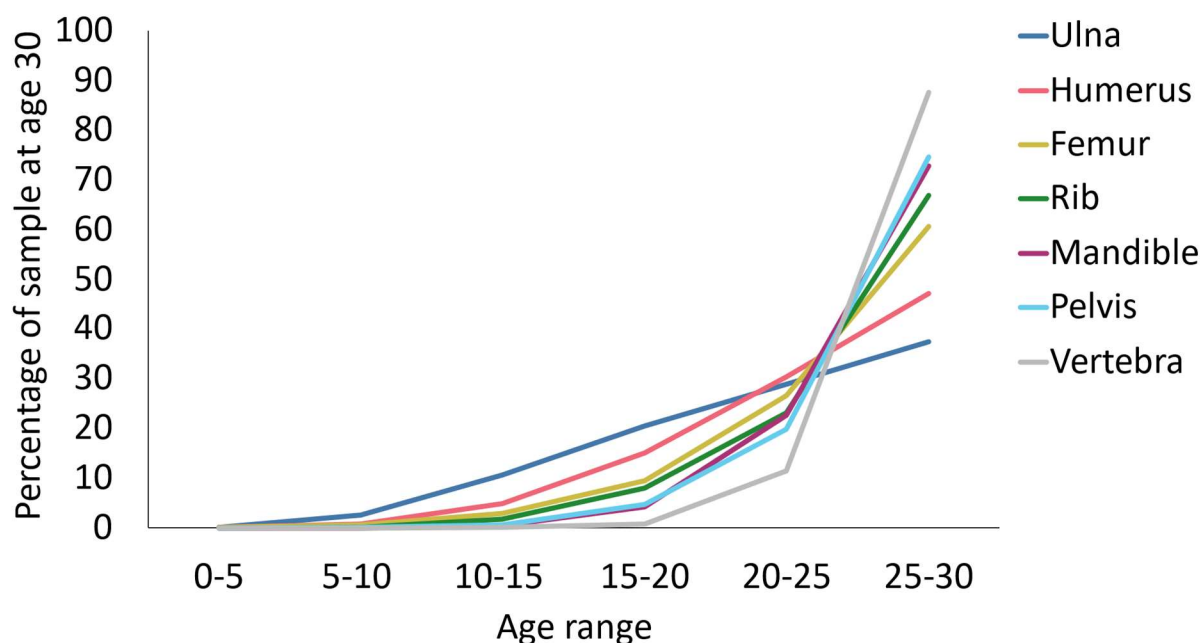
**Figure 5.12.** Average percentage of bone formed in each decade of life for the seven elements analyzed from the REST[ES] donors.

Table 5.08 and figure 5.12 show the average percentage of bone collagen that was produced in each decade of life across the elements analyzed from all donors. Due to the turnover rate declining as an individual ages, the percent bone collagen formed in each decade of life is dependent on age, and so these data only represent the average for people who died at a relatively advanced age, with an average age at death of 71. The ulna and humerus are better suited to indicate diet and activities from ages 0-40, whereas the pelvis and vertebra are more heavily weighted towards age 40-80. The femur was more evenly weighted throughout each decade, however, most accurately reflects between age 20-70. It is important to note that many of these data have high standard deviations and vary among individuals.

**Table 5.09.** The average percent of collagen that was produced in five year intervals up until age 30, across the elements analyzed. Values were calculated using the same decay constants that produced the data in Table 5.08. Periods from which the majority of bone collagen was synthesized for each element are highlighted in green.

	Decade
--	--------

	0-5	5-10	10-15	15-20	20-25	25-30
<b>Ulna</b>	0.1 ± 0.1	2.5 ± 2.1	10.6 ± 7.8	20.4 ± 9.9	28.9 ± 1.6	37.4 ± 20.1
<b>Humerus</b>	0.0 ± 0.0	0.7 ± 1.0	4.9 ± 4.5	15.1 ± 6.8	30.3 ± 2.6	47.2 ± 11.2
<b>Femur</b>	0.0 ± 0.1	0.6 ± 1.7	2.8 ± 5.4	9.4 ± 7.2	26.6 ± 4.2	60.6 ± 16.0
<b>Rib</b>	0 ± 0	0.2 ± 0.2	1.8 ± 2.0	8.0 ± 7.3	23.2 ± 10.1	66.7 ± 19.4
<b>Mandible</b>	0 ± 0	0.0 ± 0.0	0.4 ± 0.2	4.2 ± 1.3	22.7 ± 2.8	72.8 ± 4.4
<b>Pelvis</b>	0 ± 0	0.0 ± 0.1	0.7 ± 0.8	4.7 ± 4.3	19.9 ± 9.8	74.7 ± 14.6
<b>Vertebra</b>	0 ± 0	0 ± 0	0.0 ± 0.0	0.8 ± 0.4	11.5 ± 2.2	87.7 ± 2.6



**Figure 5.13.** Age 30 average percentage attributed of each decade of life for the seven elements analyzed from the REST[ES] individuals.

As an estimate of what these donors' bone composition looked like earlier in life, each donor's turnover rates were modeled as the average percent of collagen that was produced in five year periods of time up until age 30 (Table 5.09, Figure 5.13). At age 30, a much higher proportion of bone collagen was formed in the preceding few years. While the ulna is still the best indicator of early life, every element has their highest percent of tissue attributed to the age 25-30. The long bones have turnover intervals that span the whole life and still have BMUs that were formed within the first five years of life, whereas the vertebra has 99% of its BMUs coming from age 20-30.

#### 5.4.2. Supplemental Datasets.

The nature of some of the data from the Johnstone-Belford et al. (2022) dataset provided some challenges. The individuals sampled from this study had a wide range of ages, with individuals being up to 94 years old at the time of death. With the years of death being from 2016-2018, this meant that the older individuals spent a significant amount of their lives before the atmospheric  $\Delta^{14}\text{C}$  levels spiked, which allowed for more than one possible decay constant to produce the final measured  $\Delta^{14}\text{C}$  values in the samples. This problem is exemplified in figure 5.14, where one 94-year-old individual had a cortical femur sample that yielded a  $\Delta^{14}\text{C}$  value of +158.3 ‰, which is a value that could have been achieved via a decaying turnover constant of both 8.4% and 4.2%, both of which were reasonable constants based on the other data seen here. These two constants would yield significantly different results in terms of bone turnover rate. The oldest individuals included in the Johnstone-Belford et al. (2002) study, specifically those that were older than 18 before the major spike in atmospheric levels around 1960, were excluded from this analysis.

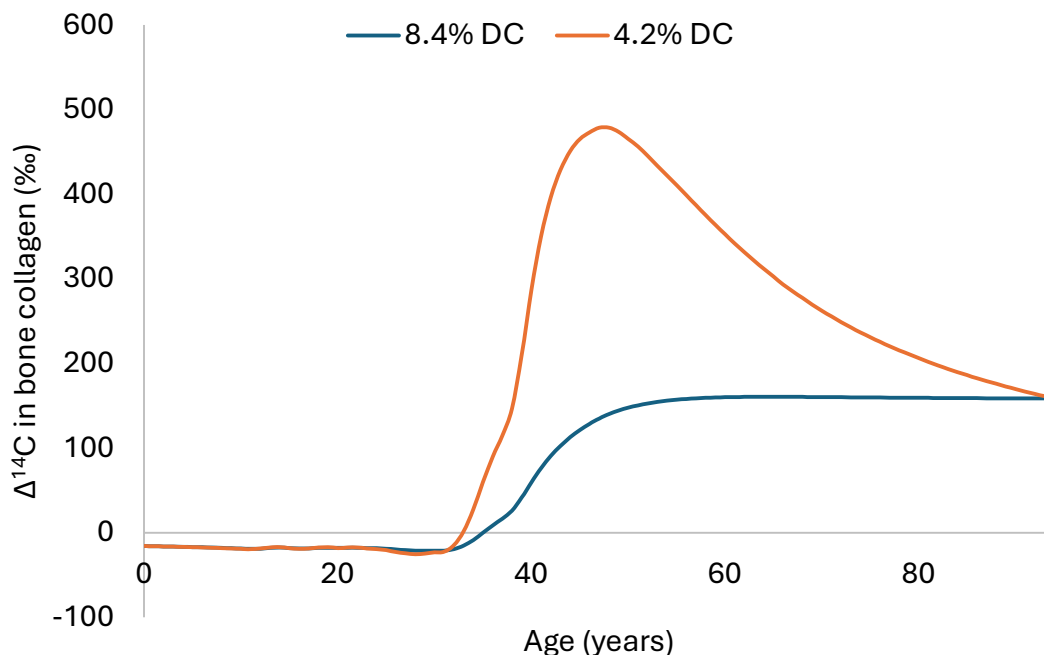


**Figure 5.14.** Modeled  $\Delta^{14}\text{C}$  throughout life for two different decay constants for an individual who died at 94 and was born in 1924. DC refers to decay constant.

The decaying turnover rate model was applied to the remaining individuals from both the additional Southern hemisphere datasets (Ubelaker et al. 2022; Johnstone-Belford et al. 2022) (Figure 5.15, Table S.3, Table S.4). A Kruskal-Wallis test indicated that there were differences among the estimated decay constants of the skeletal elements ( $\chi^2=54.56$ ,  $p<0.001$ ), the results of Dunn's post-hoc tests are presented in table 5.10. Of the skeletal elements used in these datasets, the trabecular rib generally had the fastest turnover rates (lowest average decay constant of 4.0%), which was significantly less than all other elements except the vertebra and cortical rib (Table 5.10). The cortical femur had the largest range in decay constants, ranging from 13.3% to 3.2%, also having the highest average decay constant of 8.8% (Figure 5.15).

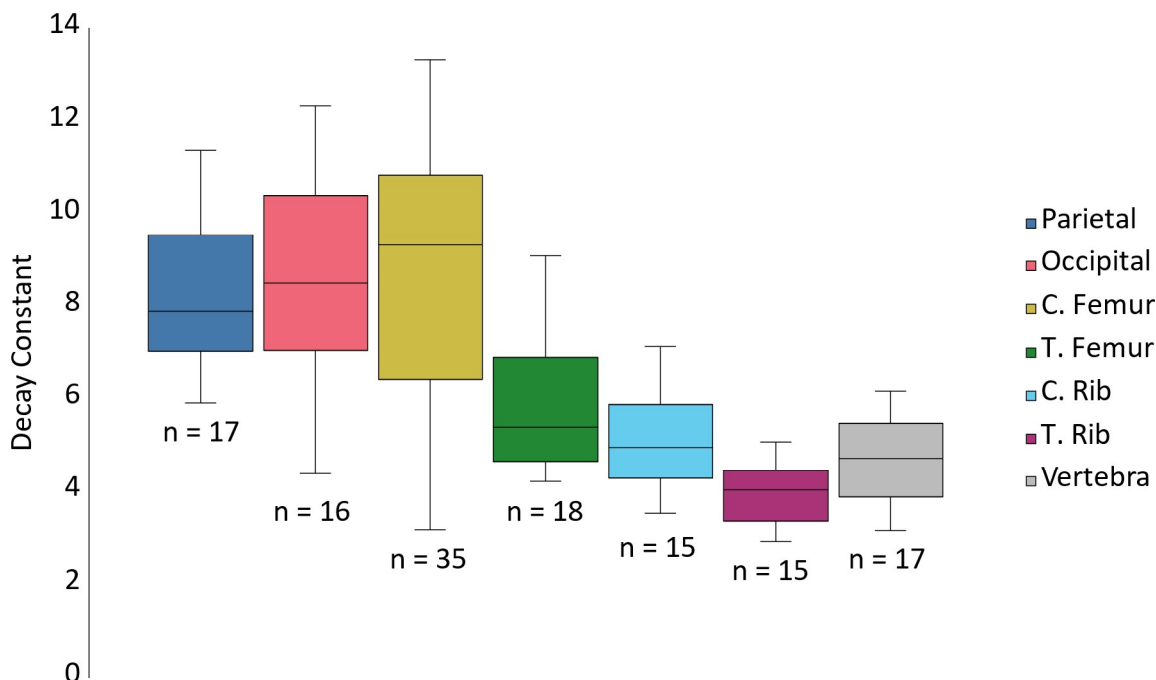


**Figure 5.15.** Decay constants (a proxy for bone turnover rate with lower decay constants equating to higher turnover rates) for each of the elements measured in the two previously published southern hemisphere studies (Ubelaker et al. 2022; Johnstone-Belford et al. 2022).

**Table 5.10.** Results of Dunn's post-hoc tests ( $p$  values) for differences in decay constants for each skeletal element group. Statistically significant differences ( $p < 0.05$ ) are indicated in red

	<b>Parietal</b>	<b>Occipital</b>	<b>C. Femur</b>	<b>T. Femur</b>	<b>C. Rib</b>	<b>T. Rib</b>	<b>Vertebra</b>
<b>Parietal</b>		0.946	0.876	0.015	<0.001	<0.001	<0.001
<b>Occipital</b>			0.821	0.019	0.001	<0.001	<0.001
<b>C. Femur</b>				0.006	<0.001	<0.001	<0.001
<b>T. Femur</b>					0.430	0.048	0.257
<b>C. Rib</b>						0.224	0.823
<b>T. Rib</b>							0.256

The two southern hemisphere datasets (Ubelaker et al. 2022; Johnstone-Belford et al. 2022) were combined to see if any differences in turnover rate (as expressed in terms of decay constant) existed on the basis of sex, with the sample consisting of eight females and nineteen males (Figure 5.16). The results show that overall, males and females had very similar bone collagen turnover rates. No significant differences in turnover rate (decay constant) were found between the sexes for any skeletal element group, however the trabecular femur as well as the two rib categories did

not have enough female data for statistical analysis. While it is a small sample, these results agree with lack of sex-based differences in bone collagen turnover observed in the REST[ES] dataset.

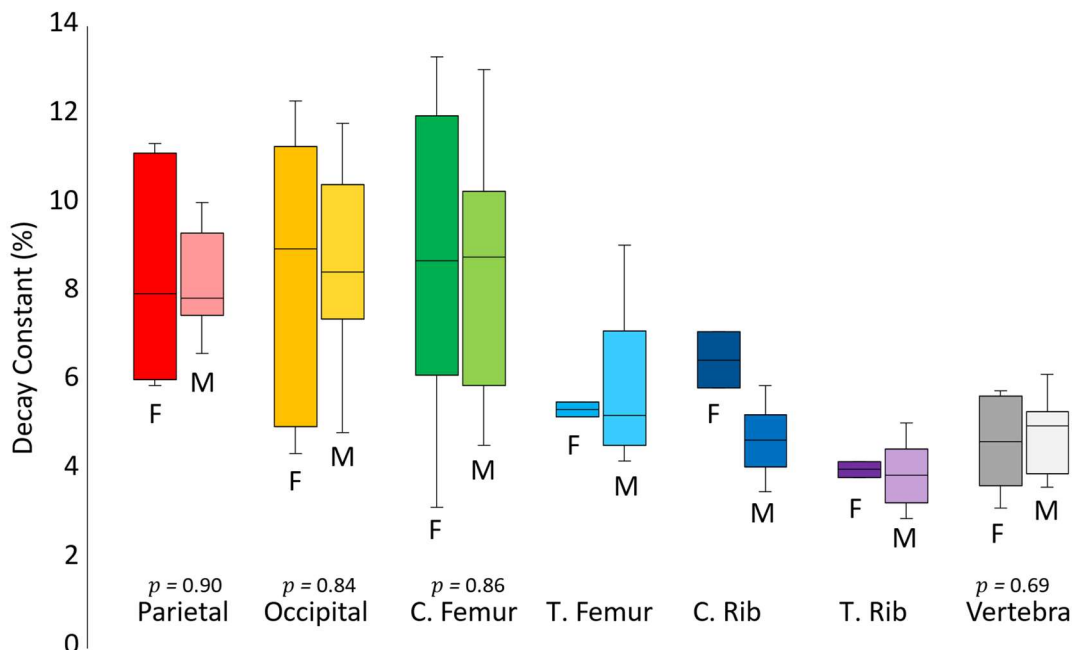


**Figure 5.16.** Decay constants (a proxy for bone turnover rate with lower decay constants equating to higher turnover rates) for the different skeletal elements analyzed in the two southern hemisphere datasets (Ubelaker et al. 2022; Johnstone-Belford et al. 2022) by sex. Male groups are signified by M and female groups are signified by F. *P* values are indicated under each grouped box plot, all were *t*-tests except for the vertebra, which was a Mann-Whitney U test

The percentage of bone collagen that was made in each decade of life across the elements analyzed from each individual was calculated and is presented in table S.5. Due to the large range in ages at death from these supplemental datasets, the average decay constants for each decade are more variable. For that reason, the averages and standard deviations for each element at each decade were separated into those that died from age 43-58 (individuals from Ubelaker et al. 2022) and from age 59-74 (individuals from Johnstone-Belford et al. 2022) (table 5.11 and table 5.12). The average percentage of bone collagen synthesized in each decade is illustrated in figures 5.17 and 5.18. Similar to the REST[ES] data, for the femur, especially the cortical femur, each decade of life is more evenly represented than elements that are more heavily weighted in

certain periods, such as the vertebra. The parietal and the occipital mimic this patter, with more collagen coming from the middle of life than from the beginning or end of life. The rib fell between these two elements.

**Table 5.11.** The average percent of collagen produced in each decade of life at the time of death, across the elements analyzed for the individuals from Ubelaker et al (2022).

	Decade					
	0-10	10-20	20-30	30-40	40-50	50-60
Parietal	1.1 ± 1.7	14.2 ± 12.7	28.8 ± 9.1	29.4 ± 6.9	21.6 ± 12.4	5.6 ± 4.6
Occipital	1.4 ± 2.5	14.6 ± 14.4	25.4 ± 14.1	24.4 ± 9.9	21.8 ± 18.6	7.2 ± 8.6
Femur (Cortical)	4.2 ± 4.6	27.6 ± 16.2	31.5 ± 8.1	21.3 ± 9.1	12.6 ± 12.6	3.2 ± 3.8
Vertebra	0.1 ± 0.3	1.5 ± 5.1	6.2 ± 9.4	20.7 ± 12.7	49.0 ± 13.6	25.5 ± 13.4

**Table 5.12.** The average percent of collagen produced in each decade of life at the time of death, across the elements analyzed for the individuals from Johnstone-Belford et al. (2022). C refers to the cortical and T refers to trabecular.

	Decade							
	0-10	10-20	20-30	30-40	40-50	50-60	60-70	70-80
Femur (Cortical)	0.4 ± 0.8	6.3 ± 10.0	14.3 ± 14.2	19.0 ± 9.8	18.9±8.6	17.4 ± 8.6	17.6 ± 19.7	9.1 ± 5.1
Femur (Trabecular)	0.1 ± 0.3	2.7 ± 5.6	9.4 ± 12.1	16.2 ± 10.3	21.0 ± 6.4	23.0 ± 8.2	20.1 ± 13.1	12.5 ± 8.6
Rib (Cortical)	0 ± 0.0	0.5 ± 1.1	4.5 ± 6.0	13.1 ± 9.4	22.6 ± 9.1	28.9 ± 9.8	22.0 ± 13.1	15.1 ± 13.7
Rib (Trabecular)	0 ± 0	0.0 ± 0.0	0.5 ± 1.0	4.1 ± 5.5	13.3 ± 11.5	27.7 ± 13.0	35.6 ± 15.8	30.1 ± 17.1

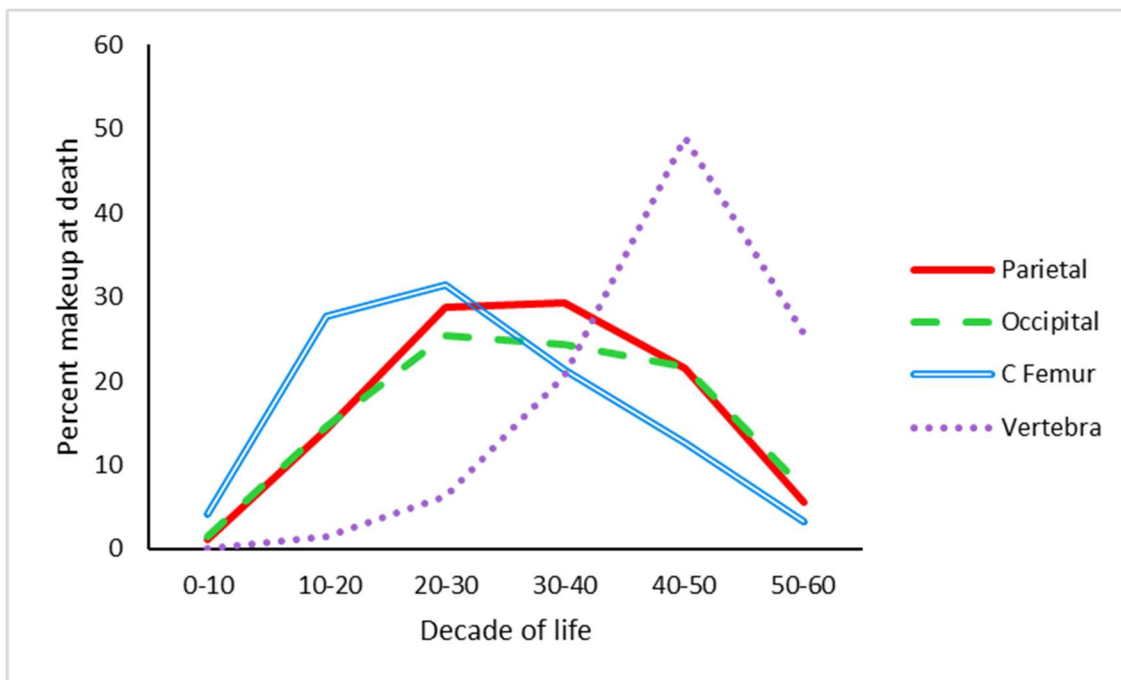


**Figure 5.17.** Average percentage of bone formed in each decade of life for the seven elements analyzed from the individuals analyzed Ubelaker et al. (2022). C refers to cortical tissue.

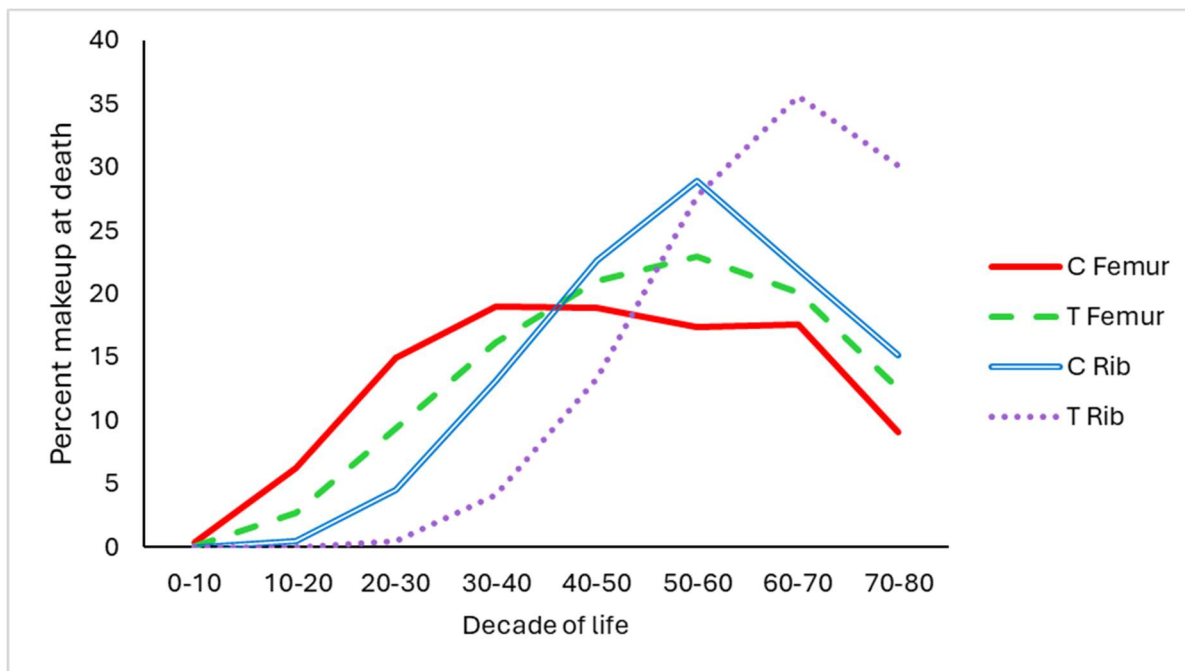


**Figure 5.18.** Average percentage of bone formed in each decade of life for the seven elements analyzed from the individuals analyzed Johnstone-Belford et al. (2022). C refers to the cortical and T refers to trabecular.

All the decay constants produced from each dataset should produce relatively similar results if the skeletal element's turnover patterns are being accurately predicted. Differences in sampling strategy and individual lifestyle differences could potentially cause differences, however any differences could also capture the extent of variability that exists within an element. The supplemental datasets were compared to the REST[ES] data where possible (for the cortical femur, cortical rib, and vertebra) (figure 5.17). Statistically significant differences were only seen between the two femur groups (Mann-Whitney U test;  $U=89$ ,  $p=0.006$ ). This difference may be due to the extreme amount of apparent variability in bone turnover as reflected in  $^{14}\text{C}$  content observed within the femur.

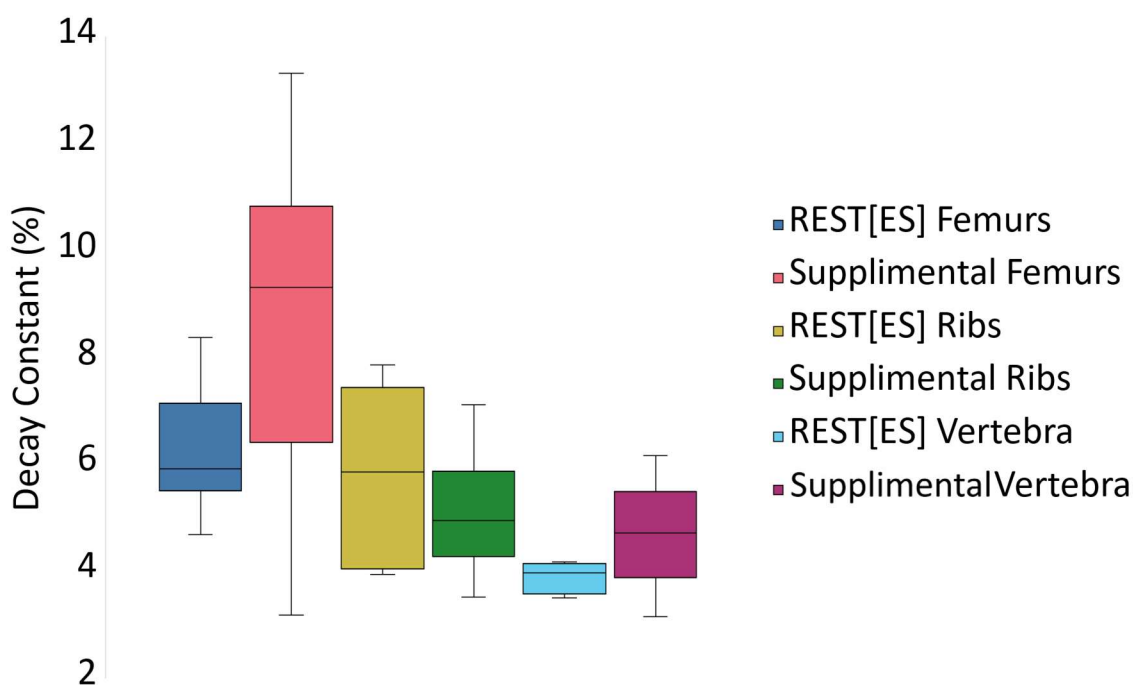


**Figure 5.19.** Estimated decay constants (a proxy for bone turnover rate with lower decay constants equating to higher turnover rates) for the skeletal elements sampled from the REST[ES] donors and in the two Southern Hemisphere studies (Ubelaker et al. 2022; Johnstone-Belford et al. 2022).

### 5.5. Hedges et al. (2007) model

The Hedges et al. (2007) study predicted inflection points as well as upper and lower turnover rates that exist at these points for females and males femurs (table S.6). If these estimates are accurate, it would be expected that all measured  $\Delta^{14}\text{C}$  values from the femurs sampled at REST[ES] would fall within the range of expected  $\Delta^{14}\text{C}$  values produced by applying the estimated rates and inflection points proposed by Hedges et al. (2007) to each donor based on sex. These ranges as well as their actual measured  $\Delta^{14}\text{C}$  are presented in figure 5.18 to highlight how often the estimated and measured values overlap. The estimated  $\Delta^{14}\text{C}$  failed to predict the actual  $\Delta^{14}\text{C}$  around half of the time. Only in the case of donor 17, donor 11, donor 5, and some of donor 6 did the estimates by Hedges et al. (2007) cover the real measured  $\Delta^{14}\text{C}$  values. This indicates that the estimated turnover rates at every inflection point for the femur predicted by Hedges et al. (2007) may be inaccurate for any person and are not reliable.

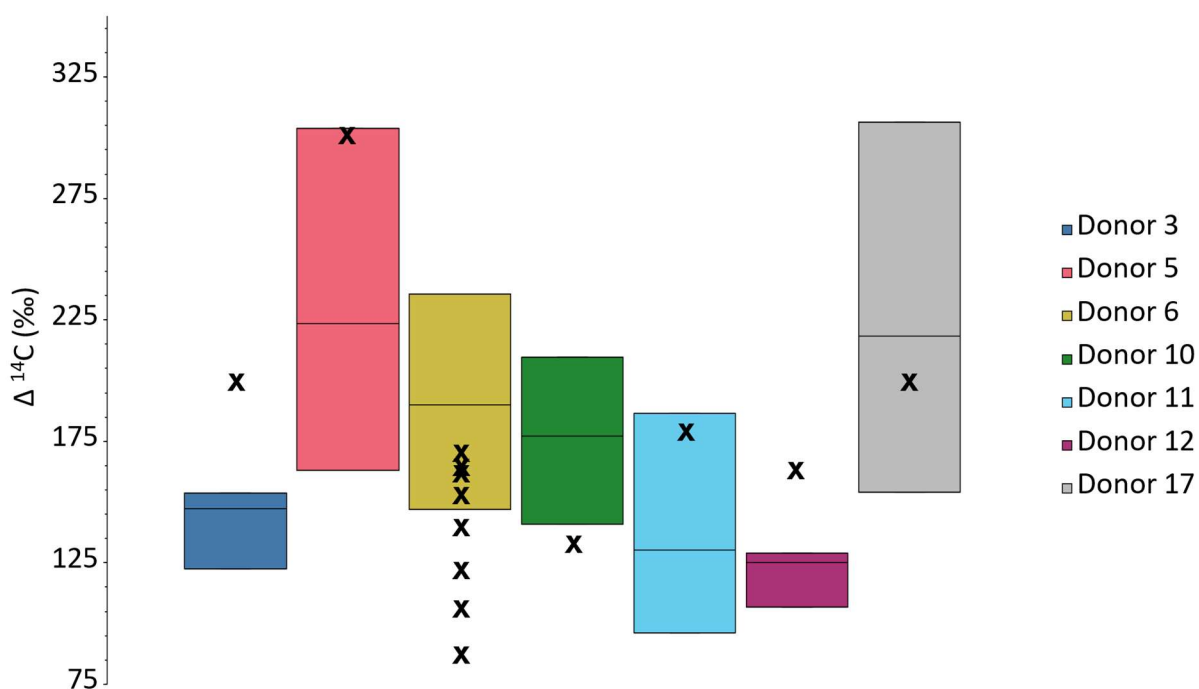


**Figure 5.20.** Estimates produced upper and lower expected  $\Delta^{14}\text{C}$  for every REST[ES] donor (boxes) as well as their actual measured  $\Delta^{14}\text{C}$  values (X). Donor 6 had 8 samples from the femur and so the highest and lowest values are indicated with a line indicating where the other values fell.

## **Chapter 6: Discussion**

The original objectives of this thesis were to:

1. Determine if there is appreciable variation in bone turnover rate between skeletal elements of one person.
2. Determine if factors such as sex, mobility, and health can influence turnover rate.
3. Quantify the period of time over which collagen forms for different skeletal elements.

### **6.1. Variation between skeletal elements**

In general, discernible trends have surfaced in the data, allowing for the arrangement of each skeletal element based on its turnover rate from slowest to fastest. Although differences between certain elements were not always statistically significant, subtle variations facilitated their ordering, as presented in Table 6.1. Regardless of the model employed for the primary dataset, the ulna consistently exhibited the slowest turnover, representing the element with the oldest BMUs across the skeleton. Following the ulna, the humerus ranked as the second slowest in the REST[ES] data, succeeded by the femur, rib, pelvis, and, on average, the vertebra emerged as the element with the fastest turnover rate. While the mandible, with a limited sample size, does not provide representative data for all individuals, it closely aligned with the rib and femur, suggesting a potentially similar turnover rate for these elements. Modeling of data from the two other datasets (Ubelaker et al., 2022; Johnstone-Belford et al., 2022) suggested that while the turnover rate for the cortical rib was statistically different than the cortical femur under the decay model, all the data from the rib samples fell within the range covered by the femur. The additional two skull bones, the occipital and parietal, exhibited similar decay constants to the femur in the Southern Hemisphere data but was not similar to the femurs in the REST[ES] data.

The skull bones had some of the highest decay constants and therefore slowest remodeling rates of any bone that was analyzed or for which data were available, except for the ulna. All datasets are consistent in suggesting that the vertebra is by far the fastest turning over element of those measured here.

**Table 6.1.** Qualitative order of skeletal elements from slowest remodeling to fastest bone collagen remodeling.

Slowest Turnover Rate	Ulna
	Occipital <sup>2</sup>
	Parietal <sup>2</sup>
	Humerus
	Femur <sup>3</sup>
	Rib
	Mandible <sup>1</sup>
	Pelvis
Fastest Turnover Rate	Vertebra

1. This bone had a small sample size and therefore this ranking is uncertain.
2. These elements represent only data derived from the Ubelaker et al. (2022) Southern Hemisphere dataset.
3. The femur varied from this position to the second slowest depending on the dataset examined. This ranking refers only to the REST[ES] donor data.

The models employed for generating turnover rates produced a few potential solutions. The fixed rate model produces one annual turnover rate per sample. While in some cases this model did not produce a logical result, which may point to the fact that this model does not reflect the true nature of bone turnover, bone turnover is frequently referred to as fixed for adults and therefore this model is still useful for comparative purposes. The decaying rate turnover model produces variable annual turnover rates that decrease with age, with one static decay constant.

The variability observed in these results extends beyond differences between skeletal elements; it also manifests across individuals within the same element. In fact, many elements

experienced more variation within an element group than between different elements (figure 5.10). This emphasizes that variations in individuals' lifestyles likely impact bone collagen turnover rates. The potential factors driving variation in collagen turnover across and within skeletal elements are discussed below.

#### *6.1.1. Does activity level influence turnover?*

The daily stress relative to the size of a bone likely plays a significant role in its turnover rate. Notably, frequent low-impact loading has been observed to stimulate bone remodeling (Bergmann et al., 2010; Turner et al., 1995). Therefore, bones subjected to more regular loading may be associated with faster turnover rates. For instance, the bones of the forearm, experiencing less regular force than the femur in day-to-day activities like walking, on average have slower turnover rates (such as the ulna and humerus, figure 5.10). Ribs, undergoing low strain loading during regular respiration (Bellemare et al., 2003), exhibit moderate turnover. In contrast, bones subject to more frequent low-impact loading, like the pelvis and vertebra, tend to have faster turnover rates. The pelvis bears the body's weight, and the vertebra supports the body's upright posture. Notably, the vertebra, being relatively small, faces a higher relative load. A relationship between loading force and turnover rate is therefore likely. This idea also matches the cranial bones being some of the bones with the slowest turnover rates, as cranial bones experience very little loading and have minimal stress placed on them at any time. Based on this idea, it is presumed that the radius would have a turnover rate similar to the ulna, where as the tibia or the fibula may be more similar to the femur.

Activities such as sports or running, which increase loading frequency, primarily affect the leg (Tozeren, 1999). Consequently, the femur, being more closely linked to an individual's activity level, is expected to exhibit greater variability in turnover rates. This could potentially

explain the differences observed in the resulting decay constants between the REST[ES] and the Southern Hemisphere data. However, since both datasets lack information about the activity levels of donors, the precise reasons for the disparity in femur results remain unclear.

Nevertheless, the wide range observed in the femur decay constants in the Southern Hemisphere data could be attributed to the individuals sampled having diverse activity levels. Additionally, since the femurs in the main (REST[ES]) dataset does not show the largest range in remodeling rates, this may be due to relatively similar rates of activity among the donors. This observation makes sense in light of the fact that they were all at an age where activity levels tend to decrease compared to earlier in life (Buchman et al., 2014). Variation in bone turnover within a skeletal element category can likely be attributed to individual differences in loading. The overall decrease in remodeling rate through life for all bones, as indicated by the decay model, may be influenced by the general decline in loading with age.

Donor 17, an individual who was paralyzed for the last years of his life, provides an interesting case study on how activity level and movement influences the rate of collagen turnover. This donor was paralyzed from the waist down and did have some movement ability in his upper body, however it is unknown how the paralysis effected his upper body movement. Some people without the ability to move their legs move to wheelchairs where they push themselves with their arms, thereby increasing the demands of the upper body. Other people move to wheelchairs and rely on motors for movement or for other people to push them, decreasing their whole-body movement. The latter is more probable in this case, as this donor was older at the time of paralysis, and it is less likely that his arms would have been strong enough to frequently wheel himself. As well, it was communicated that this individual, while having upper arm movement, also had injuries to the hands, and so it is more likely that hand and

arm movement decreased overall. Studies on paralysis discuss that almost immediately after disuse of a bone, osteoclastic activity increases and bone density decreases (Ausk et al., 2013; Roberts et al., 1998), signaling an uncoupling of osteoclastic and osteoblastic cells. Specifically, osteoclastic activity has been said to increase in the medullary cavity and in the surrounding bone tissue more than in outer layers of bone (Ausk et al., 2017).

While there are no data on the turnover rates of donor 17 prior to paralysis, comparing this individual to other donors may highlight these changes in cell activity within the present results. Looking at his overall decay constants, donor 17 is typically above the average for each element (and therefore has relatively slower turnover rates), except for the vertebra and the humerus which is just below the average. In fact, donor 17 has the highest decay constant (slowest relative turnover) in the elements group for the pelvis and the ulna. While these data do not overwhelmingly highlight the changes that can occur in bone with paralysis, it does allow for some points to be considered. It has been noted that when disuse of bone occurs, trabecular rich bones such as the pelvis may experience the effects of increased osteoclastic activity and decreased osteoblastic activity more than cortical-rich bones (Bergmann et al., 2010). This would account for the increase in decay constant (slower turnover) seen in donor 17's pelvis. It is also important to point out that an increase in random osteoclastic activity alone would not necessarily change the  $\Delta^{14}\text{C}$  of bone, and only selective removal of new collagen would result in an increase in decay constant as seen in the ulna. Some preliminary animal studies have noted that bone tissue closest to the medullary cavity is frequently newer tissue than the tissue on the outside of a bone (Matsubayashi et al., 2019). If osteoclastic activity increases in the medullary cavity of disused bone (Ausk et al., 2017), this could account for the selective removal of new bone and the overall higher decay constants in donor 17's skeletal elements.

### 6.1.2. Does health influence collagen turnover?

A health factor that could influence turnover rates is osteoporosis. While it is possible that some, if not all, donors had some form of osteoporosis due to their advanced age, it is likely that this disease would not significantly affect their ratios of  $\Delta^{14}\text{C}$ . Osteoporosis typically involves an increase in osteoclastic activity without necessarily changing osteoblastic activity (Garnero and Delmas, 1998), thus maintaining the  $\Delta^{14}\text{C}$  ratios at a relatively static level. Notably, in some cases, a reduction in osteoblastic activity in aged individuals has been observed (Becerikli et al., 2017), while in other instances, osteoblasts may increase with osteoporosis (Garnero and Delmas, 1998). Both scenarios could alter the apparent turnover rates calculated in this study. It is therefore not presently known how osteoporosis might impact collagen turnover rates. The increasing probability of osteoporosis as a person ages and the general decrease in collagen content that older people experience (Rouhi, 2012) may contribute to the turnover rate decreasing with age as modelled in the decaying turnover rate model.

Donor 12 was diagnosed with osteoporosis and was prescribed and taking a drug called alendronate. Alendronate is a proven treatment for osteoporosis and has been shown to increase overall bone density by decreasing osteoclastic activity, effectively forcing each skeletal element to hold onto its bone tissue instead of dissolving it as it normally would (Arlot et al., 2005; Kućukalić-Selimović et al 2011). It has also been noted that alendronate can specifically induce the production of type 1 collagen through osteoblastic activity in some studies (Boanini et al., 2008; Tsuchimoto et al., 1994), however these findings are not always consistent (Tormod et al., 2016). Therefore, the drug can either decrease osteoclastic activity alone, or decrease osteoclastic activity while increasing the production of type 1 collagen. The donor using alendronate had the lowest decay constants and therefore the highest turnover rates in her humerus, rib, and vertebra

when these elements were compared to the same elements from all other donors in this study. A low decay constant (relatively fast turnover) is either indicative of a coupled high activity in both osteoblasts and osteoclasts, or a decoupled increase in osteoblasts while osteoclasts can either decrease or stay the same. Based on the properties of alendronate, it is possible that the low decay constant and relatively high turnover rates of this individual were caused by the drug decreasing osteoclastic activity while simultaneously increasing osteoblastic activity. This would increase overall bone density and reduce the symptoms of osteoporosis.

When discussing how individual health may impact bone collagen turnover rate, it is important to acknowledge that the majority of the donors used in this study had cancer, as donors 5 and 6 had melanoma and donors 10, 11, and 12 had lung cancer. Donors 5, 6 and 11 had metastatic cancer, meaning that the cancer had spread to other parts of the body. Of importance here is how these cancers may interact with bone and bone collagen. In advanced lung cancer, approximately 30-40% of cases also affect the bone in some way (Roato, 2014). Melanoma, though less likely to impact bone than lung cancer, still presents the possibility (Hiraga et al., 1995). Cancer can influence bone through two potential mechanisms: osteolytic metastases, involving the cancerous increase of osteoclastic cells, leading to lesions in the bone (Roato et al., 2010; Sela, 1977), and sclerotic metastases, involving an increase in osteoblastic cells, resulting in thicker bone tissue and the formation of thick spots on bone (Roato et al., 2010). For both melanoma and lung cancer, osteolytic metastasis is more likely than sclerotic metastases (Roato et al., 2010; Hiraga et al., 1995). Although it is not specifically noted whether the donors had metastasis that impacted bone, it is unlikely that this disease would affect the results of this study. While sclerotic growth on bone would increase the amount of bone tissue and therefore introduce new  $^{14}\text{C}$  into the newly synthesized bone, osteolytic metastases would only involve the

removal of bone, and assuming it would remove bone tissue randomly (with respect to  $^{14}\text{C}$  content), this would not affect the relative abundance of  $^{14}\text{C}$  from each year of life. No visible osteolytic lesions were observed on any bone at the time of sampling, however there was no concerted effort to search for these lesions either. Regardless, it is unlikely that the effects of cancer on bone affected the results of this study.

### *6.1.3. Does sex influence collagen turnover?*

Although the REST[ES] dataset had a limited number of female donors, the Southern Hemisphere data provided more representation of female individuals for comparison. Surprisingly, using the decay model revealed no discernible difference in the results between male and female samples. This finding is intriguing because it is commonly assumed that there are differences in bone remodeling with respect to sex (Hedges et al., 2007). Physiologically, one might expect differences in remodeling due to the fact that girls typically begin puberty and growth before boys (Rosenfield et al., 2000), potentially causing variations in remodeling patterns. Additionally, hormonal differences later in life could also influence the rate of remodeling (Feik et al., 1996). Despite these expectations, this study found no evidence to suggest overall differences, indicating that variations in turnover rates between and within individuals (among skeletal elements) might surpass any differences observed between the two sexes. However, it is also possible that the differences in remodeling according to sex decline in older adults and that the individuals from the study were too old to display these differences, which may have been more pronounced earlier in life. It is essential to note that a more comprehensive analysis with a larger sample size and age range would be necessary to confirm these preliminary findings.

#### *6.1.4. Does collagen turnover vary within a skeletal element?*

In this study, samples were taken from neighboring locations on an element (rib, mandible), from various spots on the same element (pelvis) or as a whole cross section of an element (femur). There were also samples taken from different vertebra, with both the lumbar and the thoracic vertebra sampled. The results showed that there can be variation within a skeletal element to varying degrees.

In general, the turnover rates between neighboring regions of bone were more similar than within a whole cross section of bone. Both the rib and the mandible began as one sample and was subsequently divided into two parts. For the rib, the difference in  $\Delta^{14}\text{C}$  between the two subsamples from donor 12 was smaller than the difference in  $\Delta^{14}\text{C}$  between the rib and any other bone for this donor. The mandible was similar, with a small difference in decay constants compared to the range of the whole donor. The cross section of the femur, however, indicated that any random sample from a femoral midshaft can yield relatively high or low turnover rates. The decay constants of samples from this cross section have both the second highest, as well as the third lowest for all samples from this donor (total n=15). The ulna, mandible, and rib of this donor are within the range of decay constants for the femur subsamples (table 5.06). There is no pattern in sampling location that would explain the difference, but the relatively coarse sampling resolution employed may obscure such patterning.

Differences in turnover rate between cortical and trabecular bone was visible between the rib samples, with the cortical bone (sample B) having a slightly lower decay constant (slightly slower turnover rates) than the sample that had more trabecular bone (sample A). Overall, bones that contain higher amounts of trabeculation were the fastest remodeling skeletal elements out of those that were sampled, such as the pelvis and the vertebra. This pattern is also found in the

Southern Hemisphere data, where the trabecular and cortical sections of both the femur and rib were tested. While there was not always a significant difference between the two tissue types within the same skeletal element, there was at least a small trend between the tissues, with the trabecular bone averaging lower decay constants. These findings are consistent with the general understanding that in most cases, cortical bone will have faster remodeling than trabecular bone (Bryant and Louitt, 1963; Hill, 1998; Cox and Sealy, 1997). It is also important to point out that this trabecular to cortical bone difference only applies within a skeletal element. Trabecular bone from one skeletal element may still have a slower turnover rate than cortical bone from another skeletal element, as was seen with in the Southern Hemisphere data, with the trabecular femur samples still averaging slightly higher turnover rates than the cortical rib samples.

Within the pelvis, different results were observed based on sampling location, consistent with previous results (Parfitt, 2002). When both the pubic symphysis and the iliac crest were sampled from the same donor, the iliac crest always had a lower decay constant than the pubic symphysis. The iliac crest is known to have some of the lowest amount of trabeculation in the pelvis (Zaharie and Phillips, 2018), and so this difference between the two locations is likely based on difference in bone tissue type. Interestingly, these two regions also experience differences in physical demand, as the pubic symphysis is affected by low strain activities that frequently occur, such as walking, while the iliac crest is most influenced by actions such as stair descent, which is an infrequent but more forceful action on the bone (Zaharie and Phillips, 2018). The greater sciatic notch and ischiopubic ramus were also sampled, however the sample size was too small to infer any patterns. This study confirms that trabeculation location is linked to the needs of the skeletal elements in that region, and that trabecular bone typically has a higher turnover rate than cortical bone within a skeletal element.

The utilization of both lumbar and thoracic vertebrae allows for the examination of potential differences between these bone types. The thoracic vertebra, on average, had a higher decay constant when compared to the lumbar vertebra. Although the difference is subtle, it aligns with expectations, considering that lumbar vertebrae, being lower on the spine, experience slightly more load than thoracic vertebrae. This slight increase in regular stress may result in higher overall turnover rates each year, and this is consistent with other observations in this study and others (Bergmann et al., 2010), however, a larger sample size is needed to confirm these findings.

The differences in  $\Delta^{14}\text{C}$  and thus collagen turnover rate observed within the same bone indicate that in some cases it may be possible to *a priori* predict the relative difference in turnover rate within a sample selected for stable isotope analysis, such as by sampling cortical or trabecular bone. However, the location of the sampling site may influence results in an unexpected manner. Consistently sampling cortical bone from the midshaft of a femur, the turnover rates may be highly variable with no predictable pattern. This finding highlights that while there should be better identification of sample location on a skeletal element when researchers discuss their sampling strategy, it is still difficult to definitively know the turnover rate of any sample taken from a relatively large skeletal element without an in depth analysis.

## **6.2. Models of Bone Turnover**

### *6.2.1. Fixed rate turnover model*

The “fixed rate turnover model” held annual bone collagen turnover consistent throughout life. While what is known about human growth and development (higher rates of

bone formation and turnover in young individuals; Bryant and Loutit, 1963; Hedges et al., 2007) contradict the basic precepts of this model, this is the way that bone turnover is often discussed in papers presenting stable isotope measurements of human bone collagen. Frequently, papers refer to a bone having a specific annual turnover rate, yet they often do not explicitly discuss how this rate might change at different stages of adulthood (e.g. Simpson et al., 2021; Higuero Pliego and Beaumont, 2023; Clauzel et al., 2022). Some researchers group human samples into adult and subadult categories, but even then, any change in turnover rate is generally not acknowledged across the ‘adult’ category. There were instances in which the fixed rate model could not be applied to a bone due to the measured  $\Delta^{14}\text{C}$  being too high to fit the equation (as discussed in section 5.3.1., and illustrated in figure 5.03). In these cases, even if the turnover interval was equal to the whole life, the equation would not be balanced, with the calculated  $\Delta^{14}\text{C}$  being less than the measured  $\Delta^{14}\text{C}$ . Since a turnover interval cannot be more than the age at death, the fixed rate model could not produce a feasible solution for these samples. Therefore, for at least some bones, their remodelling rate must have been higher when atmospheric  $\Delta^{14}\text{C}$  values were also higher (i.e., closer to but not earlier than the bomb curve peak), meaning that their turnover rates must be higher earlier in life. Since it is unlikely that some bones would have a fixed remodelling rate and some bones would not, we can exclude the results of the fixed rate model as the conclusions are likely not representative of the remodelling method in skeletal elements.

#### *6.2.2. Decaying rate turnover model*

Due to the unlikeliness of a static turnover rate throughout life, and a need for a higher turnover rate earlier in life, the decaying turnover model is more likely to be closer to the true turnover model that characterizes bones. Numerous studies have documented that bone

formation reduces with age, linked to a decrease in muscle use and general loading on the bone (e.g. Feik et al., 1996; Han et al., 1997; Fahy et al., 2017). Typically, prior to roughly age 30, there is the possibility of osteoblastic activity outweighing osteoclastic activity in response to activity levels and stimulation (Frost, 1997; Birkhold et al., 2014), and this allows for higher amounts of  $\Delta^{14}\text{C}$  to be incorporated into the bone and would allow for a higher relative turnover rate. With increasing age, osteoblastic activity slows down and will always be less than osteoclastic activity in normal adults, decreasing the amount of new carbon being added to bone, and decreasing the turnover rates each year (Muruganandan et al., 2018; Frost, 1997; Birkhold et al., 2014). Using the decaying turnover rate model in this study, turnover rates before age 30 were estimated to be relatively high, with the annual turnover rate averaging roughly 20% at age 25 across all skeletal elements for all donors, dropping to an average 5% at age 65 across all bone.

For the decay rate model, the turnover rates at any age can be estimated after the decay constant has been determined. While some models that have been used in the past allow for specific manipulation of turnover rates at different points of life (inflection points; e.g., Hedges et al., 2007), these models provide numerous possible variables to manipulate (the age for each inflection point as well as the rate at each inflection point) and make the comparison of skeletal elements to each other very difficult. These types of models are only possible to test if there are many individuals sampled from many different age categories but prove difficult when only older individuals are sampled. Fluctuating turnover rate models are such that they are highly age-specific and require the stage of life be known for a sample. While the bone turnover rate earlier in life will be higher than in old age, the exact rates in these early years cannot be accurately determined using  $^{14}\text{C}$  measurements of older individuals because many of the bones contain no

tissue from these early years. In many samples analyzed in this thesis, 0% of the bone tissue that formed early in life remained at death, and so any estimations of turnover rates for these early years are unlikely to be accurate. However, it is only for bones such as the ulna (with very slow turnover rates and therefore very high  $\Delta^{14}\text{C}$  values) where differences in turnover rate in these early years would greatly alter their measured  $\Delta^{14}\text{C}$  at death, as they do contain a higher proportion of bone formed in these early years. Since the donors in this study are all older adults, the exact rates per year for old individuals can be estimated with a relatively high degree of confidence. The accuracy of the estimated annual turnover rates necessarily decreases for earlier and earlier years, especially for bones with relatively high turnover rates (Table 6.2)

**Table 6.2.** The relative confidence in estimated annual turnover rates for bone collagen for different types of bones when using a decaying turnover rate model based on  $^{14}\text{C}$  data derived from old individuals.

Type of Bone	Estimated Turnover Rate for Early Life	Estimated Turnover Rate for Old Age
Slow Turnover Rate	Moderate-low confidence	High confidence
Fast Turnover Rate	Low-no confidence	High confidence

### 6.2.3. Hedges et al. (2007) model

Since the study by Hedges et al. (2007) only looked at the femur, only the femur results from REST[ES] were used to determine if the ranges of turnover rates at each year of life presented by Hedges et al. (2007) could accurately predict their measured  $\Delta^{14}\text{C}$  values. The Hedges et al. (2007) model did not always accurately predict the  $\Delta^{14}\text{C}$  values for the REST[ES] donors' femurs. The  $\Delta^{14}\text{C}$  measured values were not consistently higher or lower than the values predicted by the Hedges et al. (2007) model. The Hedges et al. (2007) model therefore does not

accurately capture the amount of variation in bone collagen turnover rate that can exist within a skeletal element like the femur.

It is possible that the model put forward by Hedges et al. (2007) does accurately reflect the way that bone turnover rate changes over time. This inflection point model mirrors the way that the decaying turnover rate model sharply decreases turnover rate each year in early life, and the difference between each year becomes less as the individual ages. The age of the inflection points, the turnover rates at each inflection point (especially the early ones), or some combination of these factors may be inaccurate in the Hedges et al. (2007) model. Another possible limitation of this model is that it was generated based on a single femur sample from each individual, which fails to capture the large range of potential intra-bone variation in collagen turnover that was observed in this study. It is interesting to note that the specific inflection points and turnover rates laid out by Hedges et al. (2007) vary based on the sex of the individual, with annual collagen turnover being 37% higher in females relative to males at the cessation of growth and 100% higher in females relative to males at the end of life. As has been discussed, there were no differences in bone collagen turnover between male and female skeletal elements for the REST[ES] donors, and so the sex-based differences in turnover rate for the femur presented by Hedges et al. (2007) may not be accurate.

#### *6.2.4. Model accuracy*

Using only the methods outlined in this study, it is challenging to definitively determine the accuracy of the decaying turnover model or identify if there are alternative models that better capture the processes of turnover occurring within bone. This model was informed by the available data on bone mechanics, with an effort to simplify them for comparative purposes. It is

likely that different skeletal elements may adhere to slightly different models, and an individual's life changes may cause their turnover rates to increase or decrease inconsistently. There can be variations in turnover rates within a single skeletal element and these differences could be due to slight fluctuations outside of the predicted decaying model. Samples taken in close proximity may be characterized by slightly different turnover rates, possibly caused by different loading demands on these sites. Innumerable variations in models of bone turnover could yield identical  $\Delta^{14}\text{C}$  values. For instance, the vertebra could slow down remodelling earlier in life and then accelerate later in life. Addressing these variations that are mathematically feasible but inconsistent with what is known about bone mechanics would not be productive. The general conclusions and relative estimates of bone turnover provided by these models are more valuable than any precise estimates of turnover, which will always be associated with some level of variation and uncertainty as discussed above.

### **6.3. Conceptualizing bone collagen turnover**

#### *6.3.1. Is remodeling random?*

Currently, bone collagen is largely assumed to randomly remodel, with no specific BMUs targeted for remodeling before any other BMUs on a microscopic level (Katsimbri, 2017). Specifically, older BMUs are not thought to be targeted for remodeling, and instead at any time, any BMU is equally likely to be remodeled within a section of bone, with the majority of remodeling being 'non-targeted' (Burr, 2002; Katsimbri, 2017). The percentage of collagen attributed to each decade of life in this study was a result of randomly applying the annual turnover rate to all BMUs each year. However, the actual mechanics for the turnover on this

microscopic scale is largely unstudied and could follow a model in which every year, only the oldest BMUs are selected to remodel (hereafter ‘oldest first’ remodeling). With truly random remodeling, the oldest BMU could have come from any point in life, however it is less likely to come from earlier ages in elements that remodel faster as there are more opportunities for that specific BMU to remodel. These two different remodeling scenarios are illustrated in figure 6.1 where two skeletal elements from donor 3 are visualized according to the different scenarios for remodeling: random and oldest first.

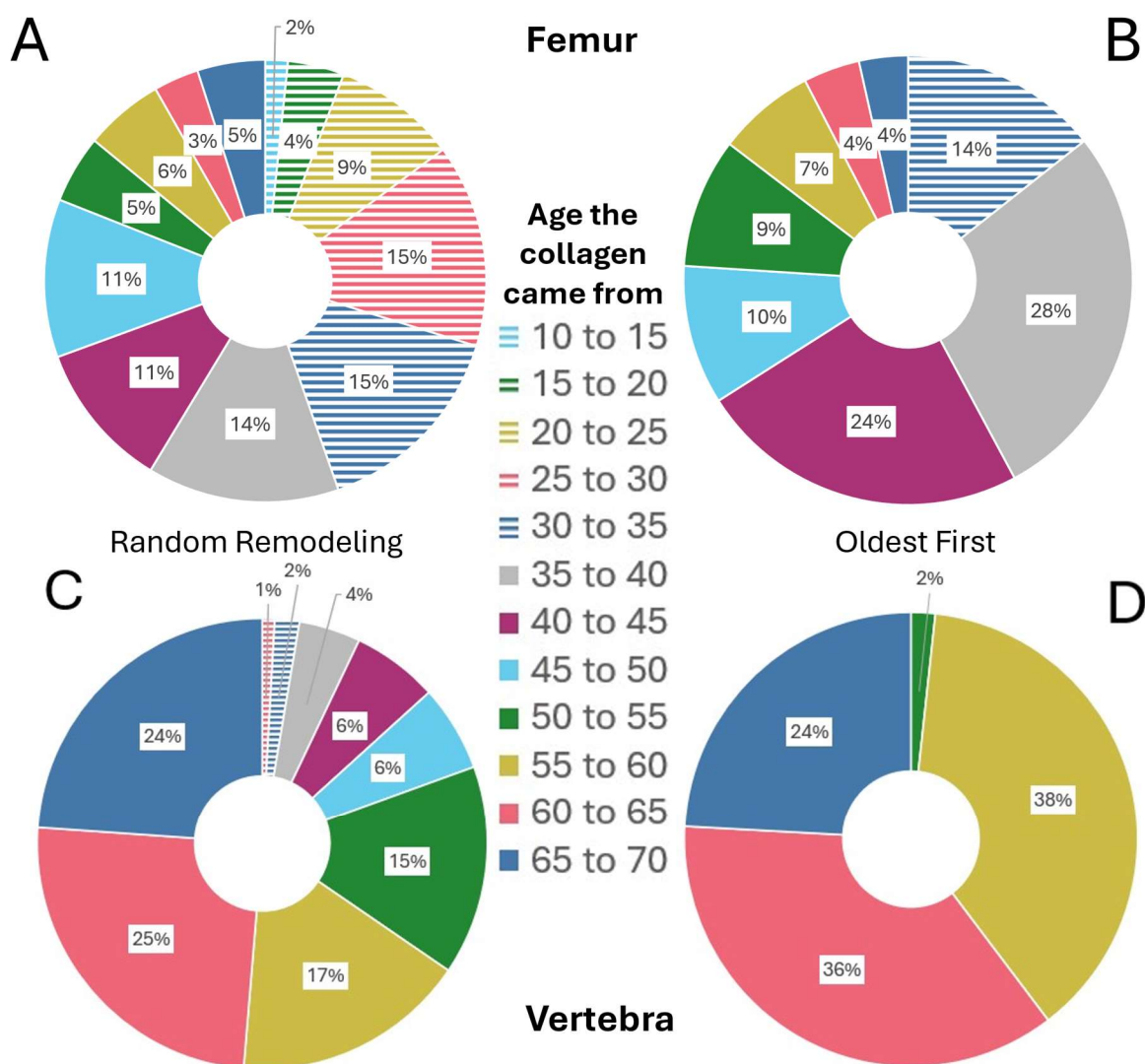


**Figure 6.1.** The percentage of a bone sample at death attributed to each age range from the femur (A and B) and vertebra (C and D) from donor 3. Random remodeling is displayed on the left (A and C) and oldest first remodeling is displaying on the right (B and D).

There is a large difference in what periods of the life history are represented in a sample depending on whether a random or oldest first remodeling model is applied. Overall, the random remodeling scenarios have a much longer turnover interval, as older BMUs may remain untouched until death, especially for bones with a lower annual rate of turnover. More than 25% of the whole sample makeup for both skeletal elements in the random remodeling scenario are from years that would have been fully remodeled and replaced under an oldest first remodeling scenario. The percentage of sample attributed to the years closer to death are less impacted by either scenario, and instead the oldest BMUs that still exist in the ‘oldest first’ model become much larger. This is because in the ‘random remodeling’ scenario, the BMUs from earlier period have a greater chance at experiencing remodeling throughout life as more time has passed and more remodeling cycles have occurred, whereas these older BMUs from the ‘oldest first’ model will not have had the chance to remodel and thus decrease in relative abundance until they are the oldest possible BMU in the sample.

Bone remodeling is typically conceptualized as if BMUs will remodel randomly within small regions. However, it is known that various factors can influence the turnover rate of a skeletal element on a large and small scale. The factors include phenomena such as microcracks and other microscopic damages within the bone (Burr, 2002; Clark, 2008; Katsimbri, 2017). However, it is important to consider why microcracks may form. As discussed in Chapter 2, BMUs continue to mineralize with age, resulting in decreased water content within a BMU and rendering it drier and more brittle over time (Burr, 2019; Farlay and Boivin, 2012). Under these

circumstances, older BMUs are likely more prone to microcracks and therefore more susceptible to remodeling than newer bone, which is still resilient to cracking. Roughly 30% of bone remodeling is thought to be for repairing damaged tissue (Burr, 2002). Consequently, bone remodeling is not likely to be completely random, but it also does not strictly follow an ‘oldest first’ model. Instead, remodeling consists of a combination of random alongside selective remodeling to replace old and damaged BMUs. Therefore, older BMUs are more likely to be replaced than younger BMUs, but the relative probabilities are unknown.

### *6.3.2. The Influence of Age on Collagen Makeup*

Since the annual turnover rate of each bone decreases as one ages, the age at death significantly influences the relative age composition of collagen. To illustrate how the composition of bone changes throughout life, figure 6.2 highlights the percentage of a sample that would be attributed to each decade of life across different ages (data in table 6.3 and 6.4). In a bone with slow turnover like the ulna, there is less change between ages as one gets older, as in the example from figure 6.2 it can be seen that the percentage of bone that was made between age 10 and age 20 remains relatively even as the individual ages. In the case of the bone with more rapid turnover, collagen that was produced in earlier decades is replaced as the individual ages and the majority bone at any age is made within the last decade.



Age is not typically explicitly discussed when researchers refer to the turnover rate of bone collagen in the context of life history information derived from stable isotope measurements. In some cases, adults and subadults are separated, but typically all adults are discussed as one homogenous group (e.g. Fernández-Crespo et al., 2022; Gaydarska et al., 2022; Pickard and Bonsall, 2022). However, there is a significant difference with respect to the period of the life history that is represented by the isotopic composition of bone collagen for a 30 year old adult and a 60 year old adult. In these younger individuals, the majority of bone was produced within roughly the last decade of life, but in older individuals, a wider range of decades are represented (Figure 6.2). It is therefore important for the age of the individual being sampled to be known if specific turnover rates are to be used. In many cases, the specific age of individuals sampled from is unknown to researchers, especially if the remains being sampled were fragmentary or poorly preserved. At the very least, it is important to convey the uncertainty in collagen turnover rates that exist when an adult individual cannot be more specifically aged.

### 6.3.3. Collagen as a “Life Average”

It is typical for researchers conducting stable isotope studies to discuss bone collagen and indicate that its isotopic composition is reflective of the average diet over the last years prior to death (e.g. Velte et al., 2023; Gregoricka and Ullinger, 2022; Miller et al., 2023; Pickard and Bonsall, 2022). While developing a more precise assessment of exactly what period prior to death is represented in bone collagen was the primary purpose of this thesis, it is important to acknowledge that collagen does not represent an equally-weighted average of this period either (Figures 6.1, 6.2). There are two factors working against the even distribution of tissue formation across the turnover interval. First, the turnover rate of bone slows down with age, such that fewer BMUs are introduced to the tissue each year. Second, even if the turnover rate remained equal

throughout life, those BMUs that were produced in earlier years have had more opportunities to be randomly selected for remodeling and therefore would likely make up less of the collagen tissue. With these two factors, the speed at which turnover rates decline will have an effect on the bone collagen makeup. As with a bone like the ulna, the turnover rates become low at a younger age and so there are not enough remodeling events to significantly remove the BMUs made in earlier periods of life. Bones like the ulna with slow turnover rates are therefore more effected by the first factor. A skeletal element with a more gradual decline in turnover rates (i.e., one that retains a relatively high turnover rate late in life) has enough remodeling occurring at any period such that there is a higher probability of older BMUs being selected for remodeling, and therefore is more effected by the second factor. Both of these factors have the possibility to skew the collagen composition in any direction and make it incredibly unlikely that a collagen sample will represent an even 'average' over life.

## **6.4. Implications for palaeodietary studies**

### *6.4.1. Suggestions for future work*

The results of this study can be applied to future studies that use bone collagen as an analyte, as a better understanding of what a sample of bone collagen actually represents will allow for these studies to be more precise and will possibly open up new opportunities. A fixed rate turnover model does not accurately capture the remodelling pattern of bone collagen, and that turnover rate must be higher earlier in life. If turnover rate is influenced by activity levels as well, it is likely that the collagen in many skeletal elements reflects the activities of an individual

while they were in the *prime of their life*, that is, in young adulthood the bone will reflect the diet leading up to death and in old age, the bone will likely reflect the diet in young adulthood.

Stable isotope research very frequently uses bone collagen in order to assess the diet and activities of archaeological individuals. As previously stated, these researchers typically assume that all cortical bone from any skeletal element will have collagen that formed during more-or-less the same period of time. Based on the results of this thesis, there are clearly vast differences in the period of life that each bone collagen sample's isotopic composition will represent. In many cases, turnover rates and turnover intervals are not especially meaningful in these types of studies as they are subject to change or are unevenly weighted throughout life. Researchers must highlight the decline in annual turnover rates over life and indicate that what they are analyzing does not evenly represent the years leading up to death. The use of turnover intervals (i.e., stating that "collagen represents diet from the last 10 years of life") must be prefaced with the fact that earlier life is more heavily weighted and that the exact age of the individual will dramatically change the temporal composition of the sample depending on the skeletal element analyzed. If possible, results from palaeodietary studies should be interpreted accordingly, framing the interpretations of the dietary patterns in the context of what is known about bone turnover.

The difference in turnover rates between skeletal elements provides researchers with two opportunities for research. In the case of bones with fast turnover rates, researchers may be able to ask questions about a short period of time leading up to death. For example, if a group of individuals were thought to undergo some sort of dietary change prior to death (perhaps they were fed a different diet in the years before being sacrificed, or a group of individuals died after a famine and determining what they ate in the years prior to death is the goal of the research) this can be assessed using fast turning over bones, such as the pelvis and the vertebra. If capturing the

diet earlier in life is the goal (perhaps the individuals were identified as migrants based on genetic or other isotopic data and reconstructing their diet before relocating is the goal of the analysis) then bones with slow turnover rates such as the ulna will give a better representation of the diet earlier in life. If the goal is in fact to assess the average diet of a group of individuals, it is recommended that samples from a few different skeletal elements be taken from each person so that dietary variation within an individual can be assessed.

This study also highlights the potential for researchers to perform diachronic analysis within a single individual using bones rather than teeth. Teeth have primarily been used for this purpose because they form incrementally and are inert once formed, but any insights are limited to early in life (e.g. Eerkens et al., 2011; Beaumont and Montgomery, 2016). Using bones to examine diachronic variation has been attempted in the past, and often are ribs selected as the short-term diet element and the femur is chosen as the long-term diet element (e.g., Cheung et al., 2017; Cox and Sealy, 1997; Drtikolova Kaupova et al., 2021; Dauven et al., 2017; Lamb et al., 2014; Pollard et al., 2012). This study highlights that this way of particular paired comparison is likely unreliable, as the femur and the rib do not have statistically different turnover rates (table 5.07). Any variation in isotopic compositions between these elements could likely be attributed to intra-element variation, which can be substantial as demonstrated with the multiple femur samples taken from the same individual in this study (table 5.06). It is problematic that the rib and the femur are still so frequently used to show diachronic variation (e.g. Deng et al., 2024 as a recent example) as their similarity in turnover rates has been noted in the past (Fahy et al., 2017; Jørkov et al. 2009) and is confirmed by the results of this thesis.

The results of this study highlight that the long bones of the arm or skull are the best elements to use for a long-term diet indicator and suggests using vertebrae or the pelvis as a short

scale diet indicator. As well, trabecular bone is likely a good indicator of short-term diet and can be sampled to target diet closer to death, however comparisons of trabecular to cortical bone should be limited to those made within the same skeletal element, as trabecular bone of one skeletal element can still be slower to turnover than cortical bone of a different skeletal element.

#### *6.4.2. Comparison of results to previous estimates of turnover*

To gauge how the outcomes of this study align with prior research, we will revisit some of the studies outlined in Chapter 3. The most frequently cited bone collagen turnover rate study in archaeological science, including in this study, is by Hedges et al. (2007), which specifies a specific turnover rate for the cortical femur alone. Another pertinent study is by Bryant and Loutit (1963), which offers specific rates for various bones. Those overlapping with this study encompass the rib, vertebra, pelvis, and femur. The study also provides rates for the skull; however turnover rates using  $^{14}\text{C}$  measurements have only been estimated for the occipital and parietal bone, with information derived from the Ubelaker et al (2022) study. Fahy et al. (2017) provided a qualitative order for various skeletal elements, although it lacks annual turnover rates for these skeletal elements.

The Hedges et al (2007) study had the following conclusions:

1. From age 20–80, femur collagen on average turns over annually 4–3% for females and 3–1.5% for males.
2. Adolescents have a much higher collagen turnover rate than adults.
3. There is variation between individual turnover rates that can lead to differences in life history representation in the bone collagen.
4. The turnover interval of human femoral collagen is at least 10 years, but likely more.

The major conclusions of this thesis agree with those of Hedges et al. (2007) study. For instance, turnover rates are higher in adolescence than in adulthood, and this is the case for all bones, not just the femur. This conclusion is strengthened in this thesis, as some bones had measured  $\Delta^{14}\text{C}$  that were so high that the majority of the bone collagen must have formed in youth with higher turnover rates, followed by very low turnover rates later in life. As well, the conclusion that there are variations between individuals is also supported, with some variation in  $\Delta^{14}\text{C}$  and thus turnover rate observed within the same skeletal element across different donors. Variation in  $\Delta^{14}\text{C}$  within same element of a single person was also observed.

In section 5.5, the measured  $\Delta^{14}\text{C}$  of the REST[ES] femurs were compared to the expected  $\Delta^{14}\text{C}$  that would be expected using the inflection points and turnover rates laid out in Hedges et al. (2007). While sometimes the measured femur  $\Delta^{14}\text{C}$  values fell within the expected range, often the measured  $\Delta^{14}\text{C}$  fell outside of the expected range. This indicates that the upper and lower turnover rates at each age outlined in Hedges et al. (2007) does not accurately reflect the extent of variation in annual turnover that may exist between femur samples of different individuals. It is clear from this study that the amount of variation in bone collagen turnover, not just between femur samples from different individuals, but all skeletal elements from different individuals is high enough to make it hard to ascertain the turnover rate of any bone *a priori*.

There are other differences between the findings of the Hedges et al. (2007) study and the current one. Notably, this study shows no discernible distinctions between the two sexes, contrary to the indications in Hedges et al. (2007). The limited sample size here precludes definitive conclusions, but this warrants consideration in future research. Moreover, for femurs aged 20-80, this thesis reveals a higher average turnover rate (with the average found through summing each annual turnover rate produced within a decay model between age 20-80 across

donors) of 5.8% per year with the decay model from age 20-80. This contrasts with Hedges et al. (2007), and the higher average in this thesis is likely due to different estimates for early adulthood turnover rates. In this study, the decay rate model consistently estimated the turnover rate around age 20 to be roughly 20% per year and estimated the turnover rate at the time of birth to be 100% whereas Hedges et al. (2007) estimated a turnover rate of 50% at birth and an annual turnover rate of roughly 5% at age 20. Without direct sampling of individuals of a younger age, it is not possible to evaluate the relative accuracy of either model at these younger ages.

As well, Hedges et al. (2007) do not suggest that there is a substantial enough change in turnover rate between age 20 to age 80 to warrant separating the adult category into different age groups. This study suggests the presence of large differences in annual turnover rate between young adults and old adults. Younger individuals in this range might still exhibit bone modeling and high osteoblastic activity, while older individuals experience a notable reduction in bone cell activities (Frost, 1997; Birkhold et al., 2014; Muruganandan et al., 2018). Additionally, Hedges et al. (2007) proposed a 10-year or more turnover interval for individuals up to age 80, mentioning that a larger portion is produced in adolescence. This does not emphasise enough that the concept of turnover interval is problematic due to the uneven weighting of turnover rate throughout life, and many researchers do not mention these findings from Hedges et al. (2007) when discussing turnover rates. An important conclusion of this research is that turnover rate decreases throughout life, meaning that each period of life is represented in a sample of bone collagen to differing degrees. Using a turnover interval (e.g., 10 years) does not immediately illustrate this complexity and can therefore misrepresent conclusions.

The Fahy et al. (2017) study sampled individuals who were likely between 25 to 35 years old from the Medieval period. They list the order of elements from fastest to slowest turnover

rate as follows: humerus, metacarpals, rib, femur, tibia, radius, clavicle, occipital. The rib and femur having similar turnover rates is consistent with the findings of this study, as well as the occipital having the slowest turnover rate of the bones sampled. Fahy et al. (2017) list the humerus as the fastest remodelling bone, while in this study the humerus is one of the slower bones. This difference could be due to a few factors, one being that a different method (osteon population density counts) was used in their study, and their method may be less well-suited to producing accurate turnover rates in this scenario as OPD is highly reliant on visual characteristics of bone which may be difficult with archaeological samples, as they were in the case of Fahy et al. (2017). It is also possible that either humerus samples from the REST[ES] individuals or from Fahy et al. (2017) unintentionally sampled a location on the humerus that favours faster or slower turnover. Since there is a high degree of variation in turnover rate that has been observed within the femur, it is possible that this variation is the source of the discrepancy between the two studies. A third factor could be the biomechanics of the two populations that were sampled. In the Fahy et al. (2017) study, only relatively young adults from the Medieval period were sampled. The donors from this study were modern individuals roughly 40 years older than this group. The difference seen in the humerus only may mean that there is some fundamental difference between the sample groups. The Medieval samples may represent individuals that typically experienced a higher degree of loading on their humerus. It is also possible that the humerus has a faster remodelling rate earlier in life and sharply declines to be a very slow remodelling bone later in life. Any of these scenarios, or some combination, are possible.

The study by Bryant and Loutit (1963) described in table 3.1 lists turnover rate in both adolescent and adult categories, and here only the comparison of the adult values will be

considered. Notably though, their study does specify that adolescent turnover rates are faster than the adult ones, which is in agreement with the findings of this study. Considering the elements measured in this study, Bryant and Loutit (1963) rank the vertebra as the fastest remodelling element, and next the ilium, the proximal femur, the rib, the distal femur/average femur, and finally skull. This fits generally with the order seen within this study, with vertebra being the fastest, then pelvis, the femur and rib being similar, and the skull being the slowest turning over element. As for specific turnover rates, Bryant and Loutit (1963) group adults into the category of those age 35-85. While the results of this study indicate that the turnover rate changes across this age range, taking the average turnover rate across this same time period for each bone and then taking an average across donors could indicate whether or not differences are visible between the two sets of turnover rates. The result of this comparison is shown in table 6.3 and shows that the turnover rates in the Bryant and Loutit (1963) study are all slightly lower than the turnover rates seen in this study, however they are comparable. This difference could indicate that either Bryant and Loutit (1963) systematically underestimate the turnover rate average across this time period, or that the decay rate model from this study has turnover rates that are too high in this age range and therefore less bone is made after age 35 than predicted in this model for at least the four bones that were measured in both studies. Its important to point out that the results from Bryant and Loutit (1963) are more likely to be problematic, as their method of determining the replacement rate of strontium within each skeletal element is highly reliant on an assumed diet.

**Table 6.5.** Average annual turnover rate (%) from age 35-85 in this study using the decay rate model and the study by Bryant and Loutit (1963) for the elements which were measured in both studies.

Element	Bryant and Loutit (1963)	This Study

Femur	2.9	3.5
Rib	4.7	5.5
Pelvis	6.5	7.6
Vertebra	8.3	11.1

Its important to keep in mind that while there are differences between the “average” bone turnover rate taken from this study and the average bone turnover rate in other studies, the average is not especially meaningful. As discussed previously, turnover rate can change drastically within the adult category and so the accuracy of the average turnover rate is less important, and it is more important to depict how time is represented in a sample of bone collagen.

## **Chapter 7: Conclusion**

This study has aimed to address what the specific turnover rates are for multiple skeletal elements in humans in order to help better define what period of an individual's life is being analyzed when bone collagen is used in stable isotope analysis. It is very important for researchers that use bone collagen as an analyte to mention over what period the collagen they are analyzing was formed, as this indicates the period of life of the individual that they are deriving their information from. Until now, there is only one major study on the turnover rate of bone collagen, and this study only covers the turnover period of the femur (Hedges et al., 2007). Due to a lack of research for all skeletal elements, researchers have had to apply the results from the Hedges et al. (2007) study to other skeletal elements that they may be analyzing. As well, researchers using multiple skeletal elements in the hopes of performing diachronic analysis have looked to use the femur as an indicator of long term life history information and the rib as an indicator of short term information, and this approach was popularized by Cox and Sealy (1997) but its effectiveness has not been well studied.

I employed a method from Hedges et al. (2007), using a radiocarbon spike in the 1960s to assess collagen's intake of environmental data and tissue turnover. Seven adults to late adult donors were sampled from the facility for Research in Experimental and Social Thanatology / *Recherche en Sciences Thanatologiques [Experimentales et Sociales]* in Québec, with seven different skeletal elements sampled across the donors. This data was supplemented with two south American studies that had previously published radiocarbon data from more skeletal elements (Ubelaker et al. 2022; Johnstone-Belford et al. 2022) Results revealed varied turnover rates across skeletal elements, ranked from slowest to fastest as follows: ulna, humerus, femur, rib, pelvis, vertebra. This demonstrates that femur turnover rates from Hedges et al. (2007)

cannot be extrapolated to other elements due to inherent differences. There was also a high degree of variation in turnover rate within a single skeletal element group, showing that it is extremely difficult to know what the turnover rate of any element will be due to multiple factors that can influence its variation from person to person. As well, there can be a high degree of variation within a single skeletal element, showing how just a difference in sample site can lead to differences in what data is being taken from the bone.

A major finding of this study was that the rib and the femur have no significant difference in turnover rates and that if the goal is to look at diachronic change in an individual, these bones should not be selected for analysis. Instead, a much slower turning over element such as the ulna or the parietal and a much faster turning over element such as the vertebra or the pubic symphysis of the pelvis would be best at showing two distinct periods of life. Moreover, this study found that bone is not always going to be averaged over the period of time of formation, as the rate of synthesis of collagen is unevenly weighted throughout life. This is especially true for slow turning over bones and bones of older individuals, where bone may be more heavily weighted towards the earlier years of the turnover interval whereas faster bones are more heavily weighted towards the later years of its interval. As well, this study confirms that bone remodels faster in youth. Frequency of forces placed on bones likely play a role in influencing the speed of turnover, with frequently loaded bones such as the spine being fast and infrequent bones such as the skull being slow. Decline in activity with age likely plays a role in the decay of turnover rate and overall bone health. This study also found no differences in turnover rate between the sexes that had previously been thought to exist (Hedges et al. 2007), however this may be attributed to the age of the individuals sampled in this study.

This study provides the most extensive compilation of bone collagen turnover rates across various human skeletal elements to date. By offering precise turnover data, researchers can accurately determine the time period reflected in their analyses, enhancing the accuracy of their interpretations. Moreover, these findings improve the precision of diachronic analyses and offer valuable insights into factors like activity level and sampling site, which influence turnover rates. More research should be done in the future to continue to better quantify the turnover rate of various skeletal elements in humans, expanding to assess skeletal elements which were not analyzed here such as phalanges or the tibia, as well as increase the sample size of the skeletal elements from this study. It is important to also look at a broader range of ages to understand how turnover rate changes through life in more detail. As well, expanding this method to better quantify the turnover rates of animal skeletal elements will help bring together the whole picture of not just past humans but also their environment and food sources in stable isotope analysis. Given the resilience of bone collagen in archaeological contexts, this research significantly improves archaeological science which contributes to our understanding of past civilizations and cultures, extending our knowledge far beyond the decay of other informative tissues.

## References

- Alves E.Q., Macario K, Ascough P, Bronk C.R., 2018. The Worldwide Marine Radiocarbon Reservoir Effect: Definitions, Mechanisms, and Prospects. *Reviews of Geophysics* 56, 278-305.
- Ambrose SH, 2000. Controlled diet and climate experiments on nitrogen isotope ratios of rats, in: Ambrose SH, Katzenberg MA (Eds.), *Biogeochemical Approaches to Paleodietary Analysis*. Kluwer Academic, New York, pp. 243-259.
- Ambrose, S. H., & Norr, L. (1993). Experimental evidence for the relationship of the carbon isotope ratios of whole diet and dietary protein to those of bone collagen and carbonate. In *Prehistoric human bone: archaeology at the molecular level* (pp. 1-37). Berlin, Heidelberg: Springer Berlin Heidelberg.
- Arens, D., Sigrist, I., Alini, M., Schawalder, P., Schneider, E., & Egermann, M. (2007). Seasonal changes in bone metabolism in sheep. *The Veterinary Journal*, 174(3), 585–591.
- Arlot, M., Meunier, P.J., Boivin, G., Haddock, L., Tamayo, J., Correa-Rotter, R., Jasqui, S., Donley, D.W., Dalsky, G.P., Martin, J.S. and Eriksen, E.F. (2005). Differential effects of teriparatide and alendronate on bone remodeling in postmenopausal women assessed by histomorphometric parameters. *Journal of Bone and Mineral Research*, 20(7), 1244-1253.
- Ascough, P., Cook, G., & Dugmore, A. (2005). Methodological approaches to determining the marine radiocarbon reservoir effect. *Progress in Physical Geography: Earth and Environment*, 29(4), 532–547.
- Balena, R., Shih, M.-S., & Parfitt, A. M. (2009). Bone resorption and formation on the periosteal envelope of the ilium: A histomorphometric study in healthy women. *Journal of Bone and Mineral Research*, 7(12), 1475–1482.
- Bataille, C. P., Chartrand, M. M. G., Raposo, F., St-Jean, G. (2020). Assessing geographic controls of hair isotopic variability in human populations: A case-study in Canada. *PLOS ONE*, 15(8), e0237105.
- Baxter, B. J., Andrews, R. N., & Barrell, G. K. (1999). Bone turnover associated with antler growth in red deer (*Cervus elaphus*). *The Anatomical Record*, 256(1), 14–19.
- Beaumont, J., & Montgomery, J. (2016). The Great Irish Famine: Identifying starvation in the tissues of victims using stable isotope analysis of bone and incremental dentine collagen. *PLoS One*, 11(8), e0160065.
- Bell, L. S., Cox, G., & Sealy, J. (2001). Determining isotopic life history trajectories using bone density fractionation and stable isotope measurements: A new approach. *American Journal of Physical Anthropology*, 116(1), 66–79.
- Bennell, K. L., Malcolm, S. A., Khan, K. M., Thomas, S. A., Reid, S. J., Brukner, P. D., Ebeling, P. R., & Wark, J. D. (1997). Bone mass and bone turnover in power athletes, endurance athletes, and controls: A 12-month longitudinal study. *Bone*, 20(5), 477–484.

- Bergmann, P., Body, J. J., Boonen, S., Boutsen, Y., Devogelaer, J. P., Goemaere, S., ... Rozenberg, S. (2010). Loading and Skeletal Development and Maintenance. *Journal of Osteoporosis*, 2011, 1–15.
- Birkhold, A. I., Razi, H., Duda, G. N., Weinkamer, R., Checa, S., & Willie, B. M. (2014). The influence of age on adaptive bone formation and bone resorption. *Biomaterials*, 35(34), 9290-9301.
- Blair, H.C., Larrouture, Q.C., Li, Y., Lin, H., Beer-Stoltz, D., Liu, L., Tuan, R.S., Robinson, L.J., Schlesinger, P.H. and Nelson, D.J. (2017). Osteoblast differentiation and bone matrix formation in vivo and in vitro. *Tissue Engineering Part B: Reviews*, 23(3), pp.268-280.
- Bonani G, Ivy SD, Niklaus TR, Suter M, Housley RA, Bronk CR, van Klinken GJ, Hedges REM. (1992). Altersbestimmung von milligrammprouben der Oetztaler Gletscherleiche mit der Beschleunigermassenspektrometrie-methode (AMS). In: Ho ¨pfel F, PlatzerW, SpindlerK, editors. DermannimEis, Bandi. Innsbruck, Austria: Eigenverlag der Universita ¨t Innsbruck, 108–116.
- Bronk, C.R. (2008). Radiocarbon Dating: Revolutions in Understanding. *Archaeometry*, 50(2), 249–275.
- Brown TA, Nelson DE, Vogel JS, Southon JR. (1988). Improved collagen extraction by modified Longin method. *Radiocarbon* 30(2), 171–7.
- Bryant, F. J., and J. F. Loutit. (1963). The entry of strontium-90 into human bone, *Proc. Roy. Soc.* 159, 449-465
- Buchardt, B., Bunch, V., Helin, P. (2007). Fingernails and diet: Stable isotope signatures of a marine hunting community from modern Uummannaq, North Greenland. *Chemical Geology*, 244, 316-329.
- Buchman, A. S., Wilson, R. S., Yu, L., James, B. D., Boyle, P. A., & Bennett, D. A. (2014). Total daily activity declines more rapidly with increasing age in older adults. *Archives of gerontology and geriatrics*, 58(1), 74-79.
- Burr, D. B. (1992). Estimated intracortical bone turnover in the femur of growing macaques: Implications for their use as models in skeletal pathology. *The Anatomical Record*, 232(2), 180–189.
- Burr, D. B. (2002). Targeted and nontargeted remodeling. *Bone*, 30(1), 2-4.
- Burr, D. B. (2019). Bone Morphology and Organization. In Burr, D.B. and Allen, M.R. (Eds.) *Basic and applied bone biology* (Second edition). Elsevier/Academic Press.
- Carbone, M. S., Ayers, T. J., Ebert, C. H., Munson, S. M., Schuur, E. A., & Richardson, A. D. (2023). Atmospheric Radiocarbon for the Period 1910–2021 Recorded by Annual Plants. *Radiocarbon*, 65(2), 357-374.
- Cheung, C., Jing, Z., Tang, J., Weston, D. A., & Richards, M. P. (2017). Diets, social roles, and geographical origins of sacrificial victims at the royal cemetery at Yinxu, Shang China: New evidence from stable carbon, nitrogen, and sulfur isotope analysis. *Journal of Anthropological Archaeology*, 48, 28-45.

- Clark, C. T., Horstmann, L., & Misarti, N. (2017). Quantifying variability in stable carbon and nitrogen isotope ratios within the skeletons of marine mammals of the suborder Caniformia. *Journal of Archaeological Science: Reports*, 15, 393–400.
- Cox, G., & Sealy, J. (1997). Investigating Identity and Life Histories: Isotopic Analysis and Historical Documentation of Slave Skeletons Found on the Cape Town Foreshore, South Africa. *International Journal of Historical Archaeology*, 1(3), 207–224.
- Craig OE, Bondioli L, Fattore L, Higham T, Hedges R. (2013). Evaluating marine diets through radiocarbon dating and stable isotope analysis of victims of the AD79 eruption of vesuvius. *American Journal of Physical Anthropology* 152, 345-352.
- Currey, J. D. (2006). *Bones: structure and mechanics*. Princeton university press.
- Daegling, D. J., & Hotzman, J. L. (2003). Functional significance of cortical bone distribution in anthropoid mandibles: An in vitro assessment of bone strain under combined loads. *American Journal of Physical Anthropology*, 122(1), 38–50.
- DeNiro, M. (1987). Stable isotopy and archaeology. *American scientist*, 75(2), 182-191.
- DeNiro, M., Epstein, S. (1978). Influence of diet on the distribution of carbon isotopes in animals. *Geochimica et Cosmochimica Acta*, 42, 495-506.
- DeNiro, M., Epstein, S. (1981). Influence of diet on the distribution of nitrogen isotopes in animals. *Geochimica et Cosmochimica Acta*, 45, 341-351.
- Deng, C., Gao, Z., Wu, Q., Zhou, Y., & Guo, Y. (2024). Millet agriculture and social complexity in the Central Plains of the Neolithic (9000-5000 BP): Isotopic reconstruction of human diet from the Shanggangyang site in China. *Journal of Archaeological Science*, 161, 105893
- Dutta, K. (2016). Sun, ocean, nuclear bombs, and fossil fuels: Radiocarbon variations and implications for high-resolution dating. *Annual Review of Earth and Planetary Sciences*, 44, 239-275.
- Dyke AS, Savelle JM, Szpak P, Southon JR, Howse L, Desrosiers PM, Kotar K. (2019). An Assessment of Marine Reservoir Corrections for Radiocarbon Dates on Walrus from the Foxe Basin Region of Arctic Canada. *Radiocarbon* 61, 67-81.
- Eerkens, J. W., Berget, A. G., & Bartelink, E. J. (2011). Estimating weaning and early childhood diet from serial micro-samples of dentin collagen. *Journal of Archaeological Science*, 38(11), 3101-3111.
- Enlow, D.H. & Brown, S.O. (1957). A comparative histological study of fossil and recent bone tissues\_part II. *The Texas Journal of Science* 9, 186–214.
- Enlow, D.H. & Brown, S.O. (1958). A comparative histological study of fossil and recent bone tissues\_part III. *The Texas Journal of Science* 9, 186–214.
- Eriksen, E. F. (2010). Cellular mechanisms of bone remodeling. *Reviews in Endocrine & Metabolic Disorders*, 11(4), 219–227.

- Fahy, G. E., Deter, C., Pitfield, R., Miszkiewicz, J. J., & Mahoney, P. (2017). Bone deep: Variation in stable isotope ratios and histomorphometric measurements of bone remodelling within adult humans. *Journal of Archaeological Science*, 87, 10–16.
- Farlay, G., Boivin, G. (2012) Bone Mineral Quality. In Dionyssiotis, Y. (Ed.). *Osteoporosis*. InTech.
- Fatayerji, D., & Dr. Eastell, R. (1999). Age-related changes in bone turnover in men. *Journal of Bone and Mineral Research*, 14(7), 1203-1210.
- Fehling, P. C., Alekel, L., Clasey, J., Rector, A., & Stillman, R. J. (1995). A comparison of bone mineral densities among female athletes in impact loading and active loading sports. *Bone*, 17(3), 205–210.
- Feik, S. A., Thomas, C. D. L., & Clement, J. G. (1996). Age trends in remodeling of the femoral midshaft differ between the sexes. *Journal of Orthopaedic Research*, 14(4), 590–597.
- Folch J., Lees M., Stanley G.H.S. (1957). A simple method for the isolation and purification of total lipides from animal tissues. *Journal of Biological Chemistry*, 226, 497-509.
- Fourel F, Martineau F, Seris M, Lécuyer C, 2014. Simultaneous N, C, S stable isotope analyses using a new purge and trap elemental analyzer and an isotope ratio mass spectrometer. *Rapid Communications in Mass Spectrometry* 28, 2587-2594. doi:https://doi.org/10.1002/rcm.7048
- Frost, H. M. (1969). Tetracycline-based histological analysis of bone remodelling. *Calcified Tissue Research*, 3(1), 211–237.
- Frost, H. M. (1997). On our age-related bone loss: insights from a new paradigm. *Journal of Bone and Mineral Research*, 12(10), 1539-1546.
- Glimcher, M.J., 1998. The nature of the mineral phase in bone: biological and clinical implications. In: Avioli, L.V., Krane, S.M. (Eds.), *Metabolic Bone Disease and Clinically Related Disorders*. Academic Press, San Diego, pp. 23e50.
- Godwin, H. (1962). Half-life of radiocarbon. *Nature* 795:984.
- Graven, H, R Keeling and X Xu, (2022). Radiocarbon dating: Going back in time. *Nature*.
- Graven, H., Allison, C. E., Etheridge, D. M., Hammer, S., Keeling, R. F., Levin, I., White, J. W. C. (2017). Compiled records of carbon isotopes in atmospheric CO<sub>2</sub> for historical simulations in CMIP6. *Geoscientific Model Development*, 10(12), 4405–4417.
- Graven, H., Allison, C. E., Etheridge, D. M., Hammer, S., Keeling, R. F., Levin, I., Meijer, H. A. J., Rubino, M., Tans, P. P., Trudinger, C. M., Vaughn, B. H., & White, J. W. C. (2017). Compiled records of carbon isotopes in atmospheric CO<sub>2</sub> for historical simulations in CMIP6. *Geoscientific Model Development*, 10(12), 4405–4417.
- Guiry E.J., Szpak P., Richards M.P. (2016). Effects of lipid extraction and ultrafiltration on stable carbon and nitrogen isotopic compositions of fish bone collagen. *Rapid Commun. Mass Spectrom.*, 30, 1591-1600.

- Guiry, E. J., & Szpak, P. (2020). Quality control for modern bone collagen stable carbon and nitrogen isotope measurements. *Methods in Ecology and Evolution*, 11(9), 1049–1060.
- Han, Z.-H., Palnitkar, S., Rao, D. S., Nelson, D., & Parfitt, A. M. (1997). Effects of Ethnicity and Age or Menopause on the Remodeling and Turnover of Iliac Bone: Implications for Mechanisms of Bone Loss. *Journal of Bone and Mineral Research*, 12(4), 498–508.
- Hedges, R. E. M., Clement, J. G., Thomas, C. D. L., & O'Connell, T. C. (2007). Collagen turnover in the adult femoral mid-shaft: Modelled from anthropogenic radiocarbon tracer measurements. *American Journal of Physical Anthropology*, 133(2), 808–816.
- Hill, P. A. (1998). Bone Remodelling. *British Journal of Orthodontics*, 25(2), 101–107.
- Hiraga, T., Nakajima, T. and Ozawa, H. (1995) Bone resorption induced by a metastatic human melanoma cell line. *Bone*, 16(3), 349-356.
- Holdaway, Hawke, D. J., Bunce, M., & Allentoft, M. E. (2011). Identification of an optimal sampling position for stable isotopic analysis of bone collagen of extinct moa (Aves: Emeidae). *Notornis*, 58(1), 1–7.
- Hua, Q., Turnbull, J., Santos, G., Rakowski, A., Ancapichún, S., Pol-Holz, R., Hammer, S., Lehman, S., Levin, I., Miller, J., Palmer, J., Turney, C. (2022). Atmospheric Radiocarbon for the Period 1950–2019. *Radiocarbon*, 64(4), 723–745
- Hudson DM, Weis M, Eyre DR. (2020). Collagen cross-linking and bone pathobiology. In Bilezikian JP, Martin TJ, Clemens TL, Rosen CJ (Eds.), *Principles of Bone Biology* (4th ed., pp. 339-358). London: Academic Press.
- Huiskes, R., Ruimerman, R., van Lenthe, G. H., & Janssen, J. D. (2000). Effects of mechanical forces on maintenance and adaptation of form in trabecular bone. *Nature*, 405(6787), Article 6787.
- Huja, S. S., & Beck, F. M. (2008). Bone Remodeling in Maxilla, Mandible, and Femur of Young Dogs. *The Anatomical Record: Advances in Integrative Anatomy and Evolutionary Biology*, 291(1), 1–5.
- Huja, S. S., Fernandez, S. A., Hill, K. J., & Li, Y. (2006). Remodeling dynamics in the alveolar process in skeletally mature dogs. *The Anatomical Record. Part A, Discoveries in Molecular, Cellular, and Evolutionary Biology*, 288(12), 1243–1249.
- Hyland, C., Scott, M. B., Routledge, J., & Szpak, P. (2022). Stable Carbon and Nitrogen Isotope Variability of Bone Collagen to Determine the Number of Isotopically Distinct Specimens. *Journal of Archaeological Method and Theory*, 29(2), 666–686.
- Ingle, B. M., Hay, S. M., Bottjer, H. M., & Eastell, R. (1999). Changes in Bone Mass and Bone Turnover Following Ankle Fracture. *Osteoporosis International*, 10(5), 408–415.
- Itkonen, S. T., Päivärinta, E., Pellinen, T., Viitakangas, H., Risteli, J., Erkkola, M., Lamberg-Allardt, C., & Pajari, A.-M. (2021). Partial Replacement of Animal Proteins with Plant Proteins for 12 Weeks Accelerates Bone Turnover Among Healthy Adults: A Randomized Clinical Trial. *The Journal of Nutrition*, 151(1), 11–19.

- Jackson SH, Heininger JA. Proline recycling during collagen metabolism as determined by concurrent  $^{18}\text{O}_2$ - and  $^3\text{H}$ -labeling. *Biochim Biophys Acta* 1975; 381:359–67.
- Jahren AH, Kraft RA, 2008. Carbon and nitrogen stable isotopes in fast food: Signatures of corn and confinement. *Proceedings of the National Academy of Sciences* 105, 17855-17860.
- Jim S, Ambrose SH, Evershed RP, 2004. Stable carbon isotopic evidence for differences in the dietary origin of bone cholesterol, collagen and apatite: implications for their use in palaeodietary reconstruction. *Geochimica et Cosmochimica Acta* 68, 61-72.
- Johnstone-Belford, E., Fallon, S. J., Dipnall, J. F., & Blau, S. (2022). The importance of bone sample selection when using radiocarbon analysis in cases of unidentified human remains. *Forensic science international*, 341, 111480.
- Jones, A. M., O'Connell, T. C., Young, E. D., Scott, K., Buckingham, C. M., Iacumin, P., & Brasier, M. D. (2001). Biogeochemical data from well preserved 200 ka collagen and skeletal remains. *Earth and Planetary Science Letters*, 193(1–2), 143–149.
- Jørkov, M. L. S., Heinemeier, J., & Lynnerup, N. (2009). The petrous bone—A new sampling site for identifying early dietary patterns in stable isotopic studies. *American journal of physical anthropology*, 138(2), 199-209.
- Katsimbri, P. (2017). The biology of normal bone remodelling. *European Journal of Cancer Care*, 26(6), e12740.
- Kirkwood, T. B. L. (1992). Comparative life spans of species: Why do species have the life spans they do? *The American Journal of Clinical Nutrition*, 55(6), 1191S-1195S.
- Kivirikko, K. (1970) Urinary Excretion of Hydroxyproline in Health and Disease. *International Review of Connective Tissue Research*, 5, 93-163
- Kong, J., Ding, Y., Zhang, C., Fu, Y., Du, J., Lu, C., Dou, X., Chen, Y., Li, Y. C., & Zhao, Q. (2013). Severe Vitamin D-Deficiency and Increased Bone Turnover in Patients with Hepatitis B from Northeastern China. *Endocrine Research*, 38(4), 215–222.
- Kromer B, Manning SW, Kuniholm PI, Newton MW, Spurk M, Levin I, 2001. Regional  $^{14}\text{C}$  Offsets in the Troposphere: Magnitude, Mechanisms, and Consequences. *Science* 294, 2529-2532.
- Kucharz, E. J. (1992). *The Collagens: Biochemistry and Pathophysiology*. Springer Berlin Heidelberg.
- Kutschera W. (2022). The versatile uses of the  $^{14}\text{C}$  bomb peak. *Radiocarbon* 64, 1295-1308. doi:10.1017/RDC.2022.13
- Kučukalić-Selimović, E., Valjevac, A., Hadžović-Džuvo, A., Skopljak-Beganović, A., Alimanovic-Alagić, R., & Brković, A. (2011). Evaluation of bone remodelling parameters after one year treatment with alendronate in postmenopausal women with osteoporosis. *Bosnian journal of basic medical sciences*, 11(1), 41–45.
- Kutschera, W. (2022). The Versatile Uses Of The  $^{14}\text{C}$  Bomb Peak. *Radiocarbon*, 64(6), 1295–1308.

- Leichliter JN, Lüdecke T, Foreman AD, Duprey NN, Winkler DE, Kast ER, Vonhof H, Sigman DM, Haug GH, Clauss M, Tütken T, Martínez-García A, 2021. Nitrogen isotopes in tooth enamel record diet and trophic level enrichment: Results from a controlled feeding experiment. *Chemical Geology* 563, 120047. doi:10.1016/j.chemgeo.2020.120047
- Levin and Kromer The Tropospheric  $^{14}\text{C}$  Level In Mid-Latitudes Of The Northern Hemisphere (1959–2003)
- Levin, I., Kromer, B., Schoch-Fischer, H., Bruns, M., Münnich, M., Berdau, D., Vogel, J. C., & Münnich, K. O. (1985). 25 Years of Tropospheric  $^{14}\text{C}$  Observations in Central Europe. *Radiocarbon*, 27(1), 1–19.
- Lingenfelter, R. E. (1963) Production of Carbon 14 by cosmic-ray neutrons. *Review of Geophysics* 7:3555.
- Longin, R. (1971). New method of collagen extraction for radiocarbon dating. *Nature* 250:241-242.
- Makarewicz CA, Sealy J, 2015. Dietary reconstruction, mobility, and the analysis of ancient skeletal tissues: Expanding the prospects of stable isotope research in archaeology. *Journal of Archaeological Science* 56, 146-158.
- Marotti, G. (1963). Quantitative Studies on Bone Reconstruction. *1. Cells Tissues Organs*, 52(4), 291–333.
- Marotti, G., & Marotti, F. (1966). Topographic-quantitative Study of Bone Tissue Formation and Reconstruction in Inert Bones. In H. Fleisch, H. J. J. Blackwood, & M. Owen (Eds.), *Calcified Tissues 1965: Proceedings of the Third European Symposium on Calcified Tissues* (pp. 89–93). Springer.
- Matsubayashi, & Tayasu, I. (2019). Collagen turnover and isotopic records in cortical bone. *Journal of Archaeological Science*, 106, 37–44.
- McGee, M. E., Maki, A. J., Johnson, S. E., Nelson, O. L., Robbins, C. T., & Donahue, S. W. (2008). Decreased bone turnover with balanced resorption and formation prevents cortical bone loss during disuse (hibernation) in grizzly bears (*Ursus arctos horribilis*). *Bone*, 42(2), 396–404.
- McGee-Lawrence, M., Buckendahl, P., Carpenter, C., Henriksen, K., Vaughan, M., & Donahue, S. (2015). Suppressed bone remodeling in black bears conserves energy and bone mass during hibernation. *Journal of Experimental Biology*, 218(13), 2067–2074.
- Melton, L. J., Khosla, S., Atkinson, E. J., O’Fallon, W. M., & Riggs, B. L. (1997). Relationship of Bone Turnover to Bone Density and Fractures. *Journal of Bone and Mineral Research*, 12(7), 1083–1091.
- Minagawa M, Wada E. (1984). Stepwise enrichment of  $^{15}\text{N}$  along food chains: Further evidence and the relation between  $\delta^{15}\text{N}$  and animal age. *Geochimica et Cosmochimica Acta* 48, 1135-1140. doi:10.1016/0016-7037(84)90204-7

- Montoya-Sanhueza, G., & Chinsamy, A. (2017). Long bone histology of the subterranean rodent *Bathyergus suillus* (Bathyergidae): Ontogenetic pattern of cortical bone thickening. *Journal of Anatomy*, 230(2), 203–233.
- Montoya-Sanhueza, G., Bennett, N. C., Oosthuizen, M. K., Dengler-Crish, C. M., & Chinsamy, A. (2021). Bone remodeling in the longest living rodent, the naked mole-rat: Interelement variation and the effects of reproduction. *Journal of Anatomy*, 239(1), 81–100.
- Mulhern, D. M. (2000). Rib remodeling dynamics in a skeletal population from Kulubnarti, Nubia. *American Journal of Physical Anthropology*, 111(4), 519–530.
- Muruganandan, S., Govindarajan, R., & Sinal, C. J. (2018). Bone marrow adipose tissue and skeletal health. *Current osteoporosis reports*, 16, 434-442.
- Nacarino-Meneses, C., Jordana, X., & Köhler, M. (2016). Histological variability in the limb bones of the Asiatic wild ass and its significance for life history inferences. *PeerJ*, 4, e2580.
- Newsome, S. D., Koch, P. L., Etnier, M. A., & Aurioles-Gamboa, D. (2006). Using Carbon and Nitrogen Isotope Values to Investigate Maternal Strategies in Northeast Pacific Otariids. *Marine Mammal Science*, 22(3), 556–572.
- O'Connell TC, Hedges REM, Healey MA, Simpson AHRW, 2001. Isotopic Comparison of Hair, Nail and Bone: Modern Analyses. *Journal of Archaeological Science* 28, 1247-1255.
- O'Connell TC, Kneale CJ, Tasevska N, Kuhnle GGC, 2012. The diet-body offset in human nitrogen isotopic values: A controlled dietary study. *American Journal of Physical Anthropology* 149, 426-434.
- O'Connor, J. A., Lanyon, L. E., & MacFie, H. (1982). The influence of strain rate on adaptive bone remodelling. *Journal of Biomechanics*, 15(10), 767–781.
- Okuyama, K. (2008). Revisiting the Molecular Structure of Collagen. *Connective Tissue Research*, 49(5), 299–310. h
- OpenAI. (2024). ChatGPT-3.5 [Software]. Retrieved from <https://openai.com> via Python script in Google Colaboratory [Software]. Retrieved from <https://colab.research.google.com>
- Ortner, D. J. (2011). Human skeletal paleopathology. *International Journal of Paleopathology*, 1(1), 4-11.
- Parfitt, A. M. (1982) The coupling of bone formation to bone resorption: a critical analysis of the concept and of its relevance to the pathogenesis of osteoporosis. *Metabolic Bone Disease Related Research*, 4, 1–6.
- Parfitt, A. M. (2002). Misconceptions (2): Turnover is always higher in cancellous than in cortical bone. *Bone*, 30(6), 807–809. 3223
- Parfitt, A.M. (1996). Hormonal Influences on Bone Remodeling and Bone Loss: Application to the Management of Primary Hyperparathyroidism. *Annals of Internal Medicine*, 125, 413-415.

- Peters C, Wang Y, Vakil V, Cramb J, Dortch J, Hocknull S, Lawrence R, Manne T, Monks C, Rössner GE, Ryan H, Siversson M, Ziegler T, Louys J, Price GJ, Boivin N, Collins MJ, 2023. Bone collagen from subtropical Australia is preserved for more than 50,000 years. *Communications Earth & Environment* 4, 438.
- Pfeilschifter, J. and Mundy, G. R. (1987) TGF $\beta$  stimulates osteoblast activity and is released during the bone resorption process. *Calcium Regulation and Bone Metabolism: Basic and Clinical Aspects*, 9, 450–454.
- Pollard, A. M., Ditchfield, P., Piva, E., Wallis, S., Falys, C., & Ford, S. (2012). ‘Sprouting like cockle amongst the wheat’: the St Brice's Day massacre and the isotopic analysis of human bones from St John's College, Oxford. *Oxford Journal of Archaeology*, 31(1), 83-102.
- Qi H, Coplen TB, Geilmann H, Brand WA, Böhlke JK. (2003). Two new organic reference materials for  $\delta^{13}\text{C}$  and  $\delta^{15}\text{N}$  measurements and a new value for the  $\delta^{13}\text{C}$  of NBS 22 oil. *Rapid Communications in Mass Spectrometry* 17, 2483-2487.
- Reed, K. (2021). Food systems in archaeology. Examining production and consumption in the past. *Archaeological Dialogues*, 28(1), 51-75.
- Reimer P.J., Brown, T., and Reimer, R. (2004) Discussion: Reporting and Calibration of Post-Bomb  $^{14}\text{C}$  Data. *Radiocarbon*, 46(3), 1299–1304.
- Reimer PJ, Baillie MGL, Bard E, Bayliss E, Beck JW, Blackwell PG, Bronk C.R., Buck CE, Burr GS, Edwards RL, Friedrich M, Grootes PM, Guilderson TP, Hajdas I, Heaton TJ, Hogg AG, Hughen KA, Kaiser KF, Kromer B, McCormac FG, Manning SW, Reimer RW, Richards DA, Southon JR, Talamo S, Turney CSM, van der Plicht J, Weyhenmeyer CE. (2009). IntCal09 and Marine09 radiocarbon age calibration curves, 0-50,000 years cal BP. *Radiocarbon* 51, 1111-1150.
- Reimer PJ, Bard E, Bayliss A, Beck JW, Blackwell PG, Ramsey CB, Buck CE, Cheng H, Edwards RL, Friedrich M, Grootes PM, Guilderson TP, Haflidason H, Hajdas I, Hatté C, Heaton TJ, Hoffmann DL, Hogg AG, Hughen KA, Kaiser KF, Kromer B, Manning SW, Niu M, Reimer RW, Richards DA, Scott EM, Southon JR, Staff RA, Turney CSM, van der Plicht J. (2013). IntCal13 and Marine13 Radiocarbon Age Calibration Curves 0–50,000 Years cal BP. *Radiocarbon* 55, 1869-1887. doi:10.1017/S0033822200048864
- Reimer PJ, 2014. Marine or estuarine radiocarbon reservoir corrections for mollusks? A case study from a medieval site in the south of England. *Journal of Archaeological Science* 49, 142-146.
- Rey-Iglesia A, García-Vázquez A, Treadaway EC, van der Plicht J, Baryshnikov GF, Szpak P, Bocherens H, Boeskorov GG, Lorenzen ED, 2019. Evolutionary history and palaeoecology of brown bear in North-East Siberia re-examined using ancient DNA and stable isotopes from skeletal remains. *Scientific Reports* 9, 4462.
- Riofrío-Lazo, & Aurióles-Gamboa, D. (2013). Timing of isotopic integration in marine mammal skull: comparative study between calcified tissues. *Rapid Communications in Mass Spectrometry*, 27(9), 1076–1082.

- Roato, I. (2014). Bone metastases: When and how lung cancer interacts with bone. *World journal of clinical oncology*, 5(2), 149.
- Roato, I., Caldo, D., Godio, L., D'Amico, L., Giannoni, P., Morello, E., Quarto, R., Molfetta, L., Buracco, P., Mussa, A. and Ferracini, R. (2010). Bone invading NSCLC cells produce IL-7: mice model and human histologic data. *BMC cancer*, 10, 1-7.
- Rouhi, G. (2012) Biomechanics of Osteoporosis: The Importance of Bone Resorption and Remodeling Processes. In Dionyssiotis, Y. (Ed.). *Osteoporosis*. InTech.
- Safadi, F. F., Barbe, M. F., Abdelmagid, S. M., Rico, M. C., Aswad, R. A., Litvin, J., & Popoff, S. N. (2009). Bone Structure, Development and Bone Biology. In J. S. Khurana (Ed.), *Bone Pathology* (pp. 1–50).
- Schimmelmann A, Qi H, Coplen TB, Brand WA, Fong J, Meier-Augenstein W, Kemp HF, Toman B, Ackermann A, Assonov S, Aerts-Bijma AT, Brejcha R, Chikaraishi Y, Darwish T, Elsner M, Gehre M, Geilmann H, Gröning M, Hélie J-F, Herrero-Martín S, Meijer HAJ, Sauer PE, Sessions AL, Werner RA. (2016). Organic Reference Materials for Hydrogen, Carbon, and Nitrogen Stable Isotope-Ratio Measurements: Caffeines, n-Alkanes, Fatty Acid Methyl Esters, Glycines, l-Valines, Polyethylenes, and Oils. *Analytical Chemistry* 88, 4294-4302.
- Schoeninger, M. J., & DeNiro, M. J. (1984). Nitrogen and carbon isotopic composition of bone collagen from marine and terrestrial animals. *Geochimica et Cosmochimica Acta*, 48(4), 625–639.
- Sealy, J., Armstrong, R., & Schrire, C. (1995). Beyond lifetime averages: Tracing life histories through isotopic analysis of different calcified tissues from archaeological human skeletons. *Antiquity*, 69(263), 290–300.
- Sela J. (1977). Bone remodeling in pathologic conditions. A scanning electron microscopic study. *Calcified tissue research*, 23(3), 229–234. <https://doi.org/10.1007/BF02012790>
- Shigdel, R., Osima, M., Ahmed, L. A., Joakimsen, R. M., Eriksen, E. F., Zebaze, R., & Bjørnerem, Å. (2015). Bone turnover markers are associated with higher cortical porosity, thinner cortices, and larger size of the proximal femur and non-vertebral fractures. *Bone*, 81, 1–6.
- Shin, J. Y., O'Connell, T., Black, S., & Hedges, R. (2004). Differentiating Bone Osteonal Turnover Rates by Density Fractionation; Validation Using the Bomb 14C Atmospheric Pulse. *Radiocarbon*, 46(2), 853–861.
- Shipov, A., Zaslansky, P., Riesemeier, H., Segev, G., Atkins, A. & Shahar, R. (2013). Unremodeled endochondral bone is a major architectural component of the cortical bone of the rat (*Rattus norvegicus*). *Journal of Structural Biology* 183, 132–140.
- Sigman DM, Boyle EA, 2000. Glacial/interglacial variations in atmospheric carbon dioxide. *Nature* 407, 859-869.
- Sinex, F. B., and B. Faris (1959) Isolation of gelatin from ancient bones. *Science* 729:969.

- Skedros, J. G., Knight, A. N., Clark, G. C., Crowder, C. M., Dominguez, V. M., Qiu, S., Mulhern, D. M., Donahue, S. W., Busse, B., Hulsey, B. I., Zedda, M., & Sorenson, S. M. (2013). Scaling of Haversian canal surface area to secondary osteon bone volume in ribs and limb bones. *American Journal of Physical Anthropology*, 151(2), 230–244.
- Skedros, J. G., Sybrowsky, C. L., Parry, T. R., & Bloebaum, R. D. (2003). Regional differences in cortical bone organisation and microdamage prevalence in Rocky Mountain mule deer. *The Anatomical Record*, 274A (1), 837–850.
- Stenhouse, M. A., & Baxter, M. S. (1979). The uptake of bomb <sup>14</sup>C in humans. *Radiocarbon* dating, 324–341.
- Stout SD, Lueck R. 1995. Bone remodeling rates and skeletal maturation in three archaeological skeletal populations. *Am J Phys Anthropol* 98:600 – 604.
- Stuiver, M., & Polach, H. A. (1977). Discussion Reporting of <sup>14</sup>C Data. *Radiocarbon*, 19(3), 355–363.
- Sykut, M., Pawełczyk, S., Borowik, T., Pokorny, B., Flajšman, K., & Niedziałkowska, M. (2020). Intraindividual and interpopulation variability in carbon and nitrogen stable isotope ratios of bone collagen in the modern red deer (*Cervus elaphus*). *Journal of Archaeological Science: Reports*, 34, 102669.
- Szpak, P., Metcalfe, J. Z., Macdonald, R. A. (2017). Best practices for calibrating and reporting stable isotope measurements in archaeology. *Journal of Archaeological Science: Reports*, 13, 609–616.
- Taylor, R. E. (2016). *Radiocarbon Dating, An Archaeological Perspective*. Academic Press.
- Teitelbaum SL (2000) Bone resorption by osteoclasts. *Science* 289: 1504–1508.
- Tözeren, A. (1999). *Human body dynamics: classical mechanics and human movement*. Springer Science & Business Media.
- Turner, C. H., Owan, I., & Takano, Y. (1995). Mechanotransduction in bone: role of strain rate. *American Journal of Physiology-Endocrinology and Metabolism*, 269(3), E438–E442. doi:10.1152/ajpendo.1995.2
- Ubelaker, D. H., Buchholz, B. A., & Stewart, J. E. B. (2006). Analysis of Artificial Radiocarbon in Different Skeletal and Dental Tissue Types to Evaluate Date of Death. *Journal of Forensic Sciences*, 51(3), 484–488.
- Ubelaker, D.H., Plens, C.R., Soriano, E.P., Diniz, M.V., de Almeida Junior, E., Junior, E.D., Júnior, L.F. and Machado, C.E.P. (2022). Lag time of modern bomb-pulse radiocarbon in human bone tissues: New data from Brazil. *Forensic Science International*, 331, p.111143.
- Väänänen, H. K. (1993). Mechanism of Bone Turnover. *Annals of Medicine*, 25(4), 353–359.
- Vajda, E. G., Kneissel, M., Muggenburg, B., & Miller, S. C. (1999). Increased Intracortical Bone Remodeling During Lactation in Beagle Dogs. *Biology of Reproduction*, 61(6), 1439–1444.

- Viguet-Carrin, S., Garnero, P., & Delmas, P. D. (2006). The role of collagen in bone strength. *Osteoporosis International*, 17(3), 319–336.
- Weaver, C. M. (1998). Use of Calcium Tracers and Biomarkers to Determine Calcium Kinetics and Bone Turnover. *Bone*, 22(5), 103S-104S.
- Weiner, S., & Wagner, H. D. (1998). THE MATERIAL BONE: Structure-Mechanical Function Relations. *Annual Review of Materials Science*, 28(1), 271–298.  
<https://doi.org/10.1146/annurev.matsci.28.1.271>
- Weinstein RS, Bell NH. (1988). Diminished rates of bone formation in normal black adults. *N Engl J Med* 319: 1698–1701.
- Wilson T, Szpak P. (2022). Acidification does not alter the stable isotope composition of bone collagen. *PeerJ* 10, e13593. doi:10.7717/peerj.13593
- Woitge, H. W., Scheidt-Nave, C., Kissling, C., Leidig-Bruckner, G., Meyer, K., Grauer, A., Scharla, S. H., Ziegler, R., & Seibel, M. J. (1998). Seasonal Variation of Biochemical Indexes of Bone Turnover: Results of a Population-Based Study<sup>1</sup>. *The Journal of Clinical Endocrinology & Metabolism*, 83(1), 68–75.
- Wojda, S. J., Weyland, D. R., Gray, S. K., Mcgee-Lawrence, M. E., Drummer, T. D., & Donahue, S. W. (2013). Black Bears with Longer Disuse (Hibernation) Periods Have Lower Femoral Osteon Population Density and Greater Mineralization and Intracortical Porosity. *The Anatomical Record*, 296(8), 1148–1153
- Zanker, C. L., & Swaine, I. L. (2000). Responses of bone turnover markers to repeated endurance running in humans under conditions of energy balance or energy restriction. *European Journal of Applied Physiology*, 83(4), 434–440.

**Appendix 1**

Table S.1. Northern hemisphere atmospheric  $^{14}\text{CO}_2$  levels from 1941-2022. Data derived from Hua et al. (2022)

Year	D14C
1940	-20.3
1941	-20.8
1942	-21.3
1943	-21.8
1944	-22.3
1945	-22.7
1946	-23.1
1947	-23.5
1948	-23.9
1949	-24.3
1950	-24.8
1951	-24.8
1952	-24.9
1953	-23.9
1954	-21.1
1955	-8.2
1956	26.5
1957	73
1958	140.2
1959	228
1960	212.3
1961	221.7
1962	358.5
1963	718.3
1964	835.7
1965	756.3
1966	691.9
1967	623.6
1968	564.5
1969	545.4
1970	529.1

1971	499.4
1972	465.6
1973	418.6
1974	400.8
1975	369.8
1976	352.5
1977	333.9
1978	325.8
1979	295.8
1980	264.5
1981	256.7
1982	238.3
1983	224.2
1984	209.3
1985	201.1
1986	191.1
1987	183.6
1988	174.7
1989	163.7
1990	152.2
1991	142.4
1992	136.3
1993	128.7
1994	122.1
1995	115.8
1996	109.8
1997	103.1
1998	99.2
1999	94.1
2000	88.3
2001	82.2
2002	76.2
2003	70.6
2004	65.4
2005	60.7
2006	56.6
2007	52.9

2008	49.4
2009	45.8
2010	41.6
2011	37.3
2012	30.4
2013	24.3
2014	19.6
2015	13.8
2016	13
2017	9
2018	3
2019	0
2020	-2
2021	-5

**Table S.2** Southern hemisphere atmospheric  $^{14}\text{CO}_2$  levels from 1941-2022. Data derived from Hua et al. (2022)

Year	D14C
1941	-18.3
1942	-16.3
1943	-16.7
1944	-19.3
1945	-16.8
1946	-16.8
1947	-20.6
1948	-20.5
1949	-23.3
1950	-27.4
1951	-27.5
1952	-27.6
1953	-22.9
1954	-20.0

Year	D14C
1955	-20.0
1956	8.8
1957	52.6
1958	112.3
1959	172.2
1960	202.2
1961	211.2
1962	277.8
1963	481.3
1964	645.0
1965	652.3
1966	626.9
1967	601.4
1968	576.9
1969	548.5
1970	521.8
1971	515.3
1972	478.1
1973	438.7
1974	403.7
1975	383.1
1976	353.3
1977	332.2
1978	320.4
1979	298.8
1980	279.0
1981	261.8
1982	246.2

Year	D14C
1983	230.5
1984	217.0
1985	205.6
1986	194.3
1987	180.4
1988	172.6
1989	161.9
1990	148.2
1991	143.8
1992	140.9
1993	130.1
1994	121.8
1995	115.7
1996	111.2
1997	107.1
1998	100.7
1999	93.7
2000	89.7
2001	84.6
2002	81.9
2003	76.4
2004	69.8
2005	64.8
2006	60.2
2007	55.7
2008	52.5
2009	50.3
2010	48.5

Year	D14C
2011	40.3
2012	35.4
2013	31.3
2014	25.4
2015	22.8
2016	20.6
2017	16.1
2018	12.7
2019	11.4

**Table S.3** Sample information,  $\Delta^{14}\text{C}$  values, and the estimated turnover intervals using fixed rate models (Data from Ubelaker et al. 2022). Samples that had  $\Delta^{14}\text{C}$  values too high to produce a fixed rate were highlighted red. \*This sample had a measured  $\Delta^{14}\text{C}$  that was lower than any atmospheric level that existed during this individuals life. This is an impossibility and is an assumed error

Sex	Individual	Death year	Age at Death	Skeletal Element	$\Delta^{14}\text{C}$ (‰)	Turnover interval	Z (%)
F	1	2013	50	Parietal	+ 108.30	<b>29.1</b>	6.98
				Occipital	+ 22.15	<b>-3.5*</b>	
				Femur	+ 302.18	<b>N/A</b>	13.32
				Vertebra	+ 64.62	<b>14.7</b>	4.72
F	2	2014	51	Parietal	+ 85.9	<b>24.8</b>	6.1
				Occipital	+ 75.95	<b>21.3</b>	5.59
				Femur	+ 81.99	<b>23.5</b>	5.91
				Vertebra	+ 41.68	<b>6.4</b>	3.15
M	3	2013	50	Parietal	+ 110.23	<b>29.5</b>	7.06
				Occipital	+ 66.48	<b>15.5</b>	4.85
				Femur	+ 202.01	<b>44.7</b>	10.18
				Vertebra	+ 58.01	<b>11.8</b>	4.23
M	4	2014	51	Parietal	+ 174.20	<b>43.0</b>	9.34

Sex	Individual	Death year	Age at Death	Skeletal Element	$\Delta^{14}\text{C}$ (‰)	Turnover interval	Z (%)
				Occipital	+ 226.19	N/A	10.94
				Femur	+ 292.97	N/A	13.03
				Vertebra	+ 87.39	<b>25.2</b>	6.17
M	5	2014	51	Parietal	+ 172.45	<b>42.8</b>	9.29
				Occipital	+ 127.22	<b>35.2</b>	7.77
				Femur	+ 237.54	N/A	11.29
				Vertebra	+ 47.40	<b>9.0</b>	3.63
F	6	2014	51	Parietal	+ 162.71	<b>41.4</b>	8.98
				Occipital	+ 163.44	<b>41.5</b>	9.00
				Femur	+ 272.85	N/A	12.38
				Vertebra	+ 59.20	<b>14.4</b>	4.58
M	7	2016	53	Parietal	+ 195.00	<b>48.2</b>	10.03
				Occipital	+ 208.31	<b>49.7</b>	10.43
				Femur	+ 142.91	<b>40.7</b>	8.4
				Vertebra	+ 174.20	<b>45.5</b>	9.4
M	8	2016	53	Parietal	+ 192.62	<b>47.8</b>	9.72
				Occipital	+ 152.62	<b>42.3</b>	8.72
				Femur	+ 203.58	<b>49.2</b>	10.29
				Vertebra	+ 61.71	<b>19.4</b>	5.11
F	9	2016	53	Parietal	+ 77.29	<b>25.3</b>	5.91
				Occipital	+ 50.27	<b>14.4</b>	4.39
				Femur	+ 99.64	<b>31.8</b>	6.87
				Vertebra	+ 42.85	<b>10.9</b>	3.83
M	10	2016	53	Parietal	+ 116.19	<b>35.6</b>	7.49
				Occipital	+ 144.9	<b>41.0</b>	8.47
				Femur	+ 255.85	N/A	11.87
				Vertebra	+ 42.85	<b>10.9</b>	3.83
F	11	2010	47	Parietal	+ 233.08	<b>44.7</b>	11.08
				Occipital	+ 272.22	N/A	12.32

Sex	Individual	Death year	Age at Death	Skeletal Element	$\Delta^{14}\text{C}$ (‰)	Turnover interval	Z (%)
				Femur	+ 225.27	<b>43.9</b>	10.83
				Vertebra	+ 90.78	<b>19.4</b>	5.79
F	12	2006	43	Parietal	+ 254.29	N/A	11.36
				Occipital	+ 211.77	<b>35.9</b>	10.26
				Femur	+ 211.77	<b>35.9</b>	10.26
				Vertebra	+ 100.95	<b>15.2</b>	5.64
M	13	2017	54	Parietal	+ 129.75	<b>39.9</b>	8.01
				Occipital	+ 98.96	<b>33.3</b>	6.91
				Femur	+ 99.78	<b>33.5</b>	6.91
				Vertebra	+ 58.41	<b>20.0</b>	5.07
M	14	2017	54	Parietal	+ 92.14	<b>31.5</b>	6.64
				Occipital	+ 112.72	<b>36.4</b>	7.42
				Femur	+ 172.31	<b>46.7</b>	9.36
				Vertebra	+ 52.10	<b>17.2</b>	4.7
M	15	2017	54	Parietal	+ 118.28	<b>37.6</b>	7.62
				Occipital	+ 144.90	<b>42.5</b>	8.5
				Femur	+ 229.71	N/A	11.09
				Vertebra	+ 63.16	<b>22.0</b>	5.33
M	16	2017	54	Parietal	+ 125.26	<b>39.0</b>	7.89
				Occipital	+ 143.48	<b>42.3</b>	8.46
				Femur	+ 175.37	<b>47.1</b>	9.45
				Vertebra	+ 40.90	<b>11.9</b>	3.93
M	17	2016	53	Parietal	+ 126.10	<b>37.6</b>	7.84
				Occipital	+ 253.66	N/A	11.81
				Femur	+ 162.42	<b>43.8</b>	8.81
				Vertebra	+ 59.86	<b>18.6</b>	5

**Table S.4** Sample information,  $\Delta^{14}\text{C}$  values, and the estimated turnover intervals using fixed rate (data from Johnstone-Belford et al. 2022). Samples that had  $\Delta^{14}\text{C}$  values too high to produce a

fixed rate or samples that did not produce results were highlighted red. DC refers to decay constant.

Sex	Individual	Death year	Age	Skeletal Element	Bone Type	$\Delta^{14}\text{C}$ (‰)	Fixed rate turnover interval	DC
M	1	2016	65	Femur	Cortical	+ 238.9	N/A	7.9
				Femur	Trabecular	+ 165.7	44.24	6.7
				Rib	Cortical	+ 93.5	30.19	5.
				Rib	Trabecular	+ 73.9	24.11	4.5
M	2	2016	77	Femur	Cortical	+ 131.6	38.68	
				Femur	Trabecular	+ 173.5	45.35	
				Rib	Cortical	+ 171.8	45.11	
				Rib	Trabecular	+ 168.2	44.60	
M	3	2016	64	Femur	Cortical	+ 348	N/A	10.2
				Femur	Trabecular	+ 212.4	50.21	7.6
				Rib	Cortical	+ 66.3	21.28	4.3
				Rib	Trabecular		N/A	
M	4	2016	78	Femur	Cortical	+ 157.9	43.09	
				Femur	Trabecular	+ 204.6	49.31	
				Rib	Cortical	+ 535.2	N/A	
				Rib	Trabecular	+ 47.8	13.23	
M	5	2016	59	Femur	Cortical	+ 240.5	N/A	9.3
				Femur	Trabecular	+ 229.8	N/A	9.1
				Rib	Cortical	+ 80.8	26.44	5.3
				Rib	Trabecular	+ 74.8	24.43	5.1
M	6	2016	77	Femur	Cortical	+ 99.6	31.79	
				Femur	Trabecular	+ 52	15.17	
				Rib	Cortical		N/A	
				Rib	Trabecular		N/A	
F	7	2017	70	Femur	Cortical	+ 45	13.87	3.2
				Femur	Trabecular	+ 113	36.50	5.2
				Rib	Cortical	+ 148.4	43.07	5.9
				Rib	Trabecular	+ 60.7	20.95	3.9

Sex	Individual	Death year	Age	Skeletal Element	Bone Type	$\Delta^{14}\text{C}$ (‰)	Fixed rate turnover interval	DC
M	8	2017	75	Femur	Cortical	+ 189.7	48.96	5.9
				Femur	Trabecular	+ 142.3	42.07	5.2
				Rib	Cortical	+ 190.2	49.03	5.9
				Rib	Trabecular	+ 61.5	21.27	3.6
M	9	2017	91	Femur	Cortical	+ 127.5	39.43	
				Femur	Trabecular	+ 140.1	41.69	
				Rib	Cortical	+ 92.4	31.55	
				Rib	Trabecular	+ 88.1	30.36	
F	10	2017	67	Femur	Cortical	+ 203.9	50.70	7.2
				Femur	Trabecular	+ 113.8	36.67	5.5
				Rib	Cortical	+ 200.6	50.31	7.1
				Rib	Trabecular	+ 65	22.67	4.2
M	11	2017	75	Femur	Cortical	+ 102.5	34.12	4.6
				Femur	Trabecular	+ 111.2	36.11	4.7
				Rib	Cortical			
				Rib	Trabecular			
M	12	2017	89	Femur	Cortical	+ 200.6	50.31	
				Femur	Trabecular	+ 200.6	50.31	
				Rib	Cortical	+ 125.9	39.12	
				Rib	Trabecular	+ 115.6	37.05	
M	13	2017	74	Femur	Cortical	+ 167.9	46.03	5.7
				Femur	Trabecular	+ 82.6	28.74	4.2
				Rib	Cortical	+ 117.2	37.39	4.9
				Rib	Trabecular	+ 43.3	13.05	2.9
M	14	2017	80	Femur	Cortical	+ 94.5	32.11	
				Femur	Trabecular	+ 126	39.14	
				Rib	Cortical	+ 142.7	42.13	
				Rib	Trabecular	+ 99.8	33.46	
M	15	2018	88	Femur	Cortical	+ 200.3	52.28	

Sex	Individual	Death year	Age	Skeletal Element	Bone Type	$\Delta^{14}\text{C}$ (‰)	Fixed rate turnover interval	DC
				Femur	Trabecular	+ 154.4	45.97	
				Rib	Cortical	+ 133.3	42.43	
				Rib	Trabecular	+ 200.3	52.28	
M	16	2018	75	Femur	Cortical	+ 137	43.09	5.8
				Femur	Trabecular	+ 87.9	32.26	4.4
				Rib	Cortical	+ 55	20.58	3.5
				Rib	Trabecular	+ 48.4	17.55	3.3
F	17	2018	94	Femur	Cortical	+ 158.3	46.57	
				Femur	Trabecular	+ 113.2	38.47	
				Rib	Cortical	+ 64.8	24.63	
				Rib	Trabecular	+ 29.7	8.37	
M	18	2018	74	Femur	Cortical	+ 208.9	53.31	6.4
				Femur	Trabecular	+ 188.5	50.80	6.1
				Rib	Cortical	+ 86.9	31.97	4.5
				Rib	Trabecular	+ 81.8	30.47	4.3

**Table S.5.** The average percent of collagen that was produced in each decade of life at death, across the elements analyzed from the southern hemisphere (studies (Ubelaker et al. 2022; Johnstone-Belford et al. 2022)).

	Bone	0-10	10-20	20-30	30-40	40-50	50-60	60-70	70-80
U1	Parietal	0.04 ± 0.20	3.80 ± 1.90	22.56 ± 4.21	37.84 ± 4.91	33.11 ± 4.78	2.65 ± 1.60		
	Femur	14.80 ± 3.55	50.06 ± 5.14	25.78 ± 4.30	7.43 ± 2.62	1.86 ± 1.33	0.07 ± 0.27		
	Vertebra	0.00 ± 0.00	0.07 ± 0.25	3.08 ± 1.68	23.06 ± 4.16	64.83 ± 4.65	8.96 ± 2.90		
U2	Parietal	0.01 ± 0.10	1.19 ± 1.07	12.82 ± 3.37	34.48 ± 4.90	43.45 ± 4.93	8.05 ± 2.72		
	Occipital	0.00 ± 0.03	0.53 ± 0.70	8.28 ± 2.68	30.71 ± 4.60	49.84 ± 5.08	10.64 ± 3.06		
	Femur	0.00 ± 0.05	0.91 ± 0.99	10.95 ± 3.06	33.18 ± 4.67	46.01 ± 4.93	8.94 ± 2.75		

	<b>Bone</b>	<b>0-10</b>	<b>10-20</b>	<b>20-30</b>	<b>30-40</b>	<b>40-50</b>	<b>50-60</b>	<b>60-70</b>	<b>70-80</b>
	Vertebra	0.00 ± 0.00	0.00 ± 0.00	0.06 ± 0.23	4.15 ± 1.99	59.93 ± 4.78	35.86 ± 4.84		
U3	Parietal	0.06 ± 0.25	4.27 ± 2.00	23.24 ± 4.20	37.25 ± 4.94	32.61 ± 4.59	2.58 ± 1.58		
	Occipital	0.00 ± 0.00	0.11 ± 0.35	3.63 ± 1.85	24.89 ± 4.28	63.12 ± 4.85	8.24 ± 2.76		
	Femur	2.48 ± 1.54	29.57 ± 4.84	38.21 ± 4.82	20.89 ± 3.94	8.40 ± 2.76	0.45 ± 0.67		
	Vertebra	0.00 ± 0.00	0.02 ± 0.16	1.33 ± 1.16	16.76 ± 3.71	70.47 ± 4.60	11.42 ± 3.25		
U4	Parietal	1.27 ± 1.15	21.41 ± 4.28	38.38 ± 4.81	26.14 ± 4.52	12.10 ± 3.15	0.70 ± 0.84		
	Occipital	4.34 ± 2.00	35.82 ± 4.71	36.55 ± 4.73	16.74 ± 3.70	5.94 ± 2.29	0.62 ± 0.80		
	Femur	13.21 ± 3.45	49.11 ± 4.99	27.01 ± 4.52	8.27 ± 2.76	2.22 ± 1.43	0.18 ± 0.44		
	Vertebra	0.01 ± 0.09	1.38 ± 1.19	13.62 ± 3.38	34.57 ± 4.76	42.56 ± 4.88	7.86 ± 2.68		
U5	Parietal	1.07 ± 1.01	20.33 ± 4.10	38.09 ± 4.81	26.39 ± 4.44	12.63 ± 3.37	1.50 ± 1.24		
	Occipital	0.17 ± 0.42	8.03 ± 2.72	29.98 ± 4.68	34.51 ± 4.90	23.89 ± 4.45	3.42 ± 1.82		
	Femur	5.54 ± 2.26	38.96 ± 4.88	35.34 ± 4.80	14.77 ± 3.52	4.90 ± 2.11	0.49 ± 0.66		
	Vertebra	0.00 ± 0.00	0.00 ± 0.00	0.31 ± 0.56	7.97 ± 2.74	62.96 ± 4.85	28.76 ± 4.49		
U6	Parietal	0.79 ± 0.90	17.73 ± 3.81	36.84 ± 4.71	28.49 ± 4.47	14.46 ± 3.48	1.69 ± 1.30		
	Occipital	0.84 ± 0.93	17.86 ± 3.75	37.00 ± 4.80	28.14 ± 4.53	14.41 ± 3.48	1.74 ± 1.32		
	Femur	9.74 ± 2.97	46.01 ± 5.09	30.57 ± 4.50	10.45 ± 3.02	2.95 ± 1.69	0.29 ± 0.53		
	Vertebra	0.00 ± 0.00	0.06 ± 0.24	2.29 ± 1.48	19.03 ± 3.98	60.74 ± 4.93	17.89 ± 3.75		
U7	Parietal	2.22 ± 1.47	27.41 ± 4.61	37.75 ± 4.86	21.74 ± 4.09	9.11 ± 2.80	1.77 ± 1.30		

	<b>Bone</b>	<b>0-10</b>	<b>10-20</b>	<b>20-30</b>	<b>30-40</b>	<b>40-50</b>	<b>50-60</b>	<b>60-70</b>	<b>70-80</b>
	Occipital	2.95 ± 1.64	31.60 ± 4.50	37.05 ± 4.71	19.48 ± 4.11	7.51 ± 2.54	1.40 ± 1.19		
	Femur	0.38 ± 0.61	12.32 ± 3.22	33.52 ± 4.63	31.17 ± 4.72	18.22 ± 3.87	4.39 ± 2.01		
	Vertebra	1.23 ± 1.08	21.38 ± 4.13	37.77 ± 4.79	25.47 ± 4.31	11.73 ± 3.19	2.42 ± 1.58		
U8	Parietal	1.67 ± 1.22	24.70 ± 4.43	38.17 ± 4.80	23.20 ± 4.21	10.16 ± 3.16	2.11 ± 1.44		
	Occipital	0.59 ± 0.75	15.05 ± 3.69	35.19 ± 4.98	29.55 ± 4.71	16.04 ± 3.68	3.58 ± 1.80		
	Femur	2.67 ± 1.60	30.11 ± 4.41	37.74 ± 4.71	20.03 ± 3.93	7.98 ± 2.59	1.48 ± 1.18		
	Vertebra	0.00 ± 0.00	0.17 ± 0.41	4.08 ± 1.99	22.56 ± 4.23	48.73 ± 5.10	24.46 ± 4.32		
U9	Parietal	0.01 ± 0.07	0.84 ± 0.87	10.08 ± 3.09	30.93 ± 4.61	41.85 ± 5.06	16.29 ± 3.72		
	Occipital	0.00 ± 0.00	0.02 ± 0.15	1.33 ± 1.15	13.74 ± 3.42	50.63 ± 4.93	34.27 ± 4.64		
	Femur	0.03 ± 0.17	3.25 ± 1.79	20.03 ± 3.91	34.76 ± 4.48	32.10 ± 4.50	9.83 ± 2.83		
	Vertebra	0.00 ± 0.00	0.00 ± 0.05	0.38 ± 0.62	7.57 ± 2.64	48.31 ± 4.97	43.73 ± 5.00		
U10	Parietal	0.10 ± 0.32	6.04 ± 2.38	26.13 ± 4.35	34.63 ± 4.59	25.91 ± 4.28	7.18 ± 2.60		
	Occipital	0.44 ± 0.65	12.82 ± 3.36	34.18 ± 4.70	30.86 ± 4.77	17.61 ± 3.82	4.08 ± 2.01		
	Femur	7.57 ± 2.69	43.21 ± 5.02	32.60 ± 4.60	12.23 ± 3.30	3.80 ± 1.87	0.59 ± 0.77		
	Vertebra	0.00 ± 0.00	0.00 ± 0.05	0.39 ± 0.61	7.62 ± 2.69	48.02 ± 4.90	43.96 ± 5.06		
U11	Parietal	4.71 ± 2.12	37.89 ± 4.78	36.16 ± 4.67	16.27 ± 3.59	4.96 ± 2.19	0.00 ± 0.00		
	Occipital	9.49 ± 3.04	46.24 ± 4.95	30.80 ± 4.66	10.71 ± 3.14	2.77 ± 1.66	0.00 ± 0.00		
	Femur	4.27 ± 2.02	35.48 ± 4.56	37.07 ± 4.91	17.68 ± 3.82	5.51 ± 2.25	0.00 ± 0.00		

	<b>Bone</b>	<b>0-10</b>	<b>10-20</b>	<b>20-30</b>	<b>30-40</b>	<b>40-50</b>	<b>50-60</b>	<b>60-70</b>	<b>70-80</b>
	Vertebra	0.01 ± 0.07	0.93 ± 0.96	12.62 ± 3.49	39.57 ± 5.02	46.88 ± 5.10	0.00 ± 0.00		
U12	Parietal	5.91 ± 2.39	40.82 ± 5.03	35.60 ± 4.81	14.99 ± 3.61	2.68 ± 1.61	0.00 ± 0.00		
	Occipital	2.83 ± 1.55	31.43 ± 4.77	39.84 ± 5.04	21.39 ± 3.98	4.51 ± 2.04	0.00 ± 0.00		
	Femur	2.81 ± 1.67	31.37 ± 4.66	39.83 ± 4.87	21.53 ± 4.03	4.46 ± 2.07	0.00 ± 0.00		
	Vertebra	0.01 ± 0.08	0.94 ± 0.99	15.02 ± 3.48	53.02 ± 5.00	31.00 ± 4.54	0.00 ± 0.00		
U13	Parietal	0.27 ± 0.53	9.36 ± 2.88	30.41 ± 4.78	32.59 ± 4.65	20.99 ± 4.23	6.37 ± 2.46		
	Occipital	0.04 ± 0.19	3.29 ± 1.76	19.85 ± 4.04	34.19 ± 4.80	30.92 ± 4.65	11.71 ± 3.17		
	Femur	0.03 ± 0.17	3.29 ± 1.73	19.94 ± 3.95	34.18 ± 4.81	31.05 ± 4.68	11.50 ± 3.21		
	Vertebra	0.00 ± 0.00	0.16 ± 0.39	3.73 ± 1.90	20.53 ± 3.95	46.26 ± 4.90	29.32 ± 4.57		
U14	Parietal	0.02 ± 0.13	2.36 ± 1.54	17.13 ± 3.71	33.72 ± 4.67	33.46 ± 4.63	13.30 ± 3.31		
	Occipital	0.08 ± 0.28	5.67 ± 2.40	25.49 ± 4.27	34.26 ± 4.94	25.71 ± 4.54	8.79 ± 2.88		
	Femur	1.19 ± 1.12	20.75 ± 3.97	37.41 ± 4.82	25.48 ± 4.54	12.09 ± 3.25	3.08 ± 1.77		
	Vertebra	0.00 ± 0.00	0.04 ± 0.19	2.12 ± 1.46	16.22 ± 3.60	47.12 ± 4.89	34.50 ± 4.79		
U15	Parietal	0.12 ± 0.34	6.77 ± 2.49	27.22 ± 4.43	33.73 ± 4.68	24.31 ± 4.38	7.86 ± 2.69		
	Occipital	0.41 ± 0.62	13.12 ± 3.44	33.76 ± 4.77	30.43 ± 4.49	17.37 ± 3.79	4.92 ± 2.07		
	Femur	4.79 ± 2.09	37.53 ± 4.75	35.56 ± 4.82	15.61 ± 3.47	5.41 ± 2.22	1.10 ± 1.05		
	Vertebra	0.00 ± 0.03	0.24 ± 0.51	5.24 ± 2.19	23.62 ± 4.21	44.81 ± 4.88	26.08 ± 4.41		
U16	Parietal	0.20 ± 0.46	8.41 ± 2.83	29.53 ± 4.43	33.17 ± 4.69	21.86 ± 4.07	6.83 ± 2.57		

	<b>Bone</b>	<b>0-10</b>	<b>10-20</b>	<b>20-30</b>	<b>30-40</b>	<b>40-50</b>	<b>50-60</b>	<b>60-70</b>	<b>70-80</b>
	Occipital	0.46 ± 0.67	12.67 ± 3.31	33.75 ± 4.65	30.48 ± 4.58	17.68 ± 3.82	4.96 ± 2.30		
	Femur	1.34 ± 1.09	21.70 ± 4.19	37.72 ± 4.96	24.92 ± 4.30	11.46 ± 3.14	2.86 ± 1.68		
	Vertebra	0.00 ± 0.00	0.00 ± 0.06	0.45 ± 0.67	8.59 ± 2.73	49.06 ± 5.08	41.90 ± 4.91		
U17	Parietal	0.18 ± 0.43	8.24 ± 2.72	29.43 ± 4.61	33.77 ± 4.51	22.62 ± 4.12	5.76 ± 2.38		
	Occipital	0.00 ± 0.00	0.00 ± 0.00	0.00 ± 0.00	0.00 ± 0.00	0.00 ± 0.00	1.82 ± 1.34		
	Femur	0.63 ± 0.80	16.06 ± 3.69	35.79 ± 4.80	28.90 ± 4.66	15.21 ± 3.45	3.41 ± 1.80		
	Vertebra	0.00 ± 0.00	0.11 ± 0.34	3.67 ± 1.83	21.19 ± 4.18	49.46 ± 4.95	25.56 ± 4.37		
J1	C Femur	0.19 ± 0.45	7.95 ± 2.69	27.24 ± 4.55	30.46 ± 4.58	20.05 ± 3.95	10.61 ± 3.07	3.51 ± 1.80	
	T Femur	0.03 ± 0.16	1.96 ± 1.36	14.36 ± 3.49	28.07 ± 4.53	27.98 ± 4.51	19.77 ± 3.98	7.84 ± 2.72	
	C Rib	0.00 ± 0.00	0.10 ± 0.31	2.23 ± 1.49	12.66 ± 3.25	28.11 ± 4.53	35.66 ± 4.92	21.25 ± 4.15	
	T Rib	0.00 ± 0.00	0.02 ± 0.13	0.69 ± 0.83	6.59 ± 2.54	22.50 ± 4.14	40.69 ± 4.98	29.50 ± 4.58	
J3	C Femur	2.54 ± 1.61	28.40 ± 4.40	36.99 ± 4.70	20.37 ± 4.07	8.13 ± 2.72	2.89 ± 1.64	0.67 ± 0.80	
	T Femur	0.11 ± 0.33	6.21 ± 2.40	25.00 ± 4.30	30.91 ± 4.61	21.89 ± 4.29	12.31 ± 3.40	3.58 ± 1.82	
	C Rib	0.00 ± 0.00	0.00 ± 0.05	0.45 ± 0.66	5.25 ± 2.18	21.22 ± 3.95	43.91 ± 4.81	29.16 ± 4.61	
J5	C Femur	1.15 ± 1.07	20.11 ± 4.00	36.46 ± 4.67	25.22 ± 4.29	12.03 ± 3.23	5.03 ± 2.20		
	T Femur	0.83 ± 0.94	17.81 ± 3.76	35.71 ± 4.82	26.75 ± 4.38	13.35 ± 3.53	5.55 ± 2.35		
	C Rib	0.00 ± 0.00	0.18 ± 0.41	4.09 ± 1.93	18.75 ± 3.95	35.79 ± 4.84	41.19 ± 4.93		
	T Rib	0.00 ± 0.00	0.09 ± 0.31	2.81 ± 1.61	16.44 ± 3.67	35.41 ± 4.91	45.24 ± 4.98		

	<b>Bone</b>	<b>0-10</b>	<b>10-20</b>	<b>20-30</b>	<b>30-40</b>	<b>40-50</b>	<b>50-60</b>	<b>60-70</b>	<b>70-80</b>
J7	C Femur	0.00 ± 0.00	0.00 ± 0.00	0.00 ± 0.04	0.24 ± 0.48	3.36 ± 1.87	19.82 ± 3.87	66.04 ± 4.72	10.54 ± 3.06
	T Femur	0.00 ± 0.00	0.11 ± 0.34	2.49 ± 1.50	12.90 ± 3.26	25.65 ± 4.21	30.91 ± 4.57	27.93 ± 4.32	0.00 ± 0.00
	C Rib	0.00 ± 0.04	0.49 ± 0.72	6.36 ± 2.36	19.63 ± 4.06	27.95 ± 4.50	25.69 ± 4.25	18.45 ± 3.91	1.44 ± 1.15
	T Rib	0.00 ± 0.00	0.00 ± 0.00	0.08 ± 0.28	1.56 ± 1.21	9.94 ± 3.03	29.07 ± 4.62	53.07 ± 4.81	6.28 ± 2.42
J8	C Femur	0.00 ± 0.00	0.49 ± 0.71	6.52 ± 2.50	19.17 ± 4.03	26.54 ± 4.45	23.53 ± 4.12	16.82 ± 3.75	6.94 ± 2.57
	T Femur	0.00 ± 0.00	0.11 ± 0.34	2.40 ± 1.54	11.25 ± 3.17	22.86 ± 4.23	27.27 ± 4.43	24.33 ± 4.26	11.78 ± 3.23
	C Rib	0.00 ± 0.00	0.53 ± 0.71	6.36 ± 2.43	19.17 ± 3.93	26.43 ± 4.56	23.77 ± 4.35	16.71 ± 3.67	7.04 ± 2.56
	T Rib	0.00 ± 0.00	0.00 ± 0.00	0.02 ± 0.13	0.60 ± 0.73	4.75 ± 2.10	18.11 ± 3.95	40.79 ± 4.80	35.73 ± 4.77
J10	C Femur	0.05 ± 0.22	3.76 ± 1.94	19.80 ± 3.78	29.58 ± 4.47	24.58 ± 4.24	15.28 ± 3.55	6.96 ± 2.67	
	T Femur	0.00 ± 0.04	0.24 ± 0.49	4.43 ± 2.01	17.07 ± 3.68	28.55 ± 4.54	29.97 ± 4.41	19.73 ± 3.94	
	C Rib	0.04 ± 0.22	3.48 ± 1.84	19.11 ± 3.96	29.58 ± 4.60	24.90 ± 4.35	15.62 ± 3.70	7.26 ± 2.64	
	T Rib	0.00 ± 0.00	0.01 ± 0.09	0.34 ± 0.57	3.80 ± 1.91	16.54 ± 3.92	37.26 ± 4.71	42.06 ± 4.89	
J11	C Femur	0.00 ± 0.00	0.01 ± 0.12	0.59 ± 0.77	5.00 ± 2.17	15.95 ± 3.75	27.42 ± 4.40	32.31 ± 4.67	18.71 ± 3.94
	T Femur	0.00 ± 0.00	0.03 ± 0.17	0.81 ± 0.89	6.41 ± 2.55	17.81 ± 3.93	28.11 ± 4.59	30.20 ± 4.72	16.64 ± 3.71
J13	C Femur	0.00 ± 0.00	0.34 ± 0.59	5.06 ± 2.19	17.17 ± 3.79	25.95 ± 4.43	25.23 ± 4.35	19.22 ± 3.87	7.02 ± 2.53
	T Femur	0.00 ± 0.00	0.00 ± 0.05	0.26 ± 0.50	2.92 ± 1.68	11.77 ± 3.10	26.38 ± 4.58	37.98 ± 4.78	20.69 ± 3.91
	C Rib	0.00 ± 0.00	0.04 ± 0.19	1.32 ± 1.12	8.32 ± 2.76	20.24 ± 4.00	28.54 ± 4.46	28.92 ± 4.49	12.62 ± 3.33
	T Rib	0.00 ± 0.00	0.00 ± 0.00	0.00 ± 0.00	0.04 ± 0.20	1.13 ± 1.05	9.40 ± 2.81	42.52 ± 4.85	46.91 ± 4.85

	<b>Bone</b>	<b>0-10</b>	<b>10-20</b>	<b>20-30</b>	<b>30-40</b>	<b>40-50</b>	<b>50-60</b>	<b>60-70</b>	<b>70-80</b>
J16	C Femur	0.00 ± 0.00	0.44 ± 0.66	5.67 ± 2.29	18.31 ± 3.83	25.99 ± 4.32	24.13 ± 4.07	17.89 ± 3.85	7.57 ± 2.62
	T Femur	0.00 ± 0.00	0.01 ± 0.09	0.35 ± 0.59	3.81 ± 1.85	13.73 ± 3.52	26.78 ± 4.48	34.28 ± 4.83	21.02 ± 4.07
	C Rib	0.00 ± 0.00	0.00 ± 0.00	0.01 ± 0.11	0.48 ± 0.68	4.24 ± 1.99	17.35 ± 3.77	40.81 ± 5.07	37.11 ± 4.88
	T Rib	0.00 ± 0.00	0.00 ± 0.03	0.00 ± 0.05	0.22 ± 0.46	2.54 ± 1.58	13.84 ± 3.60	40.64 ± 4.91	42.76 ± 4.84
J18	C Femur	0.01 ± 0.10	1.31 ± 1.17	10.95 ± 3.07	24.30 ± 4.21	26.47 ± 4.34	20.18 ± 3.95	12.74 ± 3.28	4.03 ± 1.99
	T Femur	0.00 ± 0.05	0.74 ± 0.86	8.22 ± 2.64	21.67 ± 4.08	26.76 ± 4.30	22.43 ± 4.27	15.07 ± 3.55	5.10 ± 2.20
	C Rib	0.00 ± 0.00	0.01 ± 0.08	0.45 ± 0.68	4.21 ± 1.91	14.74 ± 3.77	28.22 ± 4.54	35.02 ± 4.81	17.36 ± 3.81
	T Rib	0.00 ± 0.00	0.01 ± 0.07	0.31 ± 0.55	3.50 ± 1.82	13.63 ± 3.25	27.55 ± 4.55	36.05 ± 4.75	18.96 ± 3.90

**Table S.6.** Annual turnover rates for males and females calculated from the suggested values from Hedges et al. (2008). Inflection points are highlighted in yellow.

Age	Annual Turnover rate			
	Male		Female	
0	0.3	0.7	0.3	0.7
1	0.289647	0.667647	0.281333	0.66
2	0.279294	0.635294	0.262667	0.62
3	0.268941	0.602941	0.244	0.58
4	0.258588	0.570588	0.225333	0.54
5	0.248235	0.538235	0.206667	0.5
6	0.237882	0.505882	0.188	0.46
7	0.227529	0.473529	0.169333	0.42
8	0.217176	0.441176	0.150667	0.38
9	0.206824	0.408824	0.132	0.34
10	0.196471	0.376471	0.113333	0.3

11	0.186118	0.344118	0.094667	0.26
12	0.175765	0.311765	0.076	0.22
13	0.165412	0.279412	0.057333	0.18
14	0.155059	0.247059	0.038667	0.14
15	0.144706	0.214706	0.02	0.1
16	0.134353	0.182353	0.0225	0.08775
17	0.124	0.15	0.025	0.0755
18	0.110375	0.136875	0.0275	0.06325
19	0.09675	0.12375	0.03	0.051
20	0.083125	0.110625	0.029877	0.050864
21	0.0695	0.0975	0.029753	0.050728
22	0.055875	0.084375	0.02963	0.050593
23	0.04225	0.07125	0.029506	0.050457
24	0.028625	0.058125	0.029383	0.050321
25	0.015	0.045	0.029259	0.050185
26	0.014907	0.044693	0.029136	0.050049
27	0.014813	0.044387	0.029012	0.049914
28	0.01472	0.04408	0.028889	0.049778
29	0.014627	0.043773	0.028765	0.049642
30	0.014533	0.043467	0.028642	0.049506
31	0.01444	0.04316	0.028519	0.04937
32	0.014347	0.042853	0.028395	0.049235
33	0.014253	0.042547	0.028272	0.049099
34	0.01416	0.04224	0.028148	0.048963
35	0.014067	0.041933	0.028025	0.048827
36	0.013973	0.041627	0.027901	0.048691
37	0.01388	0.04132	0.027778	0.048556
38	0.013787	0.041013	0.027654	0.04842
39	0.013693	0.040707	0.027531	0.048284

40	0.0136	0.0404	0.027407	0.048148
41	0.013507	0.040093	0.027284	0.048012
42	0.013413	0.039787	0.02716	0.047877
43	0.01332	0.03948	0.027037	0.047741
44	0.013227	0.039173	0.026914	0.047605
45	0.013133	0.038867	0.02679	0.047469
46	0.01304	0.03856	0.026667	0.047333
47	0.012947	0.038253	0.026543	0.047198
48	0.012853	0.037947	0.02642	0.047062
49	0.01276	0.03764	0.026296	0.046926
50	0.012667	0.037333	0.026173	0.04679
51	0.012573	0.037027	0.026049	0.046654
52	0.01248	0.03672	0.025926	0.046519
53	0.012387	0.036413	0.025802	0.046383
54	0.012293	0.036107	0.025679	0.046247
55	0.0122	0.0358	0.025556	0.046111
56	0.012107	0.035493	0.025432	0.045975
57	0.012013	0.035187	0.025309	0.04584
58	0.01192	0.03488	0.025185	0.045704
59	0.011827	0.034573	0.025062	0.045568
60	0.011733	0.034267	0.024938	0.045432
61	0.01164	0.03396	0.024815	0.045296
62	0.011547	0.033653	0.024691	0.04516
63	0.011453	0.033347	0.024568	0.045025
64	0.01136	0.03304	0.024444	0.044889
65	0.011267	0.032733	0.024321	0.044753
66	0.011173	0.032427	0.024198	0.044617
67	0.01108	0.03212	0.024074	0.044481
68	0.010987	0.031813	0.023951	0.044346

69	0.010893	0.031507	0.023827	0.04421
70	0.0108	0.0312	0.023704	0.044074
71	0.010707	0.030893	0.02358	0.043938
72	0.010613	0.030587	0.023457	0.043802
73	0.01052	0.03028	0.023333	0.043667
74	0.010427	0.029973	0.02321	0.043531
75	0.010333	0.029667	0.023086	0.043395
76	0.01024	0.02936	0.022963	0.043259
77	0.010147	0.029053	0.02284	0.043123
78	0.010053	0.028747	0.022716	0.042988
79	0.00996	0.02844	0.022593	0.042852
80	0.009867	0.028133	0.022469	0.042716
81	0.009773	0.027827	0.022346	0.04258
82	0.00968	0.02752	0.022222	0.042444
83	0.009587	0.027213	0.022099	0.042309
84	0.009493	0.026907	0.021975	0.042173
85	0.0094	0.0266	0.021852	0.042037
86	0.009307	0.026293	0.021728	0.041901
87	0.009213	0.025987	0.021605	0.041765
88	0.00912	0.02568	0.021481	0.04163
89	0.009027	0.025373	0.021358	0.041494
90	0.008933	0.025067	0.021235	0.041358
91	0.00884	0.02476	0.021111	0.041222
92	0.008747	0.024453	0.020988	0.041086
93	0.008653	0.024147	0.020864	0.040951
94	0.00856	0.02384	0.020741	0.040815
95	0.008467	0.023533	0.020617	0.040679
96	0.008373	0.023227	0.020494	0.040543
97	0.00828	0.02292	0.02037	0.040407

98	0.008187	0.022613	0.020247	0.040272
99	0.008093	0.022307	0.020123	0.040136
100	0.008	0.022	0.02	0.04

## Appendix 2

Below is the python script used to model the average percentage of tissue from each period of life contained in a sample. “#” symbols bracket lines of code in which data specific to the sample under analysis are imputed.

```
import random
import numpy as np

def regenerate_blocks(blocks, round_num, replacement_rate):
    for i in range(len(blocks)):
        if random.random() < replacement_rate / 100:
            blocks[i] = max(round_num, blocks[i])
    return blocks

total_blocks = 100
initial_blocks = [0] * total_blocks

# Specify different replacement rates for each round
replacement_rates = [# Imput each turnover rate from year 1 to the year
where the bone will be analyzed (i.e. 90, 81, 73, etc)#]

percentage_ranges = {}
std_devs = {}

for i in range(0, #upper age assessed (likely age at death)#, #years in
each grouping (period of 5 or 10 years analyzed)#):
    lower_bound = i
    upper_bound = i + #years in each grouping#
    key = f"{lower_bound}-{upper_bound}"
    percentage_ranges[key] = []
    std_devs[key] = []
```

```
# Run 1000 simulations to get average from all simulation
for _ in range(1000):
    current_blocks = initial_blocks.copy()

    for round_num, rate in enumerate(replacement_rates, start=1):
        current_blocks = regenerate_blocks(current_blocks, round_num,
rate)

# Calculate percentages for each range
for key in percentage_ranges.keys():
    lower_bound, upper_bound = map(int, key.split('-'))

    count_within_range = sum(1 for block in current_blocks if
lower_bound <= block < upper_bound)

    percentage_within_range = (count_within_range / total_blocks) *
100

    percentage_ranges[key].append(percentage_within_range)

# Calculate average percentage and standard deviation for each range
for key in percentage_ranges.keys():
    average_percentage = np.mean(percentage_ranges[key])
    std_dev = np.std(percentage_ranges[key])
    std_devs[key] = std_dev

    print(f"Range {key}: Average percentage: {average_percentage:.2f}%,
Standard deviation: {std_dev:.2f}%")
```